THE JOURNAL OF BIOLOGICAL CHEMISTRY

Vol. 271, No. 39, Issue of September 27, pp. 23792–23798, 1996
Printed in U.S.A.

Apolipoprotein A-I Structural Modification and the Functionality of Reconstituted High Density Lipoprotein Particles in Cellular Cholesterol Efflux*

(Received for publication, March 29, 1996, and in revised form, June 4, 1996)

Kristin L. Gillotte, W. Sean Davidson‡, Sissel Lund-Katz, George H. Rothblat, and Michael C. Phillips§

From the Department of Biochemistry, Allegheny University of the Health Sciences, Philadelphia, Pennsylvania 19129 and the ‡Department of Biochemistry, College of Medicine at Urbana-Champaign, University of Illinois, Urbana, Illinois 61801

The role of HDL and its major protein constituent, apolipoprotein (apo) A-I, in promoting the removal of excess cholesterol from cultured cells has been well established; however, the mechanisms by which this occurs are not completely understood. To address the effects of apoA-I modification on cellular unesterified (free) cholesterol (FC) efflux, three recombinant human apoA-I deletion mutants and plasma apoA-I were combined with 1-palmitoyl-2-oleoyl phosphatidylcholine (POPC) and FC to make reconstituted high density lipoprotein (rHDL) discoidal complexes. These particles were characterized structurally and for their efficiency as acceptors of mouse L-cell fibroblast cholesterol. The deletion mutant proteins lacked NH_2-terminal (apoA-I (Δ44–126)), central (apoA-I (Δ139–170)), or COOH-terminal (apoA-I (Δ190–243)) domains of apoA-I. The three deletion mutants all displayed lipid-binding abilities and formed discoidal complexes that were similar in major diameter (13.2 ± 1.5 nm) to those formed by human apoA-I when reconstituted at a 100:5:1 (POPC:FC: protein) mole ratio. Gel filtration profiles indicated unreacted protein in the preparation made with apoA-I (Δ190–243), which is consistent with the COOH terminus portion of apoA-I being an important determinant of lipid binding. Measurements of the percent α-helix content of the proteins, as well as the number of protein molecules per rHDL particle, gave an indication of the arrangement of the deletion mutant proteins in the discoidal complexes. The rHDL particles containing the deletion mutants had more molecules of protein present than particles containing intact apoA-I, to the extent that a similar number of helical segments was incorporated into each of the discoidal species. Comparison of the experimentally determined number of helical segments with an estimate of the available space indicated that the deletion mutant proteins are probably more loosely arranged than apoA-I around the edge of the rHDL. The abilities of the complexes to remove radiolabeled FC were compared in experiments using cultured mouse L-cell fibroblasts. All four discoidal complexes displayed similar abilities to remove FC from the plasma membrane of L-cells when compared at an acceptor concentration of 50 μg of phospholipid/ml. Thus, none of the deletions imposed in this study notably altered the ability of the rHDL particles to participate in cellular FC efflux. These results suggest that efficient apoA-I-mediated FC efflux requires the presence of amphipathic α-helical segments but is not dependent on specific helical segments.

High density lipoproteins (HDL)[1] are a heterogeneous class of particles thought to mediate the flux of unesterified (free) cholesterol (FC) from peripheral cells to the liver in the process of reverse cholesterol transport (1). However, the mechanism directing the incorporation of cell cholesterol into the HDL and the role of HDL's major protein component, apolipoprotein (apo) A-I, are subjects of controversy. Epidemiological studies (2) as well as experiments involving transgenic animal models (3) have suggested that apoA-I is the major determinant of the ability of HDL species to participate in cholesterol efflux, thus much effort has been expended to elucidate the functional domains of this protein.

It has been demonstrated that the presence of amphipathic helical segments in acceptor particles is necessary for efficient efflux of cholesterol from cells (4). The arrangement or conformation of these segments may be a factor in the ability of acceptor particles to sequester cellular cholesterol. Several groups have utilized epitope-specific apoA-I monoclonal antibodies to define segment(s) of apoA-I that may be crucial for FC efflux (5–8). Banka *et al.* (5) utilized eight such antibodies and found a region spanning amino acid residues 74–110 to be important for efficient cholesterol efflux. A similar approach was taken by Luchoomun *et al.* (6) whose experiments indicated that the domain around amino acid 165 of apoA-I is involved in the efflux of cellular cholesterol. Experiments in which genetic apoA-I variants were combined with dimyristoylphosphatidylcholine have further suggested that substitution of a proline residue at amino acid 165 interferes with a conformation that is essential for cholesterol efflux (7). In contrast, a study by Fielding *et al.* (8) has demonstrated that the amino acid region 137–144 of apoA-I is adjacent to or part of a

*This work was supported by National Institutes of Health Program Project HL22633, a predoctoral fellowship (to K. L. G.) from the American Heart Association, Southeastern Pennsylvania Affiliate, and a postdoctoral fellowship (to W. S. D.) from the American Heart Association, Illinois Affiliate. The costs of publication of this article were defrayed in part by the payment of page charges. This article must therefore be hereby marked "*advertisement*" in accordance with 18 U.S.C. Section 1734 solely to indicate this fact.

§ To whom correspondence should be addressed.

[1] The abbreviations used are: rHDL, reconstituted HDL; apo, apolipoprotein; apoA-I (Δ139–170), apoA-I deletion mutant lacking residues Glu^{139}-Leu^{170}; apoA-I (Δ190–243), apoA-I deletion mutant lacking residues Ala^{190}-Gln^{243}; apoA-I (Δ44–126), apoA-I deletion mutant lacking residues Leu^{44}-Leu^{126}; apoA-I/FC/POPC, apoA-I/FC/POPC discoidal complex; CD, circular dichroism; EM, electron microscopy; FC, free (unesterified) cholesterol; HDL, high density lipoprotein; LCAT, lecithin-cholesterol acyltransferase; PAGE, polyacrylamide gradient gel electrophoresis; PL, phospholipid; POPC, 1-palmitoyl-2-oleoyl phosphatidylcholine.

structural site in the HDL subspecies, pre-β_1-HDL, which is effective in promoting the efflux of cellular cholesterol. Another study has attempted to distinguish whether monoclonal antibodies specific to apoA-I are able to inhibit cellular cholesterol efflux from intracellular or plasma membrane pools of cholesterol (9). Two Fab fragments spanning the amino acid region 140–150 were found to inhibit the efflux of intracellular cholesterol but not the cholesterol flux from the plasma membrane. It is apparent that there is marked disagreement about which, if any, domains of apoA-I are critical for cell cholesterol efflux.

Recently, Holvoet *et al.* (10) have expressed and purified recombinant mature human apoA-I and various deletion mutants for investigating structure-function relationships with regard to activation of lecithin-cholesterol acyltransferase (LCAT). The three deletion mutants: apoA-I (ΔLeu^{44}-Leu^{126}), apoA-I (ΔGlu^{139}-Leu^{170}), and apoA-I (ΔAla^{190}-Gln^{243}) lack domains thought to be crucial for either phospholipid (PL) binding or LCAT activation. In an attempt to define the domain of apoA-I that is crucial for cholesterol efflux from cells, the present study uses acceptor particles containing these engineered apoA-I molecules reconstituted with 1-palmitoyl-2-oleoyl phosphatidylcholine (POPC) into homogeneous and highly defined discoidal complexes. The variant proteins were successfully combined with POPC and unesterified cholesterol to form reconstituted HDL (rHDL) particles of similar size, which were subsequently characterized with respect to their structure. Cholesterol efflux studies indicate that when rHDL particles are utilized as acceptors of FC, there are no significant differences in the rates of efflux to the discoidal HDL containing either intact apoA-I or the deletion mutant proteins. These data indicate that the deletion of large segments from either the NH_2-terminal, central or COOH-terminal regions of the apoA-I molecule does not significantly impair the functionality of the rHDL complexes as acceptors of cellular cholesterol.

EXPERIMENTAL PROCEDURES

Materials

1-Palmitoyl-2-oleoylphosphatidylcholine (POPC) was purchased from Avanti Polar Lipids (Birmingham, AL) (+99% grade). Bovine serum albumin, sodium cholate, gentamycin, and cholesteryl methyl ether were obtained from Sigma (St. Louis, MO). [1, 2-^{3}H]Cholesterol was purchased from DuPont NEN (Boston, MA). Fetal bovine serum and minimal essential medium were obtained from Life Technologies, Inc. (Grand Island, NY).

Methods

Purification of Apolipoprotein A-I—Human HDL isolated from the fresh plasma of normolipidemic subjects was delipidated in ethanol/diethyl ether as described by Scanu and Edelstein (11) and purified apoA-I was isolated by anion exchange chromatography on Q-Sepharose and stored in lyophilized form at −70 °C (12). Prior to use the purified A-I was resolubilized in 6 M guanidine HCl and dialyzed extensively against Tris buffer (10 mM Tris, 150 mM NaCl, 1.0 mM EDTA; pH 8.2).

Recombinant Human Apolipoprotein A-I and Deletion Mutants—Preparation of the recombinant proteins was carried out by Holvoet *et al.* as formerly described in detail (10). Wild-type apoA-I and the apoA-I mutants were expressed in the periplasmic space of *Escherichia coli* cells and purified to homogeneity to yield the three deletion mutants utilized in this study: apoA-I (ΔLeu^{44}-Leu^{126}), apoA-I (ΔGlu^{139}-Leu^{170}), and apoA-I (ΔAla^{190}-Gln^{243}).

Preparation of Reconstituted HDL (rHDL)—Particles were prepared using the cholate dispersion/Bio-Bead removal technique as described in detail previously (13). A starting POPC/cholesterol/protein ratio of 100:5:1 (mol:mol:mol) was used and final compositions were determined after concentration (Centriprep 30, Amicon) under low speed centrifugation. The homogeneity and size of the complexes were assessed by gradient gel electrophoresis using precast 8–25% polyacrylamide gels (Pharmacia Biotech Inc.). Due to indications that the complex preparations contained varying amounts of free protein, the samples were purified by high performance gel filtration (Superdex 200 HR 10/30, Pharmacia Biotech Inc.). The column was calibrated with standard proteins (13) and the hydrodynamic diameters of the particles were calculated from the elution volumes.

Characterization of rHDL—The particles were analyzed chemically using the Markwell modification of the Lowry protein assay (14), while phospholipids were determined as inorganic phosphorus by the method of Sokoloff and Rothblat (15). Unesterified cholesterol was determined after Bligh and Dyer extraction (16) by gas-liquid chromatography analysis (17); cholesteryl methyl ether was utilized as an internal standard in this assay. The number of apoA-I molecules per particle was determined by reaction with dimethyl suberimidate and determining the degree of cross-linking of the apoA-I by SDS-PAGE (18). In addition to hydrodynamic diameter determination by gel filtration chromatography, negative stain electron microscopy (EM) was utilized as described by Forte and Nordhausen (19) to determine the size of the reconstituted particles. Mean particle dimensions of 100 complexes were determined from each negative at ×189,000 magnification. The average α-helix content of apoA-I when complexed to PL was determined by circular dichroism (CD) spectroscopy using a Jasco J41A spectropolarimeter. Spectra were measured at 25 °C in a 0.1-cm path length quartz cuvette as described previously (20); the percent α-helix was determined from the molar ellipticities at 222 nm.

Efflux of Plasma Membrane Cholesterol—Mouse L-cell fibroblast monolayers were used to monitor the release of [^{3}H]cholesterol to the extracellular medium as a measure of unesterified (free) cholesterol (FC) efflux, as has been described in detail (4). The cells, present in 12-well cell plates (22 mm), were grown to confluence in minimal essential medium/bicarbonate supplemented with 10% fetal bovine serum in a 37 °C humidified incubator in the presence of 95% air and 5% CO_2. The monolayers were labeled with 2 μCi/ml [1,2-^{3}H]cholesterol in bicarbonate-buffered minimal essential medium with 2.5% fetal calf serum for 24 h. This was followed by a 12-h incubation in minimal essential medium/bicarbonate containing 1% bovine serum albumin to equilibrate the radioactivity between the various cellular sterol pools. After a brief wash with minimal essential medium/bicarbonate containing HEPES (50 mM), cholesterol efflux measurements were initiated by the application of 1.0 ml/well of the test medium, containing 0.5% bovine serum albumin and the acceptor at the indicated PL concentration. The experiment was conducted in a 37 °C incubator with an atmosphere of 95% air and 5% CO_2. The radioactivity of a 75-μl aliquot of the medium was determined at specific time intervals to estimate the fraction of FC released into the medium. Upon completion of the time course, all cell wells were washed with Dulbecco's phosphate-buffered salt solution three times and the cellular lipids were extracted with isopropanol (21). From the extraction, the total amount of radioactive cholesterol per well was determined by liquid scintillation counting.

Data Analysis—The fractional release of FC was determined experimentally and analyzed as described in detail for this system previously (4). The kinetic analysis is based on the assumption that the system is closed and that all FC therefore exists in either the cellular FC pool or in the acceptor FC pool. The equilibration of FC between these two pools was fitted to the single exponential equation $Y = Ae^{-Bt} + C$, where Y represents the fraction of radiolabeled FC remaining in the cells, t is the incubation time, A is a pre-exponential term that reflects the fraction of FC that exists in the medium at equilibrium, B is a time constant representing the release of FC, and C is a constant that represents the fraction of labeled FC that remains associated with the cells at equilibrium. A, B, and C were derived by fitting the experimental data to the above equation by nonlinear regression (Graph Pad Prism, Graph Pad Software Inc.). The above equation fit the data more accurately than a double exponential equation. The apparent rate constant for efflux (k_a), which is dependent on the acceptor particle concentration tested, is the product of A and B. The apparent $t_{1/2}$ of efflux value in hours was then calculated as follows: $t_{1/2} = \ln 2/k_a$. The $t_{1/2}$ values were statistically compared by Student's t test (Graph Pad Prism, Graph Pad Software Inc.).

RESULTS

Structural Characterization of rHDL Particles—Previously, plasma apoA-I has been shown to form discoidal complexes (rHDL) upon combination with POPC ± cholesterol (22–24), and the compositional characteristics of these discs have been well defined. Holvoet *et al.* (10) recently showed that recombinant apoA-I and specific deletion mutants of apoA-I were able to combine in a similar manner with dipalmitoylphosphatidyl-

choline to form discoidal complexes. We confirmed that recombinant apoA-I forms reconstituted complexes with POPC and cholesterol and that these complexes are structurally identical to those prepared from plasma apoA-I. In preliminary cell FC efflux studies utilizing rHDL containing either plasma apoA-I or recombinant, wild-type, apoA-I, all measurements of efflux to the two types of rHDL particles were indistinguishable, indicating that the origin of the apoA-I did not affect the ability of the particles to function as acceptors of cellular cholesterol. Therefore, plasma apoA-I was used as the control protein in the studies of recombinant variants.

To study the effects of apoA-I modification on the structure and function of rHDL particles, discoidal complexes were prepared with plasma apoA-I, apoA-I (Δ44–126), apoA-I (Δ139–170), or apoA-I (Δ190–243) at an initial molar ratio of 100:5:1 (POPC:FC:protein). The particles were sized by PAGE, which indicated the presence of free protein in addition to the complexes, particularly with rHDL constructed with apoA-I (Δ44–126) and apoA-I (Δ190–243) (approximately 20 and 50% lipid-free protein, respectively). The complexes were isolated from unreacted protein and lipid using gel filtration chromatography on a calibrated column, from which particle hydrodynamic diameters were determined. The gel filtration profiles (Fig. 1) indicated that there was no free protein in the preparations containing plasma apoA-I, apoA-I (Δ44–126), and apoA-I (Δ139–170), whereas 26% of apoA-I (Δ190–243) was found to be unassociated with lipid in its preparation. These results suggest that the extent of free protein detected by PAGE may have been an artifact of the electrophoresis due to stripping of the protein from the complexes as they migrated through the gel. Reduced lipid association of apoA-I (Δ190–243) was an expected result as this apoA-I mutant is missing the carboxyl terminus of apoA-I, which plays a major role in stabilizing the lipid-bound state of apoA-I (10, 25–27). The fractions corresponding to the rHDL species were isolated and characterized; the compositions and dimensions of the particles are listed in Table I. Electron microscopy was utilized to confirm that the particles were discoidal in shape, which is apparent from the stacks of discoidal complexes displayed for each preparation in Fig. 2. The composition and size determinations of the plasma apoA-I-FC-POPC complex are in good agreement with previously published results for a discoidal complex of composition 83:3:1 (molar ratio, POPC:FC:apoA-I) (24). This complex has been measured by PAGE and EM to have a diameter of 10.3 and 11.5 nm, respectively, which is the same as the present measurements of 10.0 and 11.2 nm (Table I). The EM measurements denote an average major diameter of 13.2 ± 1.5 nm for the four rHDL species described in Table I; the measurements are not significantly different by unpaired *t* test analysis. The PAGE and gel filtration column measurements of the hydrodynamic diameters indicated that apoA-I (Δ44–126) formed a slightly larger complex than rHDL prepared with plasma apoA-I, while apoA-I (Δ139–170) and apoA-I (Δ190–243) both resulted in slightly smaller complexes. Again, the smaller hydrodynamic diameters of the latter two complexes may be attributed to some protein removal during migration through the gel matrix. Protein cross-linking was used to estimate the number of protein molecules per complex (Fig. 3). The rHDL comprised of intact apoA-I contained a mixture of particles containing 2 (70%) and 3 (30%) molecules of apoA-I per complex. The scans of the gels in Fig. 3 for the complexes containing the mutant proteins indicate that the cross-linking

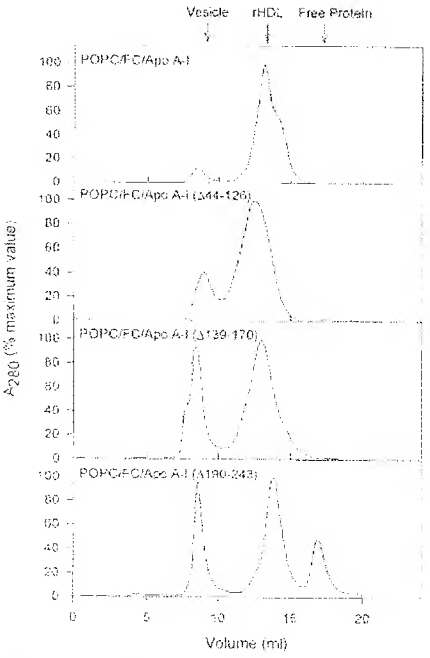

FIG. 1. **Elution profiles of POPC-FC-apoA-I reconstituted particles subjected to gel filtration chromatography.** A 1 × 30-cm Superdex HR 200 (Pharmacia Biotech Inc.) gel filtration column was used to analyze solutions of reconstituted particles that were combined at a 100:5:1 PL:unesterified cholesterol:protein molar ratio. Fractions of 0.25 ml were collected and the protein was detected by absorbance at 280 nm. The void volume of the column was 8.1 ml, and the total volume was 20.1 ml.

TABLE I
Characteristics of discoidal rHDL particles

Protein component of particle	Molar composition (POPC:FC:apoAI)[a]		Diameter of particle			No. of protein/particle[e]	α-Helix content[f]
	Initial	Final	PAGE[b]	Column[c]	EM[d]		
				nm			%
Plasma ApoA-I	100:5:1	84 ± 21:5:1	10.0 ± 0.3	9.6 ± 0.9	11.2 ± 1.9	2	80 ± 6
ApoA-I (Δ44–126)	100:5:1	42 ± 20:2:1	10.9 ± 0.7	10.9 ± 0.4	13.3 ± 1.6	4	59 ± 16
ApoA-I (Δ139–170)	100:5:1	44 ± 12:2:1	9.1 ± 0.1	8.9 ± 0.4	14.8 ± 1.7	3	68 ± 6
ApoA-I (Δ190–243)	100:5:1	42:1:1	7.9 ± 0.2	8.1 ± 0.3	13.3 ± 1.7	3	63 ± 3

[a] Determined from analysis on three separate reconstitution experiments (±1 S.D.) ($n = 1$ for apoAI (Δ190–243)). Final values were obtained after purification by gel filtration chromatography on a Superdex 200 column.
[b] Determined from nondenaturing polyacrylamide gradient gel electrophoresis using reference globular proteins.
[c] Average hydrodynamic diameter as measured on a Superdex 200 (Pharmacia) gel filtration column calibrated with reference globular proteins (±1 S.D.).
[d] Average major diameter of 100 particles determined from negative staining microscopy (±1 S.D.). Variances are not significantly different as determined by unpaired *t* test.
[e] Determined from SDS-polyacrylamide gel electrophoresis of delipidated apoAI or deletion variant after cross-linking with dimethyl suberimidate.
[f] Determined from molar ellipticities at 222 nm (±1 S.D.).

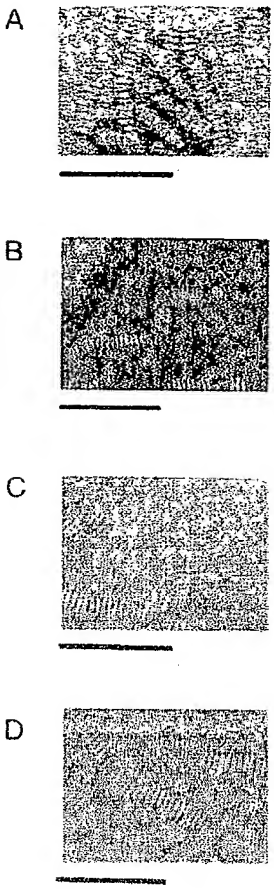

FIG. 2. **Negative stain electron micrographs of rHDL.** Electron micrographs of the reconstituted POPC·FC·apoA-I discoidal particles are shown. The protein component of the complexes is as follows: *A*, apoA-I; *B*, apoA-I (Δ44–126); *C*, apoA-I (Δ139–170); and *D*, apoA-I (Δ190–243). Magnification is × 189,000 in *A*, *C*, and *D* and 150,000 × in *B*; *bars* represent 100 nm. Major diameters of 100 discoidal particles were determined and are listed in Table I.

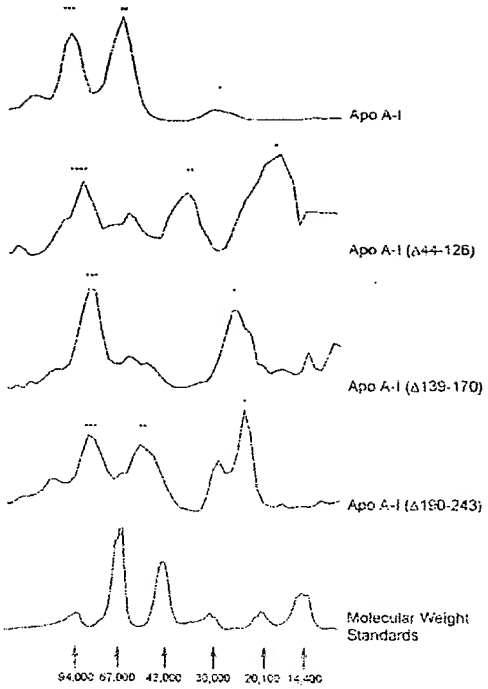

FIG. 3. **Profiles of SDS-PAGE gels used to determine the degree of apoA-I cross-linking by dimethyl suberimidate.** SDS-PAGE on 8–25% gels was performed using cross-linked rHDL. The apoA-I oligomers were visualized by Coomassie Blue staining, and a scan of the protein distribution was obtained in digital form using a flatbed scanner (Hewlett-Packard ScanJet IIP) and computer image analysis (Jandel Scientific, San Rafael, CA). The resulting profiles indicate the degree of oligomer formation by either apoA-I or the variants of apoA-I; the number of protein molecules per oligomer is indicated by the number of *asterisks* above each peak. Molecular weight standards are indicated in the *bottom panel*.

was incomplete. In these cases, the dominant cross-linked oligomer was assumed to represent the number of protein molecules on the discoidal particle (Table I). The predominant species were four molecules of apoA-I (Δ44–126), three molecules of apoA-I (Δ139–170), and three molecules of apoA-I (Δ190–243).

Circular dichroism was used to determine the effect of the various deletions in the apoA-I molecule on the average α-helix content of the proteins in the rHDL particles. Table I demonstrates that the α-helix content of the intact protein was greater than that of any of the apoA-I deletion mutants. The number of amphipathic helices per protein molecule can be predicted from the number of helical residues in the protein by assuming that there are approximately 22 amino acid residues per helical segment (28). On this basis, there are nine helices in the plasma apoA-I molecules in the rHDL particles; this number is in good agreement with prior work which suggest that with 75% α-helix there should be eight helical segments per protein molecule (22, 28). The equivalent numbers of helices for apoA-I (Δ44–126), apoA-I (Δ139–170), and apoA-I (Δ190–243) are 4, 7, and 5, respectively.

Efflux of Cellular Cholesterol to Discoidal rHDL Particles—To compare plasma apoA-I/FC/POPC and mutant apoA-I/FC/POPC discoidal complexes as acceptors of cell cholesterol, the rHDL were incubated with radiolabeled mouse L-cell fibroblasts at a concentration of 50 μg of PL/ml for periods of up to 6 h. Measurement of the fraction of radiolabeled FC present in the cells during the time course of incubation with rHDL particles showed that they exhibited similar abilities to remove cellular cholesterol (Fig. 4). Time courses of cholesterol efflux in the systems containing native apoA-I·FC·POPC and apoA-I (Δ190–243)·FC·POPC discoidal complexes are the same. Thus, the deletion of the carboxyl terminus did not impair the ability of the particle to participate in cholesterol efflux. Efflux to apoA-I (Δ44–126)·FC·POPC and apoA-I (Δ139–170)·FC·POPC rHDL was identical to efflux to particles containing intact apoA-I for the first 2 h of the experiment, after which point they showed some deviation from the control time course. After 6 h of incubation, apoA-I (Δ139–170)·FC·POPC rHDL removed slightly less FC and apoA-I (Δ44–126)·FC·POPC slightly more than the apoA-I·FC·POPC particles. All the time courses were fitted to a single exponential decay equation as described under "Methods" to obtain $t_{1/2}$ values of efflux for each complex (Table II). An average $t_{1/2}$ of 16.2 ± 1.8 h was measured, with maximum deviations of only 14% from this value. Comparison of the $t_{1/2}$ of efflux by unpaired *t* test analysis indicates that none of the time courses involving incubation with apoA-I mutant·FC·POPC complexes were statistically different. These data indicate that the apoA-I deletions introduced here do not impair the functionality of the rHDL complexes as acceptors of cellular cholesterol.

DISCUSSION

Formation of rHDL Particles—The experiments summarized in Table I and Figs. 1–3 indicate that the deletion mutants

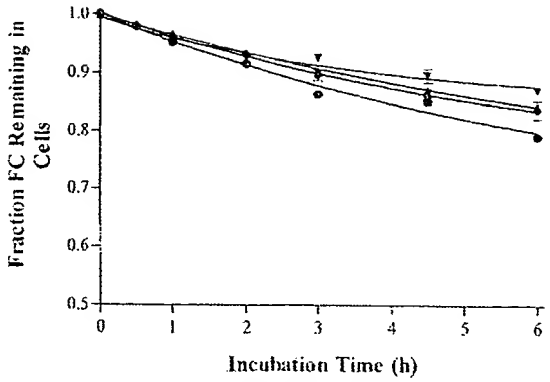

FIG. 4. **Time course of free cholesterol efflux from mouse L-cell fibroblast to reconstituted HDL particles.** Mouse L-cell fibroblasts grown to confluence in 22-mm tissue culture wells and trace-labeled with ^{3}H-free cholesterol were incubated for 6 h at 37 °C with 1 ml of test medium. Test media consisted of rHDL at 50 μg PL/ml minimal essential medium, 0.5% bovine serum albumin. Symbols indicate the protein component of the particles: ▲, plasma apoA-I; ●, apoA-I (Δ44–126); ▼, apoA-I (Δ139–170), and ◆, apoA-I (Δ190–243). Each point represents the mean fraction of radiolabeled cholesterol detected in the media of three cell wells, and the *error bars* represent 1 S.D. The curves through the time points were obtained by fitting to a single exponential decay equation (see "Methods").

TABLE II
$t_{1/2}$ values of efflux from L-cell fibroblast monolayers to discoidal rHDL

Recombinant HDL protein species[a]	Halftimes of efflux[b]
	h
Plasma ApoA-I	18.1 ± 0.5
ApoA-I (ΔLeu^{44}–Leu^{126})	13.9 ± 0.8[c]
ApoA-I (ΔGlu^{139}–Leu^{170})	17.2 ± 2.5[c,d]
ApoA-I (ΔAla^{190}–Gln^{243})	15.7 ± 1.4[c]

[a] Recombinant HDL were prepared with POPC and the indicated protein as described under "Methods." The discoidal particles were utilized in the cholesterol efflux experiment at a concentration of 50 μg of PL/ml.

[b] Efflux $t_{1/2}$ are derived by fitting the experimental timecourse of 6 h to a single exponential equation as described under "Methods." Values are the average of triplicate measurements ± 1 S.D.

[c] Time courses not significantly different from each other as determined by Student's *t* test.

[d] Time course is not significantly different from that obtained with POPC/apoA-I as determined by Student's *t* test.

were able to bind to POPC and cholesterol to form rHDL discoidal complexes. From the helix content and the amino acid residue content of the proteins, the number of α-helical segments per protein molecule can be determined through the assumption that each helix is 22 amino acids in length (28). The results indicate that the two molecules of protein present on the apoA-I·FC·POPC disc are organized such that 18 α-helical segments are present (Table III). Despite major structural modification of the apoA-I molecule, the mutant proteins packed onto a disc in such a manner that an equivalent number of α-helical segments (18 ± 3 helices) were incorporated. As shown in Table III, with native apoA-I, 20 helices could theoretically be accommodated around the disc perimeter. Since 18 helices are actually present at the disc edge, it follows that the helices in the two protein molecules are packed tightly around the perimeter of the complex. In this arrangement, electrostatic interactions between the antiparallel helices contribute to the stabilization of the protein in this close-packed conformation (29, 30). Although the apoA-I helices are tightly packed on the particles described in this study, a "hinge-domain" (28) extending away from the particle surface is probably not present, since there is room to accommodate every helix at the disc edge. Since the deletion mutant proteins are smaller and have fewer α-helical segments, more protein molecules were able to be incorporated onto the disc edge. The limiting number of α-helical segments for these rHDL particles was calculated to be 25 for discs containing the NH_2-terminal and COOH-terminal deletion mutants and 28 for the protein lacking the central domain of apoA-I (Table III). Again, there is sufficient space to accommodate every helix at the disc edge, because the numbers of helices measured experimentally were lower than these limiting values. However, the deletion mutant proteins are not as tightly packed on the disc edge as intact apoA-I, because only 60–75% of the maximum possible number of helices were incorporated at the disc edge compared with the equivalent value of 90% for the intact apoA-I molecule. It seems that when helical segments are deleted in apoA-I, the interhelix attraction is reduced, resulting in a looser packing in the discoidal particles. In summary, all four types of apoA-I molecule formed similar particles suggesting that no specific amino acid sequence or helix-helix interactions are required for this process. The particles are stable provided that sufficient amphipathic α-helices are present to cover the PL acyl chains at the disc edge.

Cholesterol Efflux to rHDL Particles—It is now generally accepted that efflux of plasma membrane cholesterol involves a passive desorption of FC molecules from the membrane followed by diffusion of these molecules through the aqueous phase surrounding the cells and incorporation of the FC into a PL-containing acceptor particle (1, 31). Studies have suggested that when FC acceptor particles contain apolipoprotein, there may be an interaction of the protein helices with specific lipid domains in the plasma membrane resulting in the modulation of cholesterol efflux (31–34), but the details of this association are not yet clear.

This study investigated the possibility that a particular region of apolipoprotein A-I is essential for the efficient release of cholesterol from the plasma membrane. Cholesterol efflux was measured to rHDL containing either wild-type apoA-I or one of the three apoA-I deletion mutants in a system in which other factors that could affect the efflux capability of the particles were eliminated. For example, acceptor particle PL properties and particle size have been shown to be determinants in cholesterol efflux (35, 36). In this study, the PL species was constant, and the acceptor particles were incubated with the cell monolayers at equal PL concentrations. In addition, differences due to varying sizes of the acceptor particles were not a factor here as the particles were constructed and isolated in a manner such that they were similar in size. Our study clearly demonstrates the need to isolate the rHDL particles from any free lipid or protein, as the gel filtration profiles indicated heterogeneous preparations. The utilization of homogeneous acceptors ensured that our results were not affected by the presence of these unreacted species. Having taken these factors into account, variations in the ability of the discs to remove cholesterol could be attributed directly to the differences in protein structure.

The results indicate that the deletion of specific segments of apoA-I did not affect the ability of the protein to participate in cholesterol efflux when combined with lipid as a rHDL particle. The $t_{1/2}$ values of efflux are the same (±14%), thus all four particles essentially displayed equivalent abilities to remove cellular FC. Furthermore, none of the deletion mutant discoidal species had slower $t_{1/2}$ values of efflux than particles containing the intact plasma apoA-I. These data suggest that specific domains within the apoA-I molecule are not required for efficient efflux. These results are in contrast to studies performed by several groups in which apoA-I-specific mono-

TABLE III
Accomodation of apoA-I α-helices in rHDL particles

Protein component of particle	Helical residues[a]	α-Helices/protein molecule[b]	Expt. number α-helices/particle[c]	Maximum number α-helices/circumference[d]
Plasma ApoA-I	194	9	18	20
ApoA-I (Δ44–126)	95	4	16	25
ApoA-I (Δ139–170)	144	7	21	28
ApoA-I (Δ190–243)	119	5	15	25

[a] Determined from the percent α-helix content (Table I) and the total amino acid residues of the protein.
[b] Number of helices was calculated from the number of helical residues assuming that each helix is 22 amino acids in length.
[c] Calculated by multiplying the number in b by the number of protein molecules per disc (Table I).
[d] The circumference of rHDL particles was calculated from the major diameter measured by EM and corrected for the apolipoprotein contribution by subtracting the diameter of an α-helix (1.5 nm). The number of α-helices packed around this circumference was estimated by dividing by the α-helix diameter. (*cf.* Ref. 22).

clonal antibodies were used to determine the regions of functional importance. Each of these studies identified a discrete region of apoA-I that was critical for apoA-I-mediated cholesterol efflux. It has been suggested that the region surrounding amino acid residue 165 of apoA-I (6) or the specific amino acid content in this position (7) determines the efficiency of apoA-I in cholesterol efflux. However, this region was deleted in this study in mutant apoA-I (Δ139–170) without any effect on the participation of the protein in the efflux process. Other regions of apoA-I have been suggested to be essential: amino acids 74–110 in studies involving rHDL species (5), and 137–144 in the HDL subspecies, pre-β HDL (8). These regions were addressed in this study with mutants apoA-I (Δ44–126) and apoA-I (Δ139–170), respectively, both of which when combined with lipid did not vary from the ability of intact apoA-I to remove cellular FC. Although small regions of the protein (1–44, 127–138, and 171–189) were not deleted in the mutants studied here, it seems likely that no specific domains of apoA-I are required for efficient apolipoprotein-mediated cholesterol efflux. The reasons for the variation in results between the present study and the monoclonal antibody studies are not entirely clear at this time. However, it is possible that inhibiting antibodies may be positioned in some cases such that they cover a significant portion of the polar phosphatidylcholine head groups, or the "faces," of the discoidal complex. Since the deletion mutant proteins utilized here demonstrate looser helix packing at the disc edge than intact apoA-I, but the discs are equally good FC acceptors, cholesterol molecules probably do not incorporate at the disc edge, but rather by way of the face of the complex. If a monoclonal antibody covers a portion of the face, it follows that cholesterol incorporation will be inhibited.

The results of this study suggest that several structural features of the apoA-I molecule are not determinants of efficient cholesterol efflux. Thus, specific domains of the protein are not essential and, furthermore, interactions between specific helices seem not to be required. The number of protein molecules or helical segments per rHDL complex has no effect on the function of the particle in a cholesterol efflux system. It seems that the essential factor provided by apoA-I is the amphipathic helices required to stabilize the small rHDL particles. This agrees with previous work with synthetic peptides (4), which suggested that amphipathic helix interactions are essential for efflux, but that the number and amino acid sequence of the helices does not affect the process.

Implications for Reverse Cholesterol Transport—In addition to the phenomenon of peripheral cell FC transfer from the plasma membrane to HDL particles that has been described in this study, reverse cholesterol transport *in vivo* involves the subsequent steps of cholesterol esterification by LCAT and cholesterol ester transfer between lipoprotein particles via cholesterol ester transfer protein (33, 37, 38). Studies have indicated that discoidal HDL are better substrates for LCAT than spherical HDL particles (39). Although the abilities of the discoidal HDL particles containing either wild-type apoA-I or apoA-I deletion mutants to accept cholesterol molecules diffusing from the plasma membrane are similar, experiments of Holvoet *et al.* (10) indicate that discoidal particles containing these deletion mutants have different reactivities with LCAT. Thus, the conformation of apoA-I probably affects the second step of the reverse cholesterol transport process. The esterification by LCAT is essential to maintain the gradient of cholesterol flux from the cellular membrane (38, 40). These results suggest that the structure of apoA-I is critical for proper activation of LCAT but not for formation of HDL particles that can accept FC molecules diffusing from the plasma membrane of a cell.

The current results relate to cholesterol efflux from mouse L-cell fibroblasts where at least 60% of the plasma membrane cholesterol effluxes from a single kinetic pool under the experimental conditions utilized.[2] However, some cell types appear to have several pools of plasma membrane cholesterol which may be accessed preferentially by apoA-I present in a particular conformation (32). Furthermore, it has been proposed that the conformation of apoA-I in pre-β HDL species is different to that in spherical HDL (33), and these small discoidal acceptors may access cholesterol in certain human fibroblast plasma membrane domains, such as caveolae, more efficiently (41). Further work is necessary to determine whether particular domains of the apoA-I molecule are important for efflux from these specific plasma membrane pools of cholesterol.

Acknowledgments—We thank Dr. Paul Holvoet of the Center for Molecular and Vascular Biology, University of Leuven, Belgium for his generous gift of the apoA-I deletion mutant proteins. We also thank Faye Baldwin, Sheila Benowitz, and Margaret Nickel for expert technical assistance.

REFERENCES

1. Johnson, W. J., Mahlberg, F. H., Rothblat, G. H., and Phillips, M. C. (1991) *Biochim. Biophys. Acta* **1085**, 273–298
2. Sharrett, A. R., Patsch, W., Sorlie, P. D., Heiss, G., Bond, M. G., and Davis, C. E. (1994) *Arterioscler. Thromb.* **14**, 1098–1104
3. Breslow, J. L. (1993) *Proc. Natl. Acad. Sci. U. S. A.* **90**, 8314–8318
4. Davidson, W. S., Lund-Katz, S., Johnson, W. J., Anantharamaiah, G. M., Palgunachari, M. N., Segrest, J. P., Rothblat, G. H., and Phillips, M. C. (1994) *J. Biol. Chem.* **269**, 22975–22982
5. Banka, C. L., Black, A. S., and Curtiss, L. K. (1994) *J. Biol. Chem.* **269**, 10288–10297
6. Luchoomun, J., Theret, N., Clavey, V., Duchateau, P., Rosseneu, M., Brasseur, R., Denefle, P., Fruchart, J. C., and Castro, G. R. (1994) *Biochim. Biophys. Acta* **1212**, 319–326
7. von Eckardstein, A., Castro, G., Wybranska, I., Theret, N., Duchateau, P., Duverger, N., Fruchart, J.-C., Ailhaud, G., and Assmann, G. (1993) *J. Biol. Chem.* **268**, 2616–2622
8. Fielding, P. E., Kawano, M., Catapano, A. L., Zeppo, A., Marcovina, S., and Fielding, C. J. (1994) *Biochemistry* **33**, 6981–6985
9. Sviridov, D., Pyle, L., and Fidge, N. (1996) *Biochemistry* **35**, 189–196
10. Holvoet, P., Zhao, Z., Vanhoo, B., Vos, R., Deridder, E., Dhoest, A., Taveirne, J., Brouwers, E., Demarsin, E., Engelborghs, Y., Rosseneu, M., Collen, D., and Brasseur, R. (1995) *Biochemistry* **34**, 13334–13342
11. Scanu, A. M., and Edelstein, C. (1971) *Anal. Biochem.* **44**, 576–588
12. Weisweiler, P., Friedl, C., and Ungar, M. (1987) *Clin. Chem. Acta* **169**,

[2] S. Davidson, unpublished results.

249–254
13. Sparks, D. L., Phillips, M. C., and Lund-Katz, S. (1992) *J. Biol. Chem.* **267**, 25830–25838
14. Markwell, M. A., Haas, S. M., Bieber, L. L., and Tolbert, N. E. (1978) *Anal. Biochem.* **87**, 206–210
15. Sokoloff, L., and Rothblat, G. H. (1974) *Proc. Soc. Exp. Biol. Med.* **146**, 1166–1172
16. Bligh, E. G., and Dyer, W. J. (1959) *Can. J. Biochem. Physiol.* **37**, 911–917
17. Klansek, J., Yancey, P., St. Clair, R. W., Fischer, R. T., Johnson, W. J., and Glick, J. M. (1995) *J. Lipid Res.* **36**, 2261–2266
18. Swaney, J. B. (1986) *Methods Enzymol.* **128**, 613–626
19. Forte, T. M., and Nordhausen, R. W. (1986) *Methods Enzymol.* **128**, 442–457
20. Sparks, D. L., Davidson, W. S., Lund-Katz, S., and Phillips, M. C. (1995) *J. Biol. Chem.* **270**, 26910–26917
21. Johnson, W. J., Ramberger, M. J., Latta, R. A., Rapp, P. E., Phillips, M. C., and Rothblat, G. H. (1986) *J. Biol. Chem.* **261**, 5766–5776
22. Jonas, A., Kezdy, K. E., and Wald, J. H. (1989) *J. Biol. Chem.* **264**, 4818–4824
23. Nichols, A. V., Gong, E. L., Blanche, P. J., and Forte, T. M. (1983) *Biochim. Biophys. Acta* **750**, 353–364
24. Sparks, D. L., Davidson, W. S., Lund-Katz, S., and Phillips, M. C. (1993) *J. Biol. Chem.* **268**, 23250–23257
25. Schmidt, H.-J., Remaley, A. T., Stonik, J. A., Ronan, R., Wellmann, A., Thomas, F., Zech, L. A., Brewer, H. B., Jr., and Hoeg, J. M. (1995) *J. Biol. Chem.* **270**, 5469–5475
26. Ji, Y., and Jonas, A. (1995) *J. Biol. Chem.* **270**, 11290–11297
27. Palgunachari, M. N., Mishra, V. K., Lund-Katz, S., Phillips, M. C., Adeyeye, S. O., Alluri, S., Anantharamaiah, G. M., and Segrest, J. P. (1996) *Arterioscler. Thromb. Vasc. Biol.* **16**, 328–338
28. Segrest, J. P., Jones, M. K., DeLoof, H., Brouillette, C. G., Venkatachalapathi, Y. V., and Anantharamaiah, G. M. (1992) *J. Lipid Res.* **33**, 141–166
29. Rosseneu, M., Vanloo, B., Lins, L., Corijn, J., Van Biervliet, J. P., Ruysschaert, J. M., and Brasseur, R. (1992) in *High Density Lipoproteins and Atherosclerosis III* (Miller, N. E., and Tall, A. R., eds) pp. 105–114, Elsevier Science Publishers B. V., Amsterdam
30. Brasseur, R., De Meutter, J., Vanloo, B., Goormaghtigh, E., Ruysschaert, J. M., and Rosseneu, M. (1990) *Biochim. Biophys. Acta* **1043**, 245–252
31. Rothblat, G. H., and Phillips, M. C. (1991) *Curr. Opin. Lipidol.* **2**, 288–294
32. Rothblat, G. H., Mahlberg, F. H., Johnson, W. J., and Phillips, M. C. (1992) *J. Lipid. Res.* **33**, 1091–1097
33. Fielding, C. J., and Fielding, P. E. (1995) *J. Lipid. Res.* **36**, 211–228
34. Hara, H., and Yokoyama, S. (1990) *J. Biol. Chem.* **266**, 3080–3086
35. Davidson, W. S., Gillotte, K. L., Lund-Katz, S., Johnson, W. J., Rothblat, G. H., and Phillips, M. C. (1995) *J. Biol. Chem.* **270**, 5882–5890
36. Davidson, W. S., Rodrigueza, W. V., Lund-Katz, S., Johnson, W. J., Rothblat, G. H., and Phillips, M. C. (1995) *J. Biol. Chem.* **270**, 17106–17113
37. Bruce, C., and Tall, A. R. (1995) *Curr. Opin. Lipidol.* **6**, 306–311
38. Phillips, M. C., Johnson, W. J., and Rothblat, G. H. (1987) *Biochim. Biophys. Acta* **906**, 223–276
39. Jonas, A. (1991) *Biochim. Biophys. Acta* **1084**, 205–220
40. Glomset, J. A. (1968) *J. Lipid. Res.* **9**, 155–167
41. Fielding, P. E., and Fielding, C. J. (1995) *Biochemistry* **43**, 14285–14292

ELSEVIER

Atherosclerosis 119 (1996) 191 -202

atherosclerosis

Reconstituted high density lipoprotein reduces the capacity of oxidatively modified low density lipoprotein to accumulate cholesteryl esters in mouse peritoneal macrophages

Masakazu Sakai[a,b], Akira Miyazaki[a], Hideki Hakamata[a], Yoshiko Suginohara[a], Yu-Ichiro Sakamoto[a], Wataru Morikawa[c], Shozo Kobori[b], Motoaki Shichiri[b], Seikoh Horiuchi*[a]

[a]*Department of Biochemistry, Kumamoto University School of Medicine, Honjo 2-2-1, Kumamoto 860, Japan*
[b]*Department of Metabolic Medicine, Kumamoto University School of Medicine, Honjo 2-2-1, Kumamoto 860, Japan*
[c]*The Chemo-Sero-Therapeutic Research Institute, Kumamoto 860, Japan*

Received 26 January 1995; revision received 13 June 1995; accepted 29 June 1995

Abstract

Oxidized low density lipoprotein (ox-LDL) was incubated with discoidal complexes of apolipoprotein A-I (apo A-I) and dimyristoylphosphatidylcholine (DMPC) (DMPC/apo A-I) in a cell-free system and re-isolated on Sephacryl *S*-400 gel filtration chromatography. Analyses of re-isolated ox-LDL showed that apo A-I was transferred from DMPC/apo A-I to ox-LDL, which accounted for 10% of the total protein of ox-LDL. Re-isolated ox-LDL also showed a 2.2-fold increase in phospholipid and a 14% decrease in cholesterol content on an apo B basis. The electrophoretic mobility of re-isolated ox-LDL was markedly reduced almost to that of native LDL. Moreover, the amounts of re-isolated ox-LDL to be degraded by mouse peritoneal macrophages as well as the capacity of re-isolated ox-LDL to accumulate cholesteryl esters (CE) in these cells were markedly reduced (60% and 80% reduction, respectively), suggesting that the ligand activity of ox-LDL for the scavenger receptor was significantly reduced upon treatment with DMPC/apo A-I. Parallel incubation of ox-LDL with free apo A-I led to a similar incorporation of apo A-I into ox-LDL. However, it had no effects on the ligand activity of ox-LDL. Thus, it is likely that the reduction in the ligand activity of ox-LDL by DMPC/apo A-I is explained by the change in the lipid moiety (mainly phospholipid) of ox-LDL. Since discoidal high density lipoprotein (HDL) is known to occur in vivo, this phenomenon might explain one of the anti-atherogenic functions of HDL.

Keywords: Oxidized LDL; Macrophage scavenger receptor(s); Foam cell formation; Discoidal HDL; Phospholipid transfer

* Corresponding author. Tel.: 81-96-364-6940; Fax: 81-96-364-6940; E-mail: horiuchi@gpo.kumamoto-u.ac.jp.

SSDI 0021-9150(95)05646-E

1. Introduction

It is generally accepted that macrophage-derived foam cells play an essential role in progression of the early stage of atherosclerosis [1,2]. Through the scavenger receptor pathway macrophages are known to take up chemically modified low density lipoproteins (modified LDLs), such as acetylated LDL (acetyl-LDL), malondialdehyde-modified LDL and oxidized LDL (ox-LDL) and become foam cells in vitro [2]. Among these modified LDLs, ox-LDL is emphasized to be a likely candidate for an atherogenic lipoprotein in vivo because its presence in human atherosclerotic plaques has been demonstrated [3,4].

In contrast to LDL, high density lipoprotein (HDL) is regarded as an anti-atherogenic lipoprotein from epidemiological evidence that the incidence of cardiovascular disease is inversely correlated with plasma HDL levels [5]. HDL is thought to play a major role in 'reverse cholesterol transport,' the transport of cholesterol from peripheral tissues back to the liver [5,6], and its anti-atherogenic property is mainly explained by a capacity to enhance cholesterol efflux from peripheral cells to HDL particles. Recent studies disclosed that Cu^{2+}-mediated oxidation of LDL in vitro is protected effectively by the presence of HDL [7–9]. Thus, in addition to enhancement of cholesterol efflux from cells [10–12], a possibility arose that HDL might protect macrophages from foam cell formation by inhibiting production of atherogenic lipoprotein in situ. In this connection, we recently made an interesting observation that acetyl-LDL-induced cholesteryl ester (CE) accumulation was inhibited almost completely by discoidal complexes of apolipoprotein A-I (apo A-I) and dimyristoylphosphatidylcholine (DMPC) (DMPC/apo A-I) [13]. Our subsequent study revealed that the interaction of DMPC/apo A-I with acetyl-LDL resulted in a significant transfer of phospholipid from DMPC/apo A-I to acetyl-LDL. As a result of the change which occurred to the lipid moiety of acetyl-LDL, the net negative charge of acetyl-LDL particles was significantly reduced, so that the ligand activity for the macrophage scavenger receptor was reduced [13]. These results obtained by acetyl-LDL suggest the possibility that atherogenic lipoproteins, even after production in vivo, might become less atherogenic by the interaction with an in vivo counterpart of DMPC/apo A-I, if it is available in situ.

In the present study, we tested whether DMPC/apo A-I similarly affected the ligand activity of ox-LDL for the scavenger receptors. The results revealed that DMPC/apo A-I interacted with ox-LDL and reduced its ligand activity as well as its cholesterol content, whereas HDL did not have such effects. The reduction in the ligand activity might be explained by the changes in lipid moiety of ox-LDL, mainly by the transfer of DMPC from DMPC/apo A-I. Since the interstitial fluids are known to contain discoidal HDL particles composed mainly of apo A-I and phospholipids with negligible amounts of free cholesterol (FC) or CE [14], and these particles share many physico-chemical properties in common with DMPC/apo A-I, it seems reasonable to hypothesize that discoidal HDL particles would weaken the atherogenicity of ox-LDL in vivo.

2. Materials and methods

2.1. Materials

Tissue culture media and reagents were obtained from Life Technologies, Inc. Horse radish peroxidase, cholesteryl ester hydrolase and *p*-hydroxyl phenyl acetic acid were from Wako Chemical Co. Cholesterol oxidase from Nocardia was purchased from Boeringer. Silica gel on aluminum sheets for thin layer chromatography (TLC) was obtained from Merck. [^{125}I]-Na (17 Ci/mg) and [9,10-^{3}H]oleate (4 Ci/mmol) were purchased from Amersham.

2.2. Lipoproteins and their modifications

LDL ($d = 1.019–1.063$) and HDL ($d = 1.063–1.21$) were isolated by sequential ultracentrifugation from fresh human plasma and dialyzed against 0.15 M NaCl and 1 mM ethylenediamine tetraacetic acid (EDTA) (pH 7.4). Traces of apo B and E were removed from HDL preparation by a heparin-agarose column [15]. Acetyl-LDL [16]

and ox-LDL [11] were prepared as described. Ox-LDL was iodinated with [^{125}I] by the method of McFarlane [17]. Protein concentrations were determined by BCA protein assay reagent (Pierce) [10]. Apo A-I concentrations were determined by the single radial immunodiffusion method (Daiichi Pure Chemical Co., Ltd.). HDL was delipidated for purification of apo A-I as described [18].

2.3. Preparation of discoidal complexes of apo A-I and DMPC (DMPC/apo A-I)

Complexes of apo A-I and DMPC were prepared by the method of Jonas [19], except that the solution buffer of apo A-I was replaced by 0.15 M NaCl and 1 mM EDTA (pH 7.4). For a standard preparation, 15 mg DMPC was sonicated in 1.0 ml of 0.15 M NaCl and 1 mM EDTA (pH 7.4) to form small unilamellar vesicles. One ml of the same buffer containing 10 mg of apo A-I was added to this solution and the mixture was equilibrated for 6 h at 25°C with gentle mixing on a vortex mixer. The final concentrations of DMPC and apo A-I were 7.5 mg/ml and 5.0 mg/ml respectively, with the molar ratio of DMPC to apo A-I being 62:1. Upon Sephacryl *S*-400 gel filtration chromatography DMPC/apo A-I thus prepared was eluted as a single peak when monitored with both absorbance at 280 nm and phospholipid determination (phospholipid test B/Wako). Electron microscopic examination showed the presence of discoidal structures about 30 Å thick and 100 Å in diameter (data not shown) [20].

2.4. Cells

Peritoneal macrophages were collected from non-stimulated male DDY mice (25–30 g) with 8 ml of ice-cold phosphate buffered saline (PBS) centrifuged at 200 × *g* for 5 min and suspended in Dulbecco's modified Eagle's medium (DMEM) containing 3% bovine serum albumin (BSA), streptomycin (0.1 mg/ml) and penicillin (100 units/ml) (medium A) [11].

2.5. Endocytic degradation and cell-association of [^{125}I]-ox-LDL

Mouse macrophages (2 × 10^6 cells) in 1.0 ml of medium A were seeded to each plastic culture dish (22 mm diameter, Corning) and incubated for 1 h at 37°C in 5% CO_2. The monolayers thus formed were washed 3 times with 1.0 ml of medium A. Each well was incubated with [^{125}I]-ox-LDL for 18 h at 37°C in the absence or presence of the unlabeled ligands to be tested. Endocytic degradation was determined by trichloroacetic acid (TCA)-soluble radioactivity in the medium as follows: To 0.75 ml of cultured medium, 0.25 ml of 40% TCA was added to a final concentration of 10%. After 30 min incubation at 4°C, 0.2 ml of 0.7 M $AgNO_3$ was added to precipitate free iodine [21]. The mixture was centrifuged and the radioactivity of the supernatant was counted. Cells were solubilized with 1.0 ml of 0.1 N NaOH and the cell-associated radioactivity was determined.

2.6. Assay for cholesterol esterification

Macrophage monolayers formed as above were incubated with ox-LDL for 18 h in the presence of 0.1 mM [^{3}H]oleate conjugated with BSA [22]. Cellular lipids were extracted for determination of radioactivity of cholesteryl[^{3}H]oleate as described previously [23].

2.7. Incubation of ox-LDL with DMPC/apo A-I and re-isolation of ox-LDL and DMPC/apo A-I

To characterize the interaction of ox-LDL with DMPC/apo A-I in a cell-free system, ox-LDL (5 mg protein/ml) was incubated at 37°C for 18 h with DMPC/apo A-I (5 mg protein/ml) in 2 ml of 0.15 M NaCl and 1 mM EDTA (pH 7.4). The incubation mixture was applied to a column of Sephacryl *S*-400 (1.5 × 100 cm, Pharmacia) and eluted with 0.15 M NaCl and 1 mM EDTA (pH 7.4) at a flow rate of 10 ml/h. A control incubation was performed with the same protein concentration of HDL instead of DMPC/apo A-I. Electron microscopic examination revealed that ox-LDL re-isolated after exposure to DMPC/apo A-I was indistinguishable in size and shape from control ox-LDL.

2.8. Lipid analysis

Lipid contents of lipoproteins were determined on a Hitachi 7450 automatic analyzer using standard enzymatic methods [24–26]. The lipid perox-

idation products in ox-LDL were determined by measuring conjugated dienes which were detected by absorbance at 234 nm after its lipid extraction [27].

2.9. Mass determination of cellular cholesterol

Both cellular FC and CE mass were quantified by a modification of the enzymatic fluorometric method of Heider and Boyett [28]. Enzyme mixtures were identical to theirs except that the Carbowax-6000 was replaced by 0.01% Triton X-100 and enzyme concentrations used were 2 times higher (cholesterol oxidase 0.16 U/ml; cholesteryl ester hydrolase, 0.16 U/ml) [29].

3. Results

3.1. Physico-chemical changes of ox-LDL after exposure to DMPC/apo A-I

Our previous report demonstrated that the interaction of acetyl-LDL with DMPC/apo A-I weakened the ligand activity of acetyl-LDL for the scavenger receptor [13]. To elucidate whether DMPC/apo A-I could also reduce the ligand activity of ox-LDL, we first examined physico-chemical changes of ox-LDL after 18 h incubation with DMPC/apo A-I in a cell-free system. When the mixture was subjected to Sephacryl S-400 gel filtration chromatography, ox-LDL in the first peak was separated from DMPC/apo A-I in the second peak (Fig. 1A). Immunological quantitation of apo A-I showed that a significant amount of apo A-I was detected in re-isolated ox-LDL (around 10% of total protein), suggesting that apo A-I was transferred from DMPC/apo A-I to ox-LDL. In a control experiment, ox-LDL was incubated with HDL instead of DMPC/apo A-I and re-isolated on the same column (Fig. 1B). However, the transfer of apo A-I from HDL to ox-LDL was not observed. To further examine the possibility that fragmented peptides of apo B-100 might be transferred in a reverse direction from ox-LDL to DMPC/apo A-I, [^{125}I]-ox-LDL was incubated with DMPC/apo A-I and re-isolated by the same column. As shown in Fig. 1A (inset), the radioactivity was detected in ox-LDL fractions but not in DMPC/apo A-I fractions, indicating that the transfer of apo B-100 fragments to DMPC/apo A-I particles did not occur.

Since apo B of LDL is known to undergo fragmentation during oxidative modification, ox-LDL did not show any visible bands on sodium dodecyl sulphate polyacrylamide gel electrophoresis (SDS-PAGE) under reducing conditions (Fig. 2A, lane c). Ox-LDL re-isolated after exposure to DMPC/apo A-I, however, was found to contain a discrete apo A-I band, suggesting that apo A-I was transferred from DMPC/apo A-I to ox-LDL (Fig. 2A, lane d). Exposure of ox-LDL to HDL did not induce any similar transfer of apo A-I (Fig. 2A, lane e).

Oxidation of LDL is well known to induce an increase in its net negative charge, a characteristic property of modified LDL which is important for recognition by the scavenger receptor [1,2]. We

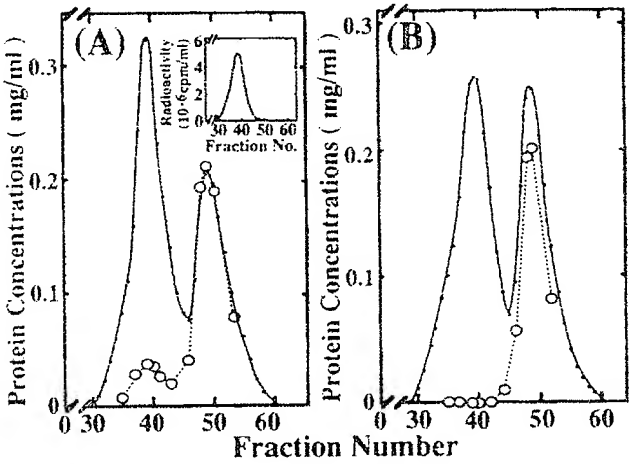

Fig. 1. Separation of ox-LDL from DMPC/apo A-I on Sephacryl S-400 gel filtration chromatography after incubation in a cell-free system. (A) Ox-LDL (5 mg protein/ml) was incubated with DMPC/apo A-I (5 mg protein/ml) at 37°C for 18 h in 2 ml of 0.15 M NaCl and 1 mM EDTA (pH 7.4). The mixture was applied to Sephacryl S-400 gel filtration chromatography and eluted with the same buffer. The concentrations of total protein (■) and apo A-I (○) were determined as described under 'Materials and methods.' (A inset) An experiment was performed under identical conditions except that ox-LDL was replaced by [^{125}I]-ox-LDL; the radioactivity was monitored. (B) Ox-LDL (5 mg protein/ml) was incubated with HDL (5 mg protein/ml) at 37°C for 18 h in 2 ml of 0.15 M NaCl and 1 mM EDTA (pH 7.4) and separated with the same column. The experimental conditions were identical to those of (A).

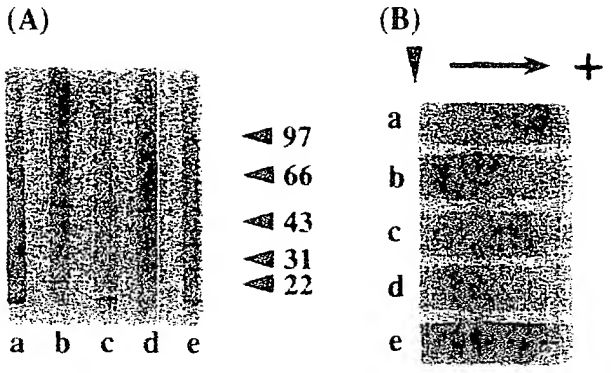

Fig. 2. SDS-PAGE (A) and agarose gel electrophoresis (B) of ox-LDL re-isolated after cell-free incubation with DMPC/apo A-I. (A) Lipoproteins were electrophoresed (5 μg protein/lane) on an SDS-polyacrylamide gradient gel (4%–20%) using 1% 2-mercaptoethanol as the reducing agent and stained with Coomassie Brilliant Blue. Molecular mass (arrowheads) is indicated in kDa. Lane a, DMPC/apo A-I; lane b LDL; lane c, ox-LDL; lane d, ox-LDL re-isolated after incubation with DMPC/apo A-I; lane e, ox-LDL re-isolated after incubation with HDL. (B) Lipoproteins were electrophoresed (5 μg protein/lane) on an agarose gel and stained with Coomassie Brilliant Blue. lane a, HDL; lane b, LDL; lane c, ox-LDL; lane d, ox-LDL re-isolated after incubation with DMPC/apo A-I; lane e, ox-LDL re-isolated after incubation with HDL.

therefore determined the net charge of ox-LDL re-isolated after exposure to DMPC/apo A-I. As shown in Fig. 2B, oxidation of LDL resulted in a marked increase in its electrophoretic mobility (lane c). While ox-LDL re-isolated after exposure to HDL showed almost the same electrophoretic mobility as control ox-LDL (lane e), ox-LDL re-isolated after exposure to DMPC/apo A-I showed a significant decrease in its electrophoretic mobility (lane d), suggesting that interaction with DMPC/apo A-I would decrease a net negative charge of ox-LDL.

Lipid analyses of ox-LDL re-isolated after exposure to DMPC/apo A-I showed a 2.2-fold increase in phospholipid and a 14% decrease in cholesterol on an apo B basis (or a 2.0-fold increase in phospholipid and a 22% decrease in cholesterol on a total protein basis) (Table 1). The corresponding decrease in phospholipid and the increase in cholesterol were observed in re-isolated DMPC/apo A-I (Table 1). A control incubation of ox-LDL with HDL, however, did not lead to a significant change in lipid contents of these particles (Table 1).

Upon oxidation of LDL with 5 μM $CuSO_4$, the level of conjugated dienes which were determined as lipid peroxidation products increased from the basal level to 135 nmol/mg protein. This level was decreased to 95 nmol/mg protein and 114 nmol/mg protein after interaction with DMPC/apo A-I and HDL, respectively. These results suggested, therefore, that lipid peroxidation products might also, in part, be transferred from ox-LDL to DMPC/apo A-I or HDL by lipid exchange reaction.

3.2. Changes in the biological properties of ox-LDL after exposure to DMPC/apo A-I

We next examined the CE accumulation capacity of ox-LDL which was re-isolated after incubation with DMPC/apo A-I. As shown in Fig. 3A, ox-LDL without any treatment was able to induce dose-dependent CE accumulation in macrophages. Ox-LDL re-isolated after exposure to HDL showed the same effect. In sharp contrast, CE accumulation by ox-LDL which was re-iso-

Table 1
Lipid contents of ox-LDL re-isolated after cell-free incubation with DMPC/apo A-I or HDL

Lipoproteins	TC	FC	CE	TG	PL
	(Lipid/protein weight ratio)				
Ox-LDL	1.46	0.49	0.97	0.33	1.02
Ox-LDL exposed to	1.15	0.30	0.85	0.18	2.01
DMPC/apo A-I	(1.27	0.33	0.94	0.20	2.20)
Ox-LDL exposed to HDL	1.42	0.42	1.00	0.29	0.95
DMPC/apo A-I	0	0	0	1.62	
DMPC/apo A-I exposed to ox-LDL	0.09	0.06	0.03	0.02	0.54
HDL	0.38	0.09	0.29	0.10	0.55
HDL exposed to ox-LDL	0.39	0.10	0.29	0.11	0.56

Ox-LDL (5 mg protein/ml) was incubated at 37°C for 18 h with DMPC/apo A-I (5 mg protein/ml) or HDL (5 mg protein/ml) in 2 ml of 0.15 M NaCl and 1 mM EDTA (pH 7.4). The mixtures were re-isolated in a Sephacryl S-400 gel filtration column (see Fig. 1) and lipid contents were determined. TC, total cholesterol; FC, free cholesterol; CE, cholesteryl esters; TG triglycerides; PL, phospholipids. Experimental errors in lipid determination were within 5%. Lipid/apo B weight ratios are shown in parentheses.

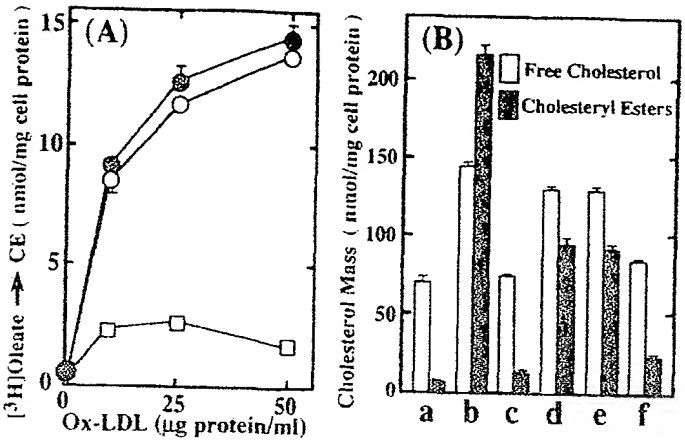

Fig. 3. CE accumulation capacity of re-isolated ox-LDL determined by [^{3}H]oleate incorporation into CE (A) and cholesterol mass (B). (A) Adhered macrophages (2 × 10^6) were incubated at 37°C for 18 h with 0.1 mM [^{3}H]oleate and the indicated protein concentrations of ox-LDL (●), ox-LDL re-isolated after exposure to HDL (○) or ox-LDL re-isolated after exposure to DMPC/apo A-I (□). Cellular lipids were extracted for determination of radioactivity of cholesteryl[^{3}H]oleate as described under 'Materials and methods.' (B) Adhered macrophages (2 × 10^6) were incubated at 37°C for 18 h with each of lipoproteins (50 μg protein/ml): a, without lipoproteins (non-loaded control); b, acetyl-LDL; c, LDL; d, ox-LDL; e, ox-LDL re-isolated after exposure to HDL; f, ox-LDL re-isolated after exposure to DMPC/apo A-I. Cellular lipids were extracted for mass determination of CE, FC as described under 'Materials and methods.'

lated after exposure to DMPC/apo A-I was markedly decreased to 20% that of control ox-LDL. Determination of cellular cholesterol mass (Fig. 3B) also showed that upon exposure to DMPC/apo A-I the capacity of ox-LDL for CE accumulation was reduced from 95.0 nmol/mg cell protein to 24.5 nmol/mg cell protein.

The ligand activity of ox-LDL exposed to DMPC/apo A-I was expected to decrease in parallel with a decrease in its CE accumulation capacity. To test this, [^{125}I]-ox-LDL was incubated with DMPC/apo A-I and re-isolated with the gel filtration column (Fig. 1A, inset). Endocytic degradation and cell-association of re-isolated [^{125}I]-ox-LDL were compared with those of the control [^{125}I]-ox-LDL treated similarly except for exposure to DMPC/apo A-I. As shown in Fig. 4A, degradation of re-isolated [^{125}I]-ox-LDL was significantly decreased when compared with that of control. A similar reduction was observed with cell-association of ox-LDL (Fig. 4B). These results indicated that a marked decrease in ligand activity occurred to ox-LDL after interaction with DMPC/apo A-I.

3.3. Effects of apo A-I incorporation on physico-chemical and biological properties of ox-LDL

To examine whether apo A-I alone could induce a similar alteration in the ligand activity of ox-LDL, ox-LDL was incubated with free apo A-I and re-isolated by gel filtration chromatography (data not shown). Re-isolated ox-LDL was found to contain a significant amount of apo A-I (~10% of protein of ox-LDL fractions) to the extent similar to ox-LDL re-isolated after incubation with DMPC/apo A-I (Fig. 1A). However, its electrophoretic mobility on agarose gel electrophoresis did not differ from control ox-LDL (data not shown). As shown in Table 2, incubation of ox-LDL with apo A-I induced a 10% decrease in each lipid (on a total protein basis), which would largely be explained by incorporation of apo A-I. We then determined the capacity of re-isolated ox-LDL for CE accumulation in macrophages. As shown in Table 3, ox-LDL re-isolated after exposure to apo A-I was indistinguishable from the control ox-LDL in its CE accumulation capacity. Moreover, the capacity of ox-LDL to be degraded by macrophages did not decrease, even after incubation with free apo A-I

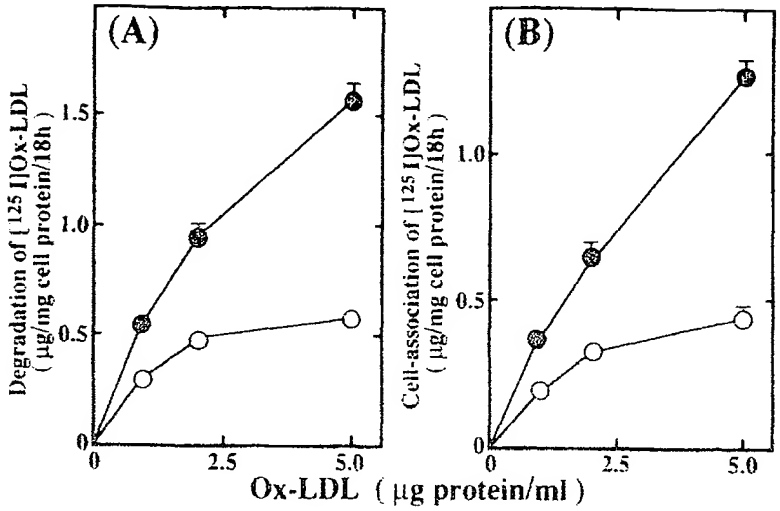

Fig. 4. Endocytic degradation and cell-association of [^{125}I]-ox-LDL re-isolated after cell-free incubation with DMPC/apo A-I. [^{125}I]-ox-LDL (5 mg protein/ml) was incubated at 37°C for 18 h with DMPC/apo A-I (5 mg protein/ml) in 2 ml of 0.15 M NaCl and 1 mM EDTA (pH 7.4) and re-isolated on a Sephacryl *S*-400 gel filtration column. Adhered macrophages (2×10^6) were incubated at 37°C for 18 h with the indicated protein concentrations of [^{125}I]-ox-LDL (●) or re-isolated [^{125}I]-ox-LDL exposed to DMPC/apo A-I (○). TCA-soluble radioactivity (A) and cell-associated radioactivity (B) were determined as described under 'Materials and methods.'

(data not shown). These results suggested that apo A-I alone did not affect the ligand activity of ox-LDL for the scavenger receptor(s).

3.4. Effect of DMPC/apo A-I on endocytic degradation and cell-association of [^{125}I]-ox-LDL

To elucidate whether DMPC/apo A-I could interact with ox-LDL in the cell-culture medium, effects of DMPC/apo A-I on endocytic degradation and cell-association of [^{125}I]-ox-LDL were examined. As shown in Fig. 5A, degradation of [^{125}I]-ox-LDL was competed for by unlabeled ox-LDL whereas neither unlabeled HDL, LDL nor apo A-I had any effect. In sharp contrast to HDL, unlabeled DMPC/apo A-I markedly suppressed degradation of [^{125}I]-ox-LDL. The extent of inhibition exceeded that of ox-LDL itself. A similar inhibitory pattern was also observed in cell-association of [^{125}I]-ox-LDL (Fig. 5B). These results suggested that DMPC/apo A-I might interact in the cell-culture medium with ox-LDL, leading to a decrease in the CE accumulation capacity of ox-LDL.

4. Discussion

In the previous report, we demonstrated that the interaction of DMPC/apo A-I with acetyl-LDL resulted in a marked reduction in its ligand activity for the macrophage scavenger receptor [13]. The present study was undertaken to obtain a pathophysiological implication(s) of this phenomenon by using ox-LDL instead of acetyl-LDL as a more likely atherogenic lipoprotein in vivo. The results make it clear that the interaction of ox-LDL with DMPC/apo A-I reduced the CE accumulation capacity of ox-LDL by reducing its cholesterol content as well as its ligand activity.

It has been suggested that ox-LDL is recognized by several types of receptors. They include (i) the scavenger receptor (type I and type II) cloned by Kodama et al. [30], (ii) the Fc receptor [31], (iii)

Table 2
Lipid contents of ox-LDL re-isolated after cell-free incubation with apo A-I

Lipoproteins	TC	FC	CE	TG	PL
	(Lipid/protein weight ratio)				
Ox-LDL	1.37	0.36	1.01	0.32	0.92
Ox-LDL exposed	1.23	0.33	0.90	0.29	0.81
to apo A-I	(1.35	0.36	0.99	0.32	0.89)

Ox-LDL (5 mg protein/ml) was incubated at 37°C for 18 h with apo A-I (20 mg protein/ml) in 2 ml of 0.15 M NaCl and 1 mM EDTA (pH 7.4). Ox-LDL, apo A-I were re-isolated on a Sephacryl S-400 gel filtration column and lipid contents were determined. TC, total cholesterol; FC, free cholesterol; CE, cholesteryl esters; TG, triglycerides; PL, phospholipids. Experimental errors in the lipid determination were within 5%. Lipid/apo B weight ratios are shown in parentheses.

CD 36 [32] demonstrated by Stanton and Endemann et al., and (iv) SR-BI, a CD 36-related molecule that was recently cloned by Acton et al. [33]. Moreover, the presence of other types of scavenger receptors has also been suggested. In mouse peritoneal macrophages, Sparrow et al. [34] and Arai et al. [35] proposed the presence of a scavenger receptor specific for ox-LDL but not for acetyl-LDL. Van Berkel et al. [36,37] identified a 95 kDa protein as a putative ox-LDL receptor in rat Kupffer cells. Melkko et al. [38] showed that the endocytic uptake of *N*-terminal peptides of procollagen by rat liver endothelial cells might be mediated by the receptor which was partially competed for by acetyl-LDL. All these results strongly suggest that there may be multiple receptors that recognize ox-LDL. It is unclear, however, which receptor(s) plays a dominant role(s) in the endocytic uptake of ox-LDL.

Table 3
Capacity for CE-accumulation in mouse macrophages of ox-LDL after exposure to free apo A-I

Sample (μg protein/ml)		[^{3}H]oleate → cholesteryl[^{3}H]oleate (nmol/mg cell protein)
Nonloaded		0.3 ± 0.1
Ox-LDL	5	4.4 ± 0.2
	10	6.5 ± 0.4
Ox-LDL exposed to	5	4.1 ± 0.5
free apo A-I	10	6.2 ± 0.6

Adhered macrophages (2×10^6) were incubated at 37°C for 18 h with 0.1 mM [^{3}H]oleate and the indicated protein concentrations of ox-LDL or ox-LDL re-isolated after incubation with apo A-I. Cellular lipids were extracted and the radioactivity of cholesteryl[^{3}H]oleate was determined as described under 'Materials and methods'. Values are the mean ± S.D. ($n = 4$)

The mechanism by which the net negative charge and ligand activity of ox-LDL were significantly reduced after exposure to DMPC/apo A-I is not known. Several studies have demonstrated that modification of lipid moieties of lipoproteins could induce a conformational change in apolipoproteins that secondarily affected the ligand activity: (i) upon conversion of very low density lipoprotein (VLDL) to LDL by triglyceride hydrolysis, conformation of apo B was altered and the affinity for the LDL receptor was increased [39,40], (ii) treatment of LDL with lipoprotein lipase or hepatic lipase [41] resulted in an increase in binding to the LDL receptor, (iii) treatment of LDL with sphingomyelinase [42] also enhanced its binding to the receptor, (iv) treatment of LDL with cholesterol esterase, on the contrary, reduced its ligand activity for the receptor [43], and (v) treatment of LDL with phospholipase A2 also reduced its ligand activity [44].

The interaction between ox-LDL and DMPC/apo A-I is mainly characterized by transfer of a large amount of DMPC, as well as a relatively small amount of apo A-I from DMPC/apo A-I to ox-LDL, with a minor transfer of other lipids in a reverse direction (Table 1). When ox-LDL was incubated with free apo A-I apo, A-I incorporation was also observed (data not shown). However, it had no effect on the ligand activity of ox-LDL as well as its CE accumulation capacity (Table 3), indicating that alteration of the lipid moiety rather than protein moiety would be responsible for the reduction in the ligand activity of ox-LDL after exposure to DMPC/apo A-I. If one can take into consideration the interaction of acetyl-LDL with DMPC/apo A-I [13], it seems reasonable to expect that DMPC incorporation into ox-LDL might also play a critical role in this phenomenon. To confirm this notion, several trials were made to characterize the interaction of ox-LDL with DMPC liposomes. However,

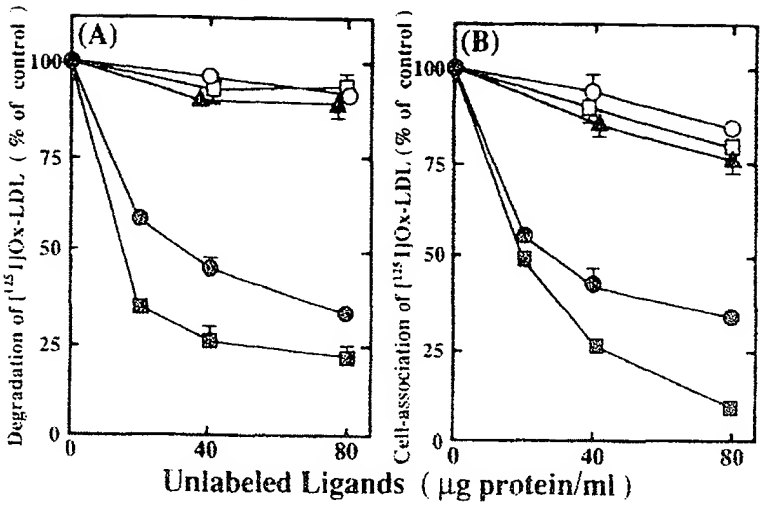

Fig. 5. Effect of DMPC/apo A-I on endocytic degradation and cell-association of [^{125}I]-ox-LDL. Adhered macrophages (2×10^6) were incubated at 37°C for 18 h with 4 μg protein/ml of [^{125}I]-ox-LDL in the absence or presence of the indicated protein concentrations of LDL (○), ox-LDL (●), HDL (□), DMPC/apo A-I (■) or free apo A-I (▲). TCA-soluble radioactivity in the medium (A) and cell-associated radioactivity (B) were determined as described under 'Materials and methods.' The 100% values of endocytic degradation (A) and cell-association (B) were 2.61 and 1.71 μg/18 h/mg cell protein, respectively.

since almost all the ox-LDL particles became insoluble aggregates upon incubation with DMPC liposome, the re-isolation and subsequent characterization of re-isolated ox-LDL was unsuccessful.

Phospholipids of reconstituted HDL were reported to be readily transferred to LDL [45,46] and HDL [47]. In the present study, when ox-LDL was incubated with DMPC/apo A-I, we observed the transfer of DMPC from DMPC/apo A-I to ox-LDL (Table 1). However, when ox-LDL was incubated with HDL instead of DMPC/apo A-I, the net transfer of phospholipid did not occur (Table 1). It is likely, therefore, that phospholipids are more tightly associated with HDL particles when compared with those in DMPC/apo A-I. Lipid-lipid interactions between phospholipids and core lipids of HDL might inhibit phospholipid transfer from HDL to ox-LDL.

In general, apo A-I is preferentially incorporated into HDL but not into LDL when incubated with plasma. This was explained by the difference in conditions of surface lipids of lipoproteins [48,49]. In contrast to LDL or acetyl-LDL [13] incubation of ox-LDL with DMPC/apo A-I resulted in incorporation of a significant amount of apo A-I into ox-LDL (Figs. 1A and 2A). This must reflect a difference in the surface lipid conditions between LDL (or acetyl-LDL) and ox-LDL. Upon oxidation, part of phosphatidylcholine and free cholesterol of LDL particles are converted to lysophosphatidylcholine and oxidized sterols, thus making the surface of ox-LDL particles much more susceptible to incorporation of apo A-I. Other examples supporting this notion are available. The surface perturbation of LDL particles with vortexing [50] or phospholipase C treatment [51] is known to induce aggregation of LDL particles. The presence of apo A-I during these treatments, however, could effectively protect LDL from aggregation because apo A-I was incorporated into LDL [50,51]. In the present study, aggregation occurred to ox-LDL when incubated with DMPC liposomes (data not shown), whereas such a thing did not occur when incubated with DMPC/apo A-I. Therefore during the interaction between ox-LDL and DMPC/apo A-I, apo A-I may have a role in preventing ox-LDL from aggregation.

Although the present results obtained from in vitro experiments clearly demonstrate a significant reduction in CE accumulation capacity of ox-LDL when treated with DMPC/apo A-I, it is not clear yet whether the CE accumulation capacity of ox-LDL would indeed be affected by an in vivo

counterpart of DMPC/apo A-I. A discoidal HDL particle is a likely candidate for a natural counterpart of DMPC/apo A-I. It was reported that interstitial fluid [14] and culture media obtained from human hepatoma cells (HepG2) [52] contain 'nascent HDL' which is composed of apo A-I and phospholipids with a negligible amount of CE and FC. In addition to the secretion of 'nascent HDL' from hepatocytes, other pathways for formation of discoidal HDL particles have also been proposed [53,54]. Thus, it is possible to speculate that discoidal HDL particles present in situ might reduce the CE accumulation capacity of ox-LDL. If this speculation is the case, this phenomenon may count for a major function of HDL as an anti-atherogenic lipoprotein.

Acknowledgments

We are grateful to Dr. Shin-Ichiro Nishimura and Dr. Takanori Takiue at the Chemo-Sero-Therapeutic Research Institute Kumamoto, Japan, for their collaborative endeavor throughout the study. This work was supported in part by a Grant-in-Aids for Scientific Research (No. 07770108) from the Ministry of Education, Science and Cultures of Japan.

References

[1] Ross R. The pathogenesis of atherosclerosis: a perspective for the 1990s. Nature 1993;362:801.
[2] Steinberg D, Parthasarathy S, Carew TE, Khoo JC Witztum JL. Beyond cholesterol. Modifications of low density lipoprotein that increase its atherogenicity. N Engl J Med 1989;320:915.
[3] Palinski W, Rosenfeld ME, Ylä-Herttuala S, Gurtner GC Socher SS, Butler SW, Parthasarathy S, Carew TE, Steinberg D. Low density lipoprotein undergoes oxidative modification in vivo. Proc Natl Acad Sci USA 1989;86:1372.
[4] Ylä-Herttuala S, Palinski W, Rosenfeld ME Parthasarathy S, Carew TE, Butler S, Witztum JL, Steinberg D. Evidence for the presence of oxidatively modified low density lipoprotein in atherosclerotic lesions of rabbit and man. J Clin Invest 1989;84:1086.
[5] Gordon DJ, Rifkind BM. High density lipoprotein: the clinical implications of recent studies. N Engl J Med 1989;321:1311.
[6] Johnson WJ, Mahlberg FH, Rothblat GH, Phillips MC. Cholesterol transport between cells and high density lipoproteins. Biochim Biophys Acta 1991;1085:273.
[7] Ohta T, Takata K, Horiuchi S, Morino Y, Matsuda I. Protective effect of lipoproteins containing apoprotein A-I on Cu^{2+}-catalyzed oxidation of human low density lipoprotein. FEBS Lett 1989;257:435.
[8] Parthasarathy S, Barnett J, Fong LG. High density lipoprotein inhibits the oxidative modification of low density lipoprotein. Biochim Biophys Acta 1990;1044:275.
[9] Kunitake ST, Jarvis MR, Hamilton RL, Kane JP. Binding of transition metals by apolipoprotein A-I-containing plasma lipoproteins: Inhibition of oxidation of low density lipoprotein. Proc Natl Acad Sci USA 1992;89:6993.
[10] Miyazaki A, Rahim ATMA, Ohta T, Morino Y, Horiuchi S. High density lipoprotein mediates selective reduction in cholesteryl esters from macrophage foam cells. Biochim Biophys Acta 1992;1126:73.
[11] Sakai M, Miyazaki A, Sakamoto Y, Shichiri M, Horiuchi S. Cross-linking of apolipoprotein is involved in a loss of the ligand activity of high density lipoprotein upon Cu^{2+}-mediated oxidation. FEBS Lett 1992;314:199.
[12] Ohta T, Nakamura R, Ikeda Y, Shinohara M, Miyazaki A Horiuchi S, Matsuda I. Differential effect of subspecies of lipoproteins containing apolipoprotein A-I on cholesterol efflux from cholesterol-loaded macrophages: Functional correlation with lecithin:cholesterol acyltransferase. Biochim Biophys Acta 1992;1165:119.
[13] Miyazaki A, Sakai M, Suginohara Y, Hakamata H Sakamoto Y, Morikawa W, Horiuchi S. Acetylated low density lipoprotein reduces its ligand activity for the scavenger receptor after interaction with reconstituted high density lipoprotein. J Biol Chem 1994;269:5264.
[14] Sloop CH, Dory L, Roheim PS. Interstitial fluid lipoproteins. J Lipid Res 1987;28:225.
[15] Murakami M, Horiuchi S, Takata K, Morino Y. Distinction in the mode of receptor-mediated endocytosis between high density lipoprotein and acetylated high density lipoprotein: evidence for high density lipoprotein receptor-mediated cholesterol transfer. J Biochem (Tokyo) 1987;101:729.
[16] Shinohara M, Miyazaki A, Shichiri M, Horiuchi S. Exposure of rat peritoneal macrophages to acetylated low density lipoprotein results in release of plasma membrane cholesterol: an efficient substrate for esterification by acyl-CoA:cholesterol acyltransferase. J Biol Chem 1992;267:1603.
[17] McFarlane AS. Efficient trace-labeling of proteins with iodine. Nature 1958;182:53.
[18] Brewer HB, Roman R, Meng M, Bishop C. Isolation and characterization of apolipoproteins A-I, A-II, and A-IV. Methods Enzymol 1986;128:223.
[19] Jonas A. Reconstitution of high density lipoproteins. Methods Enzymol 1986;128:553.
[20] Forte TM, Nordhausen RW. Electron microscopy of negatively stained lipoprotein. Methods Enzymol 1986;128:442.
[21] Hakamata H, Miyazaki A, Sakai M, Sakamoto Y-I, Matsuda H, Kihara K, Horiuchi S. Differential effects of an acyl-coenzyme A: cholesterol acyltransferase inhibitor

on HDL-mediated cholesterol efflux from rat macropgage foam cells. FEBS Lett 1995;363:29.
[22] Goldstein JL, Basu SK, Brown MS. Receptor-mediated endocytosis of low density lipoprotein in cultured cells. Methods Enzymol 1983;98:241.
[23] Miyazaki A, Rahim ATMA, Araki S, Morino Y, Horiuchi S. Chemical cross-linking alters high density lipoprotein to be recognized by a scavenger receptor in rat peritoneal macrophages. Biochim Biophys Acta 1991;1082:143.
[24] Allain CC, Poon LS, Chan CSG, Richmond W, Fu PC. Enzymatic determination of total serum cholesterol. Clin Chem 1973;20:470.
[25] Spayd RW, Bruschi B, Burdick BA, Dappen GM, Eikenberry JN, Esders TW, Figueras TW, Goodhue CT, LaRossa DD, Nelson RW Rand RN, Wu TW. Multilayer film elements for clinical analysis: applications to representative chemical determinations. Clin Chem 1978;24:1343.
[26] Takayama M, Itoh S, Nagasaki T, Tanimizu I. A new enzymatic method for determination of serum choline-containing phospholipids. Clin Chim Acta 1977;79:93.
[27] Buege JA, Aust SD. Microsomal lipid peroxidation. Methods Enzymol 1978;52:302.
[28] Heider JG, Boyett RL. The picomol determination of free and total cholesterol. J Lipid Res 1978;19:514.
[29] Miyazaki A, Sakai M, Yamaguchi E, Sakamoto Y, Shichiri M, Horiuchi S. Two independent macrophage receptors for acetylated high density lipoprotein. Biochim Biophys Acta 1993;1170:143.
[30] Kodama T, Freeman M, Rohrer L, Zabrecky J, Matsudaira P, Krieger M. Type I macrophage scavenger receptor contains α-helical collagen-like coiled coils. Nature 1990;343:531.
[31] Stanton LW, White RT, Bryant CM, Protter AA, Endemann G. A macrophage Fc receptor for IgG is also a receptor for oxidized low density lipoprotein. J Biol Chem 1992;267:22446.
[32] Endemann G, Stanton LW, Madden KS, Bryant CM, White RT, Protter AA. CD36 is a receptor for oxidized low density lipoprotein. J Biol Chem 1993;268:11811.
[33] Acton SL, Scherer PE, Lodish HF, Krieger M. Expression cloning of SR-BI, a CD36-related class B scavenger receptor. J Biol Chem 1994;269:21003.
[34] Sparrow CP, Parthasarathy S, Steinberg D. A macrophage receptor that recognizes oxidized low density lipoprotein but not acetylated low density lipoprotein. J Biol Chem 1989;264:2599.
[35] Arai H, Kita T, Yokode M, Narumiya S, Kawai C. Multiple receptors for modified low density lipoproteins in mouse peritoneal macrophages: different uptake mechanisms for acetylated and oxidized low density lipoproteins. Biochem Biophys Res Commun 1989;159:1375.
[36] Van Berkel TJC, De Rijke YB, Kruijt JK. Different fate in vivo of oxidatively modified low density lipoprotein and acetylated low density lipoprotein in rats: recognition by various scavenger receptors on Kupffer and endothelial liver cells. J Biol Chem 1991;266:2282.
[37] De Rijke YB, Van Berkel TJC. Rat liver Kupffer and endothelial cells express different binding proteins for modified low density lipoproteins: Kupffer cells express 95 kDa membrane protein as a specific binding site for oxidized low density lipoproteins. J Biol Chem 1994;269:824.
[38] Melkko J, Hellevik T, Risteli L, Risteli J, Smedsrød B. Clearance of NH_2-terminal propeptides of type I III procollagen is a physiological function of the scavenger receptor in liver endothelial cells. J Exp Med 1994;179:405.
[39] Chen GC, Zhu S, Hardman DA, Schilling JW, Lau K, Kane JP. Structural domains of human apolipoprotein B-100: differential accessibility to limited proteolysis of B-100 in low density and very low density lipoprotein. J Biol Chem 1989;264:14369.
[40] Chen GC, Lau K, Hamilton RL, Kane JP. Differences in local conformation in human apolipoprotein B-100 of plasma low density and very low density lipoprotein as identified by cathepsin D. J Biol Chem 1991;266:12581.
[41] Aviram M, Bierman EL, Chait A. Modification of low density lipoprotein by lipoprotein lipase or hepatic lipase induces enhanced uptake and cholesterol accumulation in cells. J Biol Chem 1988;263:15416.
[42] Gupta AK, Rudney H. Sphingomyelinase treatment of low density lipoprotein and cultured cells results in enhanced processing of LDL which can be modulated by sphingomyelin. J Lipid Res 1992;33:1741.
[43] Aviram M, Keidar S, Rosenblat M, Brook GJ. Reduced uptake of cholesterol esterase-modified low density lipoprotein by macrophages. J Biol Chem 1991;266:11567.
[44] Kleinman Y, Krul ES, Burnes M, Aronson W, Pfleger B Schonfeld G. Lipolysis of LDL with phospholipase A2 alters the expression of selected apo B-100 epitopes and the interaction of LDL with cells. J Lipid Res 1988;29:729.
[45] Jonas A, Kézdy KE, Williams MI, Rye K-A. Lipid transfers between reconstituted high density lipoprotein complexes and low density lipoproteins: effects of plasma protein factors. J Lipid Res 1988;29:1349.
[46] Jonas A, Bottum K, Kézdy KE. Transformation of reconstituted high density lipoprotein subclasses as a function of temperature or LDL concentration. Biochim Biophys Acta 1991;1085:71.
[47] Nichols AV, Gong EL, Blanche PJ, Forte TM. Interaction of human plasma high density lipoprotein HDL_{2b} with discoidal complexes of dimyristoylphosphatidylcholine and apolipoprotein A-I. Biochim Biophys Acta 1980;617:480.
[48] Ibdah JA, Phillips MC. Effects of lipid composition and packing on the adsorption of apolipoprotein A-I to lipid monolayers. Biochemistry 1988;27:7155.
[49] Ibdah JA, Lund-Katz S, Phillips MC. Molecular packing of high density and low density lipoprotein surface lipids and apolipoprotein A-I binding. Biochemistry 1989;28:1126.

[50] Khoo JC, Miller E, McLoughlin P, Steinberg D. Prevention of low density lipoprotein aggregation by high density lipoprotein or apolipoprotein A-I. J Lipid Res 1990;31:645.

[51] Liu H, Scrba DG, Ryan RO. Prevention of phospholipase-C induced aggregation of low density lipoprotein by amphipathic apolipoproteins. FEBS Lett 1993;316:27.

[52] McCall MR, Forte TM, Shore VG. Heterogeneity of nascent high density lipoproteins secreted by the hepatoma-derived cell line HepG2. J Lipid Res 1988;29:1127.

[53] Hara H, Yokoyama S. Interaction of free apolipoproteins with macrophages: formation of high density lipoprotein-like lipoproteins and reduction of cellular cholesterol. J Biol Chem 1991;266:3080.

[54] Musliner TA, Long MD, Forte TM, Nichols AV, Gong EL Blanche PJ, Krauss RM. Dissociation of high density lipoprotein precursors from apolipoprotein B-containing lipoproteins in the presence of unesterified fatty acids and a source of apolipoprotein A-I. J Lipid Res 1991;32:917.

Biochemical Pharmacology, Vol. 52, pp. 113–121, 1996.

ISSN 0006-2952/96/$15.00 + 0.00
PII S0006-2952(96)00170-0

Specific Targeting of a Lipophilic Prodrug of Iododeoxyuridine to Parenchymal Liver Cells Using Lactosylated Reconstituted High Density Lipoprotein Particles

Martin K. Bijsterbosch, Hendrika van de Bilt and Theo J. C. van Berkel*

Division of Biopharmaceutics, Leiden/Amsterdam Center for Drug Research, University of Leiden, P.O. Box 9503, 2300 RA Leiden, The Netherlands

ABSTRACT. We recently reported the conversion of the water-soluble antiviral drug iododeoxyuridine (IDU) into the lipophilic prodrug dioleoyl-iododeoxyuridine (IDU-Ol_2). The prodrug was incorporated into reconstituted high-density lipoprotein (NeoHDL) particles with physical and biological properties similar to those of native HDL. We also found, in initial experiments, that lactosylation of the prodrug-loaded NeoHDL increases its liver uptake. Because this offers the attractive perspective of using these particles for the delivery of drugs to the liver, we now analyze the characteristics and biological fate of lactosylated IDU-Ol_2-loaded NeoHDL. The particles (containing approximately 25 prodrug molecules) have the same size and charge as native HDL, indicating that lactosylation does not cause aggregation or oxidative modification. At 10 min after intravenous injection of lactosylated [^{3}H]IDU-Ol_2-loaded NeoHDL into rats, only 13.5 ± 2.8% of the dose was left in plasma and 75.9 ± 2.4% of the dose was recovered in the liver. The relative specific uptake by the liver was 1–2 orders of magnitude higher than that of any other tissue. The hepatic uptake of lactosylated [^{3}H]IDU-Ol_2-loaded NeoHDL was much higher than that of free [^{3}H]IDU (<20% of the dose). Both parenchymal liver cells and Kupffer cells express galactose-specific receptors. By isolating liver cells after injection of the prodrug-loaded particles, it was established that hepatic uptake occurred mainly (for 84.4 ± 3.8%) in parenchymal liver cells. Preinjection with asialofetuin substantially reduced the liver uptake of lactosylated [^{3}H]IDU-Ol_2-loaded NeoHDL, which points to uptake by the asialoglycoprotein receptor. Subcellular fractionation of the liver indicated that lactosylated [^{3}H]IDU-Ol_2-loaded NeoHDL does not merely associate to cells, but is internalized and delivered to the lysosomes. In conclusion, we show that IDU can be specifically targeted to the parenchymal liver cell. Conversion of the water-soluble parent drug into a lipophilic prodrug that is incorporated into a lactosylated reconstituted HDL particle, is an approach that may also be used to deliver other water-soluble drugs to the parenchymal liver cells. This may lead to more effective therapy for liver diseases such as hepatitis B. BIOCHEM PHARMACOL 52;1: 113–121, 1996.

KEY WORDS. asialoglycoprotein receptor; selective drug delivery; hepatitis B; antivirals; parenchymal liver cells; reconstituted lipoproteins

The selective delivery of a drug to its specific cellular target increases its therapeutic effectiveness and reduces undesired interactions with nontarget tissues [1, 2]. Drugs may be delivered to target cells by associating the drug to a carrier that is recognized by receptors present on the surface of these cells. If these receptors are only present on the target cells, highly specific delivery of the drug can be achieved.

In the liver, both Kupffer and parenchymal cells have receptors on their plasma membranes that specifically bind and internalize ligands with terminal D-galactose residues. The receptor on parenchymal cells is the classic asialoglycoprotein receptor [3, 4]. Kupffer cells express a receptor that binds galactose-exposing particles larger than 12 nm [5, 6]. This receptor (also referred to as the galactose-particle receptor) is different from the receptor on the parenchymal cells and is probably identical to a well-characterized receptor that also recognizes fucose [7, 8]. Because galactose-specific receptors show only a high expression on Kupffer and parenchymal liver cells, they are attractive targets for the delivery of drugs to these cells.

We showed previously that lipoproteins can be specifically targeted to the galactose-specific hepatic receptors [9, 10]. Lactosylation of the apoprotein moiety of HDL† induced rapid and highly specific uptake by the galactose receptor on parenchymal liver cells [10]. Lactosylation of

* Corresponding author. Tel. (071)-527 6038; FAX (071)-527 6032.

† *Abbreviations:* IDU, 5-iodo-2′-deoxyuridine; IDU-OL_2, 3′,5′-dioleoyl-5-iodo-2′-deoxyuridine; HDL, high-density lipoprotein; LDL, low-density lipoprotein; NeoHDL, HDL-like lipid particles.

receptors on Kupffer cells [9]. The different intrahepatic distributions of lactosylated LDL and lactosylated HDL can probably be ascribed to differences in the sizes of the particles [6]. Lipoproteins are attractive potential drug carriers [11–14]. They are spherical particles consisting of a core of apolar lipids surrounded by a phospholid monolayer, in which cholesterol and apoproteins are embedded. Highly lipophilic drugs can be incorporated into the apolar core and, thus, be transported, hidden inside the particles [11–14]. As drug carriers, lactosylated lipoproteins have advantages over galactose-exposing soluble molecules such as (neo)glycoproteins and lactosylated poly-L-lysine [15–17]. A (pro)drug incorporated into the lipid moiety of lactosylated lipoproteins is protected from the environment during transport in the circulation. Further, (pro)drugs incorporated in the lipid moiety are not likely to interfere with the receptor-mediated recognition of the lactose residues on the apoproteins.

A possible limitation for the use of lipoproteins as drug carriers may be their limited availability. We recently investigated the possibility of synthesizing lipoprotein-like lipid particles from commercially available lipids and isolated apoproteins. We succeeded in preparing particles with properties very similar to the naturally occurring human HDL [18]. More recently, we further investigated the potential use of reconstituted HDL particles, denoted NeoHDL, as drug carriers. We used the antiviral/antineoplastic drug IDU [19, 20] as model compound. IDU is not sufficiently lipophilic for incorporation into (neo)lipoproteins. We, therefore, synthesized the lipophilic prodrug IDU-Ol_2 (Fig. 1). The oleoyl residues were attached to IDU *via* an ester linkage [21]. Because esterases are ubiquitous, this type of linkage ensures release of the original, pharmacologically active drug at the site of delivery [22]. IDU-Ol_2 incorporated readily into NeoHDL, and the physical and biological properties of the prodrug-loaded particles were very similar to those of native HDL [21]. We also found, in initial studies, that lactosylation induced an increased liver association of the prodrug-loaded particles. This finding offers the attractive perspective of utilizing these particles as hepatotrophic carriers for lipophilic (pro)drugs. To further evaluate the feasibility of utilizing the particles as drug carriers, we analyzed in detail the physicochemical characteristics and biological fate of lactosylated IDU-Ol_2-loaded NeoHDL particles. We determined the tissue distribution of the prodrug-loaded particles to evaluate the specificity of liver uptake (i.e., to exclude major nonspecific uptake by extrahepatic tissues). In the liver, we identified the specific cell types and subcellular compartments involved in uptake, as well as the mechanism of hepatic uptake.

MATERIALS AND METHODS

Reagents

$Na^{125}I$ (carrier-free) was from Amersham International, Amersham, Bucks, U.K. [^{3}H]IDU-Ol_2 was synthesized as described earlier [21]. Cholesteryl oleate was obtained from

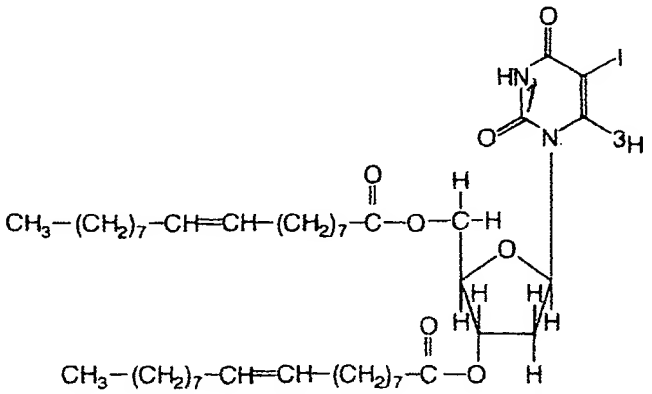

FIG. 1. 3′-5′-dioleoyl-5-iodo-2′-deoxyuridine (IDU-Ol_2).

Janssen (Beerse, Belgium). Egg yolk phosphatidyl choline was from Fluka (Buchs, Switzerland). Cholesterol and bovine serum albumin (fraction V) were obtained from Sigma (St. Louis, MO, U.S.A.). Lactose was supplied by Merck (Darmstadt, Germany). Sodium cyanoborohydride was from Aldrich (Brussels, Belgium). Emulsifier Safe™ and Hionic Fluor™ scintillation cocktails and Soluene-350 were from Packard (Downers Grove, IL, U.S.A.). Asialofetuin was prepared as described in detail earlier [10]. All other reagents were of analytical grade.

Preparation of Lactosylated [^{3}H]IDU-Ol_2-Loaded NeoHDL

HDL-like lipid particles (NeoHDL) were prepared as described in detail earlier [21]. In brief, 3.6 mg of phosphatidyl choline, 0.9 mg of cholesterol, 1.8 mg of cholesteryl oleate, and 0.9 mg of [^{3}H]IDU-Ol_2 (specific radioactivity 5.5 mCi/nmol), dispersed in sonication buffer (10 mM Tris-HCl buffer, pH 8.0, containing 0.1 M KCl, 1 mM EDTA, and 0.025% NaN_3), were sonicated for 60 min at 49–52°C. Then, the temperature was lowered to 42–44°C. Sonication was continued, and 20 mg of HDL apoproteins, dissolved in 4 M urea, were added in small portions over a period of 10 min. After a further 20 min, the sonication was stopped and large particles were removed by centrifugation. The [^{3}H]IDU-Ol_2-loaded NeoHDL particles were purified by density gradient centrifugation and by FPLC using a Superose-6 column. The purified [^{3}H]IDU-Ol_2-loaded NeoHDL was subsequently lactosylated by incubating the particles (1.0 mg of protein/mL in 0.1 M sodium phosphate buffer, pH 7.0, containing 1 mM EDTA) under sterile conditions at 37°C with lactose and sodium cyanoborohydride to final concentrations of 100 mg/mL and 50 mg/mL, respectively. After 60 hr, the reaction was stopped by the addition of 0.2 volume of 0.6 M NH_4HCO_3. The lactosylated particles were exhaustively dialyzed against phosphate-buffered saline (10 mM sodium phosphate buffer, pH 7.4, containing 0.15 M NaCl and 1 mM EDTA). Experiments with native HDL indicate that, under these conditions, apoprotein AI is the main apoprotein lactosylated.

Preparation of Radioiodinated Lactosylated [^{3}H]IDU-Ol$_2$-Loaded NeoHDL

[^{3}H]IDU-Ol$_2$-loaded NeoHDL, prepared as described in the previous section, was labeled with ^{125}I using iodine monochloride as described earlier [10]. The resulting double-labeled preparation, which contained approximately equal amounts of ^{125}I and ^{3}H, was subsequently lactosylated as described above.

Chemical Characterization of Lactosylated [^{3}H]IDU-Ol$_2$-loaded NeoHDL

The chemical composition of lactosylated [^{3}H]IDU-Ol$_2$-loaded NeoHDL was determined as follows. Protein was measured by the method of Lowry *et al.* [23], using bovine serum albumin as a standard. The amount of lactose was determined by the Anthrone assay [24]. Cholesterol and cholesteryl oleate were determined by an enzymatic method, as described earlier [25]. Phosphatidyl choline was assayed using a colorometric test kit provided by Boehringer Mannheim (Mannheim, Germany). The amount of [^{3}H]IDU-Ol$_2$ was determined by measuring radioactivity.

Determination of Plasma Clearance and Tissue Distribution

Male Wistar rats, weighing between 225 and 325 gram, were used. The animals were anesthesized by intraperitoneal injection of 15–20 mg of sodium pentobarbital, and the abdomen was opened. Radiolabeled prodrug-loaded lactosylated NeoHDL was injected *via* the vena penis. At the indicated times, blood samples of 0.2–0.3 mL were taken from the inferior vena cava and collected in heparinized tubes. The samples were centrifuged for 2 min at 16,000 × g, and the plasma assayed for radioactivity. The total amount of radioactivity in plasma was calculated using the equation: plasma volume (mL) = [0.0219 × body weight (g)] + 2.66 [9]. At the indicated times, liver lobules were tied off and excised and, at the end of the experiment, the remainder of the liver was removed. The amount of liver tissue tied off successively did not exceed 15% of the total liver mass. Radioactivity in the liver at each time point was calculated from the radioactivities and weights of the liver samples. Radioactivities in liver and other tissues were corrected for radioactivity in plasma present in the tissue at the time of sampling [26].

Determination of the Distribution Over Liver Cell Types

Rats were anesthesized and injected with radiolabeled prodrug-loaded lactosylated NeoHDL, as described above. The liver was perfused at 10 min after injection, and parenchymal, Kupffer, and endothelial cells were isolated from the liver as described in detail earlier [27]. Shortly before separation of the cells, a liver lobule was tied off and excised to determine the total liver uptake. The contributions of the various cell types were calculated from the radioactivities and weights of the liver samples. Radioactivities in liver and other tissues were corrected for radioactivity in plasma present in the tissue at the time of sampling [26].

Determination of the Distribution Over Liver Cell Types

Rats were anesthesized and injected with radiolabeled prodrug-loaded lactosylated NeoHDL, as described above. The liver was perfused at 10 min after injection, and parenchymal, Kupffer, and endothelial cells were isolated from the liver as described in detail earlier [27]. Shortly before separation of the cells, a liver lobule was tied off and excised to determine the total liver uptake. The contributions of the various cell types were calculated from the radioactivities and weights of the liver samples. Radioactivities in liver and other tissues were corrected for radioactivity in plasma present in the tissue at the time of sampling [26].

Subcellular Fractionation

Rats were anesthesized and injected with radiolabeled prodrug-loaded lactosylated NeoHDL, as described above. Twenty minutes later, the liver was perfused with ice-cold 0.25 M sucrose containing 10 mM Tris-HCl buffer, pH 7.4. Subsequently, the liver was divided into subcellular fractions as described previously [28]. In brief, the liver was dispersed in 2 volumes of sucrose/Tris-HCl (see above) using a homogenizer of the Potter-Elvehjem type. Fractions enriched in nuclei, mitochondria, lysosomes, and microsomes were obtained by collecting pellets obtained after subjecting the homogenate to consecutive centrifugation steps of 5 min at 1200 × g, 5 min at 9,000 × g, 15 min at 22,000 × g, and 30 min at 210,000 × g, respectively (g-forces in middle of tubes), with the final supernatant being the cytosol fraction. The fractions were assayed for radioactivity, protein, and the activity of marker enzymes as described in detail earlier [28].

Determination of Proteins

Protein concentrations in cell suspensions and subcellular fractions were determined by the method of Lowry *et al.* [23], with a bovine serum albumin standard.

Determination of Radioactivity

Samples containing ^{3}H were counted in a Packard Tri-Carb 1500 liquid scintillation counter, using Emulsifier Safe™ or Hionic Fluor™ scintillation cocktails. Gel slices were first digested with Soluene-350. Tissue samples were processed using a Packard 306 Sample Oxidizer. Some tissues (e.g., bone) were dissolved in 10 M NaOH at 95°C. In samples containing both ^{125}I and ^{3}H, the ^{125}I-radioactivity was counted in a Packard Auto-Gamma 5000 counter. The ^{3}H-radioactivity was subsequently measured as described above and corrected for the contribution of ^{125}I-radioactivity.

RESULT

Preparation and Characterization of Lactosylated [^{3}H]IDU-Ol$_2$-Loaded NeoHDL

Lactosylated NeoHDL particles, having incorporated the lipophilic prodrug [^{3}H]IDU-Ol$_2$ in the lipid moiety, were prepared as described earlier [21]. In short, phosphatidyl choline, cholesterol, cholesteryl oleate, [^{3}H]IDU-Ol$_2$ and HDL apoproteins were cosonicated. The resulting prodrug-

TABLE 1. Chemical composition of [^{3}H]IDU-Ol$_2$-loaded lactosylated NeoHDL

	% of total weight
Protein	49.3 ± 4.4
Phosphatidyl choline	20.8 ± 2.4
Cholesterol	2.5 ± 0.8
Cholesteryl oleate	7.5 ± 0.4
Lactose	15.7 ± 1.5
[^{3}H]IDU-Ol$_2$	4.2 ± 0.3

The chemical composition of [^{3}H]IDU-Ol$_2$-loaded lactosylated NeoHDL was analyzed as described in Materials and Methods. Values given are means ± SEM of 3 different preparations.

gation and FPLC. [^{3}H]IDU-Ol$_2$-loaded NeoHDL was subsequently provided with terminal D-galactosyl residues by incubation with lactose (D-galactosyl-D-glucose) and sodium cyanoborohydride. The latter reduces the Schiff's base formed between the glucose moiety of lactose and amino groups on NeoHDL, which results in covalent attachment of lactose to the apoproteins [29].

The chemical composition of lactosylated [^{3}H]IDU-Ol$_2$-loaded NeoHDL is given in Table 1. The formation of the prodrug-loaded particles was very reproducible; only small variations were found in the compositions of different preparations. The particles contained a substantial amount of IDU-Ol$_2$: 4.2 ± 0.3% of the total weight (12.2 ± 0.2% of the lipid moiety). From these data, it may be calculated that each particle contains approximately 25 IDU-Ol$_2$ molecules.

We showed, earlier, that the physical properties of [^{3}H]IDU-Ol$_2$-loaded NeoHDL are very similar to those of native HDL [21]. Because physical properties, such as size and electric charge, are crucial to the biological fate of a (modified) lipoprotein carrier [6, 14,.30], we investigated the effects of lactosylation on size and electric charge of [^{3}H]IDU-Ol$_2$-loaded NeoHDL. For these studies, the apoproteins of the particles were also labeled with ^{125}I. This permitted monitoring of both the incorporated ^{3}H-labeled prodrug and the ^{125}I-labeled apoproteins. Figure 2A shows the elution profile of lactosylated [^{3}H]IDU-Ol$_2$-loaded ^{125}I-NeoHDL on a calibrated Superose-6 column. Both ^{125}I and ^{3}H eluted at the same position as native HDL. This finding indicates that the size of the prodrug-loaded particles was similar to that of native HDL. Figure 2B shows the result of agarose gel electrophoresis of lactosylated [^{3}H]IDU-Ol$_2$-loaded ^{125}I-NeoHDL. Lipoproteins subjected to this type of electrophoresis are separated primarily according to their electric charge. The main peak, which migrated 2–4 cm from the origin, contained approximately 85% of the ^{125}I-radioactivity and about 95% of the ^{3}H-radioactivity. The remaining 15% of the ^{125}I-radioactivity migrated more

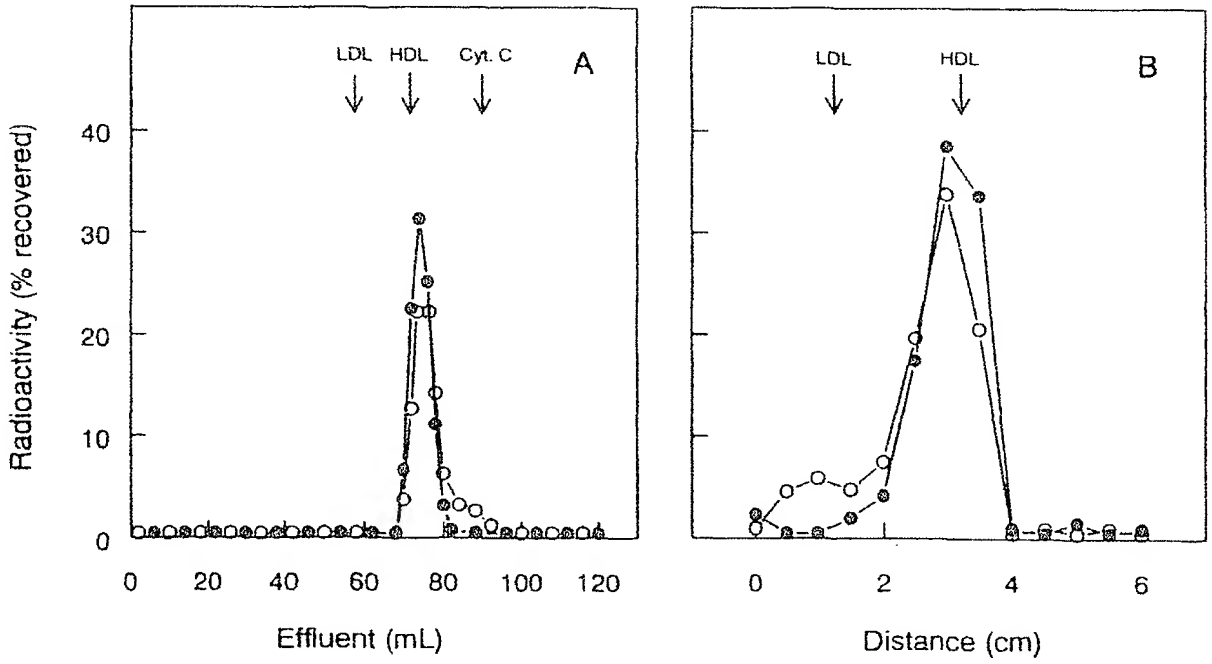

FIG. 2. Analysis of the physical properties of lactosylated [^{3}H]IDU-Ol$_2$-loaded ^{125}I-NeoHDL by gel permeation chromatography (A) and gel electrophoresis (B). A: Lactosylated [^{3}H]IDU-Ol$_2$-loaded ^{125}I-NeoHDL (0.10 mg of protein) was injected onto a Superose-6 FPLC column (60 x 1.8 cm). The column was eluted with 0.1 M sodium phosphate buffer, pH 7.0, containing 0.5 M NaCl and 10 mM EDTA (flow rate 6 mL/hr). Fractions of 2.0 mL were collected and assayed for ^{3}H (●) and ^{125}I (○). The results are expressed as % of the recovered radioactivity (recoveries > 75%). The elution volumes of LDL, HDL, and cytochrome C, which were used to calibrate the column, are indicated by arrows. B: Lactosylated [^{3}H]IDU-Ol$_2$-loaded ^{125}I-NeoHDL (5 μg of protein) was subjected to electrophoresis in a 0.75% (w/v) agarose gel at pH 8.8 (75 mM Tris-hippuric acid buffer). The gel was cut in slices that were assayed for ^{3}H (●) and ^{125}I (○). The radioactivity in each slice is given as % of the recovered radioactivity (recoveries > 101%). Arrows indicate the positions of LDL and HDL, respectively.

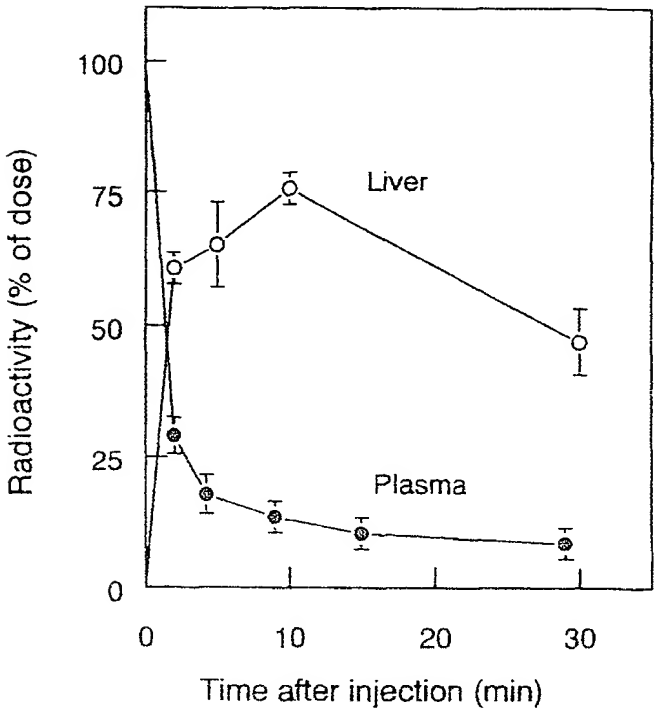

FIG. 3. Plasma clearance and liver association of lactosylated [^{3}H]IDU-Ol_2-loaded NeoHDL. Rats were intravenously injected with lactosylated [^{3}H]IDU-Ol_2-loaded NeoHDL (250 μg of protein/kg body weight). At the indicated times, the amounts of radioactivity in plasma (●) and liver (○) were determined. Values are means ± SEM of 3 rats.

slowly than the main peak, and probably represents iodinated apoproteins that had dissociated from the lactosylated NeoHDL particle. However, [^{3}H]IDU-Ol_2, which is the molecule of interest, is firmly associated with the main (NeoHDL) peak. Thus, the size and charge of lactosylated IDU-Ol_2-loaded NeoHDL are very similar to those of native HDL. Moreover, because ^{125}I and ^{3}H behaved similarly in the experiments, the results further indicate that, under the conditions employed, the particles are stable.

Plasma Clearance and Tissue Uptake of Lactosylated [^{3}H]IDU-Ol_2-loaded NeoHDL

To investigate the biological fate of lactosylated [^{3}H]IDU-Ol_2-loaded NeoHDL, rats were injected with the prodrug-loaded particles, and the plasma clearance and association of radioactivity to tissues were determined. Figure 3 shows that the injected radioactivity was very rapidly cleared from the bloodstream. At 10 min after injection, only 13.5 ± 2.8% of the dose was left in plasma. The decrease in plasma radioactivity coincided with an increase in hepatic radioactivity. At 10 min after injection, 75.9 ± 2.4% of the dose was recovered in the liver.

The results shown in Fig. 3 point to the liver playing a predominant role in the removal of lactosylated NeoHDL-associated IDU prodrug from the circulation. To investigate possible specific uptake by other organs and tissues, we determined the tissue distribution of lactosylated [^{3}H]IDU-Ol_2-loaded NeoHDL. The results are shown in Fig. 4, and are compared with the distribution of free [^{3}H]IDU. After injection of [^{3}H]IDU, the radioactivity distributed nonspecifically over the body. Most of the label was recovered in bulky tissues, such as muscles, skin, and bone, whereas the liver contained <20% of the dose. After injection of lactosylated [^{3}H]IDU-Ol_2-loaded NeoHDL, the relative specific radioactivity in the liver was found to be 1–2 orders of magnitude higher than that in any other tissue (excluding blood). Compared to the free drug, substantially lower amounts of IDU-Ol_2 were recovered in nonhepatic tissues. The ratio of liver uptake vs uptake by nonhepatic tissues (excluding blood) was 5.32 ± 0.57 after injection of the NeoHDL-associated prodrug, and 0.23 ± 0.01 after injection of the free drug.

Cellular and Subcellular Distribution of Lactosylated [^{3}H]IDU-Ol_2-Loaded NeoHDL in the Liver

In the liver, both Kupffer cells and parenchymal cells possess receptors that can bind and internalize galactose-containing ligands [3–6, 9, 10]. To identify the cell type(s) responsible for hepatic uptake, rats were injected with lactosylated [^{3}H]IDU-Ol_2-loaded NeoHDL, and parenchymal, Kupffer, and endothelial cells were isolated from the liver 10 min later. The cell isolation procedure was performed at a low temperature (8°C) to prevent processing of the internalized ligand. The results are shown in Table 2. The parenchymal cells were found to be the main site of uptake. These cells accounted for 84.4 ± 3.8% of total liver uptake, whereas Kupffer and endothelial cells contained much smaller amounts of radioactivity.

The mechanism of liver association of lactosylated [^{3}H]IDU-Ol_2-loaded NeoHDL was investigated by injecting rats with asialofetuin 1 min prior to injection of the prodrug-loaded particles. Asialofetuin specifically blocks uptake *via* the galactose-specific receptors on parenchymal liver cells [31]. Preinjection of the animals with asialofetuin (50 mg/kg body weight) inhibited the liver uptake of lactosylated [^{3}H]IDU-Ol_2-loaded NeoHDL considerably, and preinjection with the same dose of fetuin (which lacks terminal galactose residues) had no significant effect (Fig. 5). The reduction in hepatic uptake of radioactivity by asialofetuin was accompanied by a substantial increase in radioactivity in the blood plasma (not shown). These findings indicate that galactose-specific recognition sites in the liver are mainly responsible for uptake, and that [^{3}H]IDU-Ol_2 follows the fate of the lactosylated NeoHDL carrier. Because asialofetuin inhibits uptake by the asialoglycoprotein receptor, but not galactose-mediated uptake by Kupffer cells [31], this finding confirms the major role of parenchymal cells in the hepatic uptake of the prodrug-loaded lactosylated NeoHDL.

To investigate the intracellular processing of lactosylated

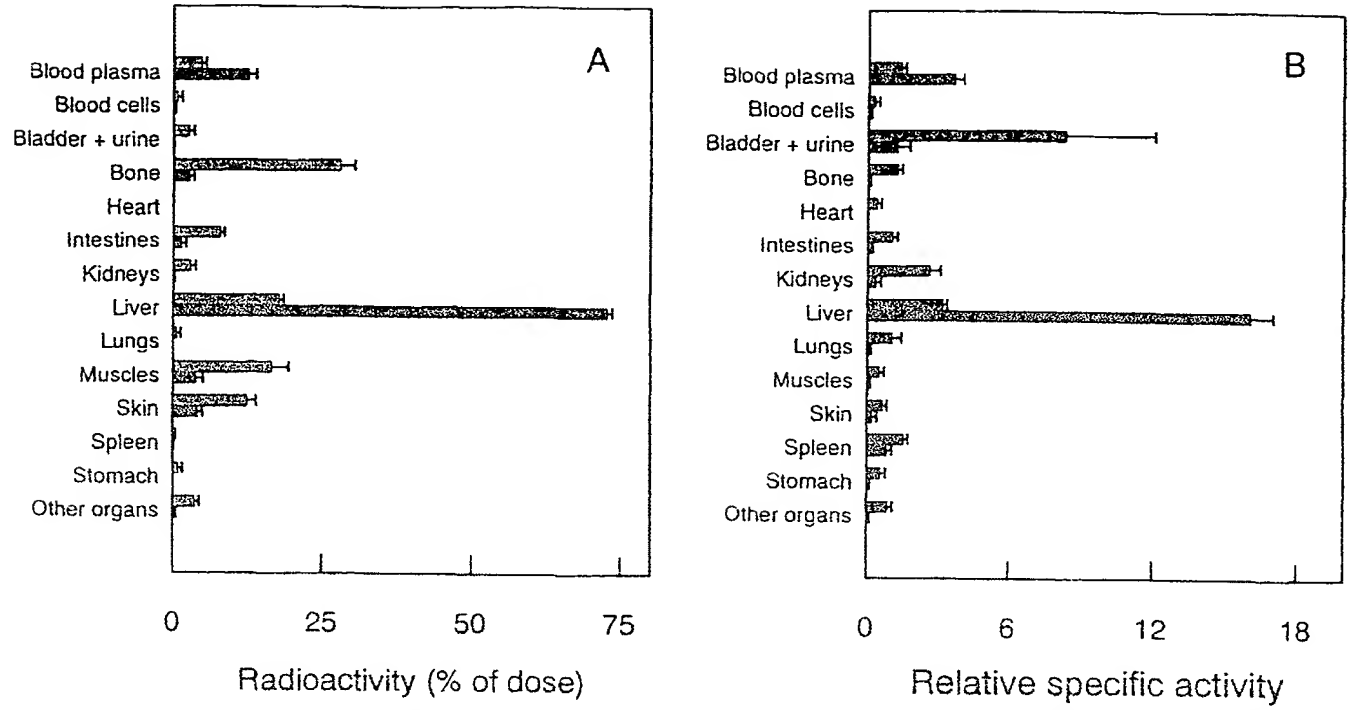

FIG. 4. **Tissue distribution of lactosylated [^{3}H]IDU-Ol$_2$-loaded NeoHDL and [^{3}H]IDU. Rats were intravenously injected with lactosylated [^{3}H]IDU-Ol$_2$-loaded NeoHDL at a dose of 250 μg of protein/kg body weight (filled bar) or with an equivalent amount of underivatized [^{3}H]IDU (shaded bar). At 10 min after injection, the radioactivities in the indicated tissues and organs were determined. The results are expressed as % of the recovered amount of radioactivity (A) and as relative specific activity (B; % of total recovered radioactivity divided by % of total recovered weight). Recoveries of radioactivity and tissues in rats injected with lactosylated [^{3}H]IDU-Ol$_2$-loaded NeoHDL were 98.9 ± 0.9% and 97.2 ± 1.3%, respectively. Recoveries of radioactivity and tissues in rats injected with [^{3}H]IDU were 72.8 ± 3.4% and 100.1 ± 0.1%, respectively. Values are means ± SEM of 3 rats.**

subcellular fractionation [28]. The distribution pattern of radioactivity showed the highest relative specific activity in the lysosomal fractions (Fig. 6). The lysosomal marker acid phosphatase also showed the highest relative specific activity in the lysosomal fraction, whereas the microsomal marker glucose-6-phosphatase had a clearly different distribution. This finding indicates that lactosylated [^{3}H]IDU-Ol$_2$-loaded NeoHDL does not merely associate with cells, but is internalized and transported to lysosomes.

DISCUSSION

We showed, recently, that the lipophilic prodrug IDU-Ol$_2$ can be efficiently incorporated into a reconstituted HDL particle (NeoHDL) with similar physicochemical properties to those of native HDL [21]. After intravenous injection into rats, the particles were relatively slowly cleared from the circulation, in a manner very similar to that of native HDL [21]. We also showed, in initial experiments, that lactosylation induced an increased liver association of the prodrug-loaded particles. In the present study, we further analyzed the characteristics and biological fate of IDU-Ol$_2$-loaded NeoHDL.

The lactosylated IDU-Ol$_2$-loaded NeoHDL particles contained a substantial amount of IDU-Ol$_2$: 4.2 ± 0.3% of the total weight, which corresponds to approximately 12% of the lipid moiety. Each particle may be calculated to contain approximately 25 IDU-Ol$_2$ molecules. Higher loads of the prodrug have not been tested, but may very well be possible. The physical properties of a lipoprotein carrier are crucial to its biological fate. Aggregation or introduction of negative charges (e.g., as a result of oxidative modification) will result in a rapid uptake by sinusoidal liver cells [14, 30]. Further, the size of a lactosylated lipoprotein particle largely determines its uptake by different liver cell types [6]. We, therefore, investigated the size and electric charge of the

TABLE 2. **Uptake of intravenously injected lactosylated [^{3}H]IDU-Ol$_2$-loaded NeoHDL by liver cell types**

Cell type	Uptake of lactosylated [^{3}H]IDU-Ol$_2$-loaded NeoHDL (% of total liver uptake)
Parenchymal cells	84.4 ± 3.4
Kupffer cells	10.6 ± 2.1
Endothelial cells	5.0 ± 2.3

Rats were injected with lactosylated [^{3}H]IDU-Ol$_2$-loaded NeoHDL at a dose of 250 μg of protein per kg body weight. Ten minutes later, parenchymal, endothelial, and Kupffer cells were isolated, and the association of radioactivity to each cell type was determined. Uptake by each cell type is expressed as the relative contribution to the total liver uptake. These values were calculated from the uptake per mg of cell protein and the contribution of each cell type to the total liver protein [27]. Values are means ± SEM of 3 rats.

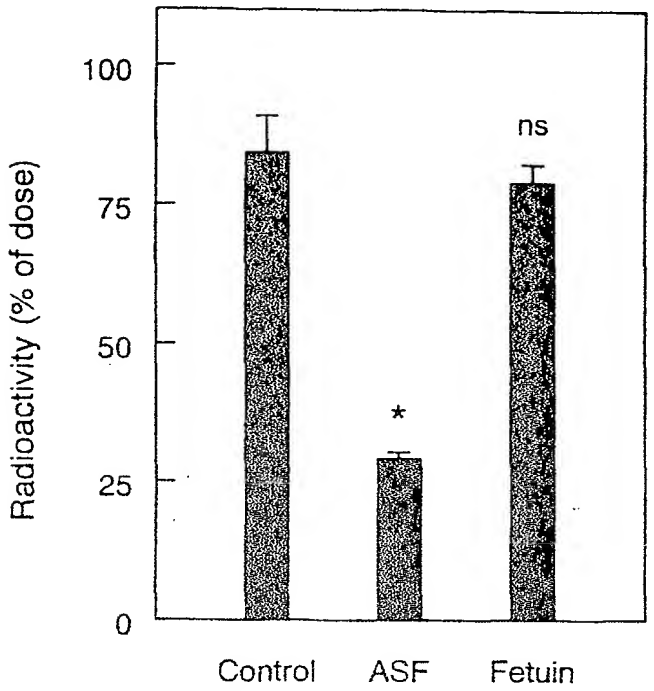

FIG. 5. Effect of asialofetuin and fetuin on the hepatic association of lactosylated [^{3}H]IDU-Ol$_2$-loaded NeoHDL. Rats were intravenously injected with lactosylated [^{3}H]IDU-Ol$_2$-loaded NeoHDL at a dose of 250 μg of protein/kg body weight. One min prior to injection, the animals received asialofetuin or fetuin, each at a dose of 50 mg/kg body weight. Controls were preinjected with solvent (phosphate-buffered saline). Ten min after injection, the radioactivity in the liver was determined. Differences with respect to the controls were tested for significance by Wilcoxon's two-sample test [37]. Values are means ± SEM of 3–4 rats. *$P < 0.05$; ns, not significant.

lactosylated prodrug-loaded NeoHDL particles. Analysis by gel permeation chromatography and agarose gel electrophoresis indicated that size and electric charge of the prodrug-loaded particles were very similar to those of native HDL. Thus, the particles were not aggregated or oxidatively modified, which reduces the risk of undesired uptake by sinusoidal liver cells. The [^{3}H]prodrug and [^{125}I]apoproteins of the particle behaved similarly in both assays, indicating that, under the conditions employed, the particles are stable. Further, the prodrug-loaded particles can be stored for at least 4 weeks at 4°C without noticeable effects on their physical properties or biological behavior.

Derivatization of IDU with oleic acid residues and subsequent incorporation of the prodrug into lactosylated NeoHDL drastically altered its biological fate. Underivatized IDU disappears very rapidly from the circulation after intravenous injection, and only a small proportion of the injected dose is recovered in the liver. The remainder was found to be evenly distributed over all tissues. IDU-Ol$_2$ incorporated into lactosylated NeoHDL also rapidly disappears from the circulation. In sharp contrast to the free drug, the cleared radioactivity was almost quantitatively recovered in the liver. The ratio of liver uptake vs uptake by prodrug was 5.32 ± 0.57, (i.e., 23 times higher than that of the free drug; 0.23 ± 0.01). Binding of lactosylated IDU-Ol$_2$-loaded NeoHDL to the galactose receptors is followed by internalization and transport to the lysosomal compartment.

In the liver, parenchymal cells are mainly responsible for uptake of lactosylated IDU-Ol$_2$-loaded NeoHDL. In cell separation experiments, it was found that parenchymal cells contained approximately 85% of the total hepatic radioactivity. Preinjection of rats with asialofetuin, a specific competitor for uptake by the galactose receptor on parenchymal liver cells, substantially reduced liver uptake of lactosylated IDU-Ol$_2$-loaded NeoHDL. Native fetuin, which has no terminal galactose residues, had no significant effect. These findings indicate that the galactose residues of the prodrug-loaded particle mediate its hepatic uptake. Kupffer cells also express a galactose-specific receptor different from the receptor on parenchymal cells [5–8]. Asialofetuin does not inhibit galactose-mediated uptake by Kupffer cells [31]. Our finding that asialofetuin inhibits the hepatic uptake of lactosylated IDU-Ol$_2$-loaded NeoHDL, thus, provides corroborative evidence for uptake of the particles by parenchymal cells. Uptake of galactose-terminated lipoproteins by the two different hepatic galactose receptors depends on the spatial arrangement of the galactose residues on the particles, as well as on their size [6, 32–34]. The receptor on Kupffer cells can only bind and internalize galactose-terminated particles larger than 12 nm [6]. Lactosylated IDU-Ol$_2$-loaded NeoHDL eluted from the Superose-6 FPLC-column at the same position as native HDL (approx. 10 nm), which indicates that the prodrug-loaded particles are probably small enough to avoid substantial uptake by the galactose receptor on Kupffer cells.

Binding of lactosylated IDU-Ol$_2$-loaded NeoHDL to the galactose receptors is followed by internalization and transport to the lysosomal compartment, where the particles are processed. The oleoyl residues in IDU-Ol$_2$ are attached to IDU *via* an ester bond. This esterase-sensitive linkage was chosen to ensure release of the original, pharmacologically active drug at the site of delivery. The lysosomes contain a wide variety of hydrolytic enzymes, including esterases [35]. Upon *in vitro* incubation of lactosylated IDU-Ol$_2$-loaded NeoHDL with a lysosomal extract, IDU-Ol$_2$ was successively converted in the monoester and free IDU (M. K. Bijsterbosch, unpublished). It is anticipated that *in vivo* IDU-Ol$_2$-loaded lactosylated NeoHDL is similarly processed after it is internalized and delivered to the lysosomal compartment. Nucleosides such as IDU can easily pass through lysosomal membranes [36]. Thus, after processing of IDU-Ol$_2$ to IDU, the pharmacologically active IDU can become available to exert its action inside the cell.

Using lactosylated NeoHDL as carrier to target lipophilic prodrugs to the galactose receptor on parenchymal liver cells affords a number of advantages over previously published carrier systems, such as (neo)glycoproteins and lac-

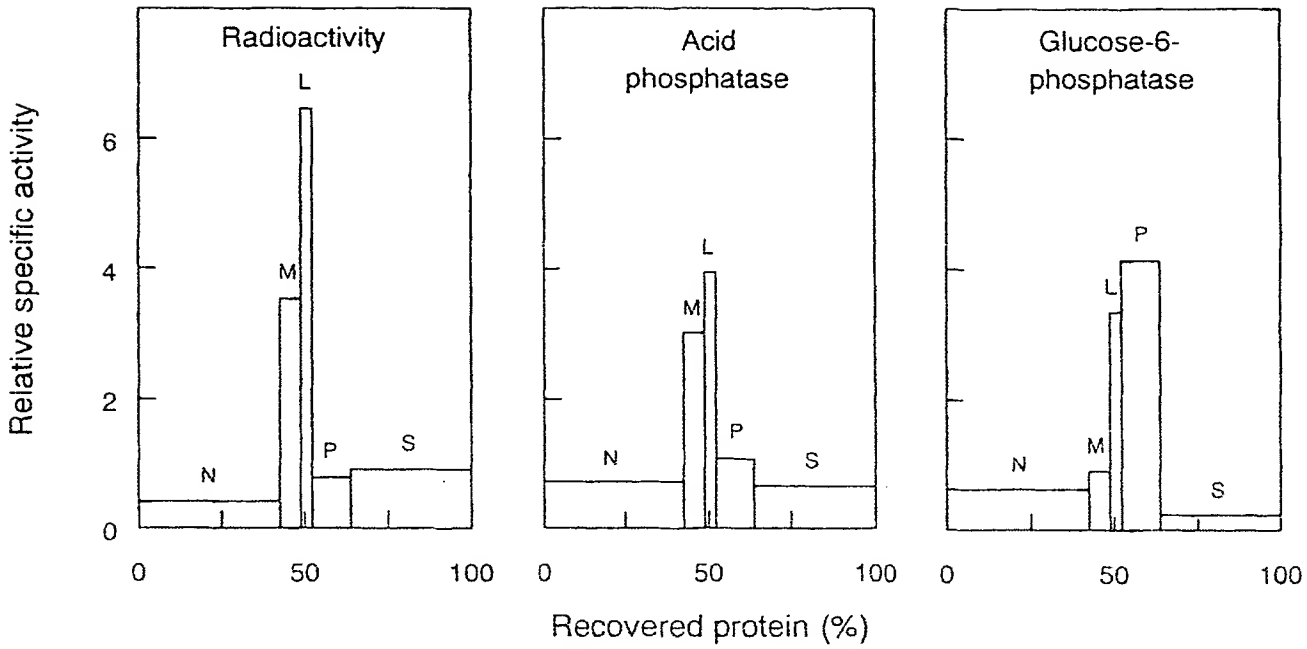

FIG. 6. Distribution patterns of radioactivity and marker enzymes over subcellular fractions of the liver after injection of lactosylated [^{3}H]IDU-Ol$_2$-loaded NeoHDL. Rats were injected with lactosylated [^{3}H]IDU-Ol$_2$-loaded NeoHDL (250 μg of protein per kg body weight). Twenty min after injection, the liver was perfused with ice-cold 0.25 M sucrose, containing 10 mM Tris-HCl buffer, pH 7.5, and divided into subcellular fractions by differential centrifugation, as described earlier [28]. The fractions were assayed for radioactivity, protein, and the activity of marker enzymes [28]; recoveries were >91%. Blocks from left to right represent: nuclear (N), mitochondrial (M), lysosomal (L), microsomal (P), and supernatant (cytosol: S) fractions. The relative protein concentration is given on the abscissa. The ordinate represents the relative specific activity (% of total recovered activity divided by % of total recovered protein).

culation, the lipophilic prodrug is hidden in the lipid moiety (probably the apolar core) and, thus, protected from the biological environment. Furthermore, as the lipophilic prodrugs are incorporated into the lipid moiety, high drug loads are possible without interfering with the receptor-mediated recognition of the lactose residues present on the apoproteins.

In conclusion, we show that IDU can be targeted highly specifically to parenchymal liver cells by incorporating its lipophilic prodrug into lactosylated NeoHDL, a particle that is recognized by galactose receptors on the target cell. These findings also have a wider significance, as the approach followed here may also be used to deliver other water-soluble drugs selectively to parenchymal liver cells. This may lead to more effective therapy for infectious diseases such as hepatitis.

References

1. Poznanski MJ and Juliano RL, Biological approaches to the controlled delivery of drugs: a critical review. *Pharmacol Rev* 36: 278–336, 1984.
2. Meijer DKF, Jansen RW and Molema G, Drug targeting systems for antiviral agents: options and limitations. *Antiviral Res* 18: 215–258, 1992.
3. Ashwell G and Harford J, Carbohydrate-specific receptors of the liver. *Ann Rev Biochem* 51: 531–554, 1982.
4. Spies M, The asialoglycoprotein receptor: a model for endocytic transport receptors. *Biochemistry* 29: 10009–10018, 1990.
5. Kolb-Bachofen V, Schlepper-Schafer J and Vogell W, Electronmicroscopic evidence for a asialoglycoprotein receptor on Kupffer cells: localization of lectin-mediated endocytosis. *Cell* 29: 859–866, 1982.
6. Biessen EAL, Bakkeren HF, Beuting DM, Kuiper J and van Berkel ThJC, Ligand size is a major determinant of high affinity binding of fucose- and galactose-exposing (lipo)proteins by the hepatic fucose receptor. *Biochem J* 299: 291–296, 1994.
7. Hoyle GW and Hill RL, Molecular cloning and sequencing of a cDNA for a carbohydrate binding receptor unique to rat Kupffer cells. *J Biol Chem* 263: 7487–7492, 1988.
8. Kuiper J, Bakkeren HF, Biessen EAL and van Berkel ThJC, Characterization of the interaction of galactose-exposing particles with rat Kupffer cells. *Biochem J* 299: 285–290, 1994.
9. Bijsterbosch MK, Ziere GJ and van Berkel ThJC, Lactosylated low density lipoprotein: a potential carrier for the site-specific delivery of drugs to Kupffer cells. *Mol Pharmacol* 36: 484–489, 1989.
10. Bijsterbosch MK and van Berkel ThJC, Lactosylated high density lipoprotein: a potential carrier for the site-specific delivery of drugs to parenchymal liver cells. *Mol Pharmacol* 41: 404–411, 1992.
11. Counsell RE and Pohland RC, Lipoproteins as potential site-specific delivery systems for diagnostic and therapeutic agents. *J Med Chem* 25: 1115–1120, 1982.
12. Samadi-Baboli M, Favre G, Canal P and Soula G, Low density lipoprotein for cytotoxic drug targeting: improved activity of elliptinium derivative against B16 melanoma in mice. *Br J Cancer* 68: 319–326, 1993.
13. Bijsterbosch MK and van Berkel ThJC, Native and modified lipoproteins as drug delivery systems. *Adv Drug Delivery Rev* 5: 231–251, 1990.

ing antitumor compounds to cancer cells. *Bioconjugate Chem* 5: 105–113, 1994.
15. Jansen RW, Kruijt JK, van Berkel ThJC and Meijer DKF, Coupling of the antiviral drug Ara-AMP to lactosaminated albumin leads to specific uptake in rat and human hepatocytes. *Hepatology* 18: 146–152, 1993.
16. Biessen EAL, Beuting DM, Vietsch H, Bijsterbosch MK and van Berkel ThJC, Specific targeting of the antiviral drug 5-iodo-2′-deoxyuridine to the parenchymal liver cell using lactosylated poly-L-lysine. *J Hepatology* 21: 806–815, 1994.
17. Ponzetto A, Fiume L, Foranzi B, Song SY, Busi C, Martioli A, Spinelli C, Marinelli M, Smedile A, Chiaberge E, Bonini F, Gervasi GB, Rapicetta M and Verme G, Adenine arabinoside monophosphate and acyclovir monophosphate coupled to lactosaminated albumin reduce woodchuck hepatitis virus viremia at doses lower than do the unconjugated drugs. *Hepatology* 44: 16–24, 1991.
18. Schouten D, van der Kooij M, Muller J, Pieters MN, Bijsterbosch MK and van Berkel ThJC, Development of lipoprotein-like lipid particles for drug targeting: Neo-high density lipoproteins. *Mol Pharmacol* 44: 486–492, 1993.
19. Prusoff WH and Goz B, Potential mechanisms of action of antiviral agents. *Fed Proc* 32: 1679–1687, 1974.
20. Santos O, Pant KD, Blank EW and Ceriani RL, 5-Iododeoxyuridine increases the efficacy of the radioimmunotherapy of human tumors growing in nude mice. *J Nucl Med* 33: 1530–1534, 1992.
21. Bijsterbosch MK, Schouten D and van Berkel ThJC, Synthesis of the dioleoyl derivative of iododeoxyuridine and its incorporation into reconstituted high density lipoprotein particles. *Biochemistry* 33: 14073–14080, 1994.
22. Sinkula AA and Yalowski SH, Rationale for design of biologically reversible drug derivatives: Prodrugs. *J Pharm Sci* 64: 181–210, 1975.
23. Lowry OH, Rosebrough NJ, Farr AL and Randall RJ, Protein measurement with the Folin phenol reagent. *J Biol Chem* 193: 265–275, 1951.
24. Spiro RG, Analysis of sugars found in glycoproteins. *Meth Enzymol* 8: 3–26, 1966.
25. Nagelkerke JF, Bakkeren HF, Kuipers HF, Vonk RJ and van Berkel ThJC, Hepatic processing of the cholesteryl ester from low density lipoprotein in the rat. *J Biol Chem* 261: 8908–8913, 1986.
26. Caster WO, Simons AB and Armstrong WD, Evans blue space in tissues of the rat. *Am J Physiol* 183: 317–321, 1955.
27. Nagelkerke JF, Barto KP and van Berkel ThJC, In vivo and in vitro uptake and degradation of acetylated low density lipoprotein by rat liver endothelial, Kupffer and parenchymal cells. *J Biol Chem* 263: 12221–12227, 1983.
28. De Duve C, Pressman BC, Gianetto R, Wattiaux R and Appelmans F, Tissue fractionation studies. 6. Intracellular distribution patterns of enzymes in rat liver tissue. *Biochem J* 60: 604–617, 1955.
29. Gray GR, The direct coupling of oligosaccharides to proteins and derivatized gels. *Arch Biochem Biophys* 163: 426–428, 1974.
30. Van Berkel ThJC, De Rijke Y and Kruijt JK, Different fate in vivo of oxidatively modified low density lipoprotein and acetylated low density lipoprotein in rats. *J Biol Chem* 266: 2282–2289, 1991.
31. Van Berkel ThJC, Dekker CJ, Kruijt JK and van Eijk HG, The interaction in vivo of transferrin and asialofetuin with liver cells. *Biochem J* 243: 715–722, 1987.
32. Bijsterbosch MK and van Berkel ThJC, Uptake of lactosylated low density lipoprotein by galactose-specific receptors in rat liver. *Biochem J* 270: 233–239, 1990.
33. Bijsterbosch MK, Bernini F, Bakkeren HF, Gotto Jr AM, Smith LC and van Berkel ThJC, Enhanced hepatic uptake and processing of cholesterol esters from LDL by specific lactosaminated Fab fragments. *Arterioscler Thromb* 11: 1806–1813, 1991.
34. Bijsterbosch MK, Bakkeren HF, Kempen HJM, Roelen HCPF, van Boom JH and van Berkel ThJC, A monogalactosylated cholesterol derivative that specifically induces uptake of LDL by the liver. *Arterioscler Thromb* 12: 1153–1160, 1992.
35. Holtzman E, *Lysosomes*. Plenum Press, New York and London, 1989.
36. Burton R, Eck CD and Lloyd JB, The permeability properties of rat liver lysosomes to nucleosides. *Biochem Soc Trans* 3: 1251–1253, 1975.
37. Wilcoxon F, Individual comparisons by ranking methods. *Biom Bull* 1: 80–83, 1945.

THE JOURNAL OF BIOLOGICAL CHEMISTRY
© 1996 by The American Society for Biochemistry and Molecular Biology, Inc.

Vol. 271, No. 32, Issue of August 9, pp. 19152–19158, 1996
Printed in U.S.A.

Sphingomyelin Inhibits the Lecithin-Cholesterol Acyltransferase Reaction with Reconstituted High Density Lipoproteins by Decreasing Enzyme Binding*

(Received for publication, April 16, 1996)

Delmas J. Bolin and Ana Jonas‡

From the Department of Biochemistry, College of Medicine at Urbana-Champaign, University of Illinois, Urbana, Illinois 61801

Lecithin-cholesterol acyltransferase (LCAT) catalyzes the formation of cholesterol esters on high density lipoproteins (HDL) and plays a critical role in reverse cholesterol transport. Sphingomyelin, an important constituent of HDL, may regulate the activity of LCAT at any of the key steps of the enzymatic reaction: binding of LCAT to the interface, activation by apo A-I, or inhibition at the catalytic site. In order to clarify the role of sphingomyelin in the regulation of the LCAT reaction and its effects on the structure of apolipoprotein A-I, we prepared reconstituted HDL (rHDL) containing egg phosphatidylcholine, cholesterol, apolipoprotein A-I, and up to 22 mol % sphingomyelin. Because the interfacial properties of substrate particles can dramatically affect LCAT binding and kinetics, we also prepared and analyzed proteoliposome substrates having the same components as the rHDL, except for a 4-fold higher ratio of phospholipid to apolipoprotein A-I. The reaction kinetics of LCAT with the rHDL particles revealed no significant change in the apparent V_{max} but showed a concentration-dependent increase in slope of the reciprocal plots and in the apparent K_m values with sphingomyelin content. The dissociation constant (K_d) for LCAT with these particles increased linearly with sphingomyelin content up to 22 mol %, changing in parallel with the apparent K_m values. No structural changes of apolipoprotein A-I were detected in the particles with increasing content of sphingomyelin, but fluorescence results with lipophilic probes revealed that significant changes in the acyl chain, backbone, and head group regions of the lipid bilayer of the particles are introduced by the addition of sphingomyelin. On the other hand, the proteoliposome substrates also had increased K_m values for LCAT at high sphingomyelin contents but compared with the rHDL particles had a 6–10-fold lower affinity for LCAT binding and exhibited kinetics consistent with competitive inhibition by sphingomyelin at the active site. These results show conclusively that the dominant mechanism for the inhibition of LCAT activity with rHDL particles by sphingomyelin is the impaired binding of the enzyme to the interface. The results also underscore the significant differences in the enzyme reaction kinetics with different substrate particles.

Lecithin-cholesterol acyltransferase (LCAT)[1] plays a critical role in the maintenance of cholesterol homeostasis. LCAT participates in the reverse cholesterol transport pathway, maintaining a gradient for the diffusion of free cholesterol from peripheral tissues into high density lipoproteins (HDL) by catalyzing cholesterol ester (CE) formation from HDL surface phosphatidylcholine (PC) and cholesterol. As a result of LCAT activity, cholesterol is removed from peripheral cell membranes and, as CE, is ultimately removed and metabolized by the liver.

Several factors contribute to the maintenance of cellular cholesterol homeostasis, including the activity of HMG-CoA reductase and acyl-CoA acyltransferase, which are responsible for production and esterification of intracellular cholesterol, respectively. In addition, the sphingomyelin (SPM) content of the cell membrane is thought to contribute to the maintenance of cellular cholesterol homeostasis. The cholesterol content of the cell membranes is positively correlated with SPM content (1). Sphingomyelin is thought to bind cholesterol with high affinity and inhibit its efflux from the plasma membrane by preventing cholesterol desorption (2); SPM also prevents the exchange of cholesterol between the plasma membrane and intracellular pools (3). Although its role in the regulation of cellular cholesterol homeostasis has become more clearly established, the role of SPM in the function of circulating lipoproteins remains unclear.

In the vasculature, LCAT encounters several potential substrate particles containing lipids (PC, cholesterol). LCAT activity with these particles is determined primarily by their apolipoprotein and lipid content and composition. Optimal substrates appear to be small HDL particles containing apolipoprotein A-I (apoA-I) (4), the principal physiological activator of LCAT (5), whereas apolipoprotein B containing lipoproteins are poor substrates (6). The activity of LCAT with these lipoproteins is inversely proportional to the size of the low density lipoproteins particles and is directly proportional to the PC/SPM ratio (7). The PC/SPM ratio correlates with LCAT activity on blood components: the PC/SPM ratio in HDL is higher (≈6.5/1) than in low density lipoproteins (≈2.6/1) or RBC membranes(≈1.2/1) (8). When SPM levels in HDL are increased, LCAT activity is reduced. Discoidal lymphatic HDL from humans (9) and dogs (10) are enriched in SPM and have low LCAT reactivity relative to their plasma counterparts. Furthermore, the apoA-I of discoidal human lymphatic HDL

* This work was supported by National Institutes of Health Grants HL 16059 and HL 29939. The costs of publication of this article were defrayed in part by the payment of page charges. This article must therefore be hereby marked "*advertisement*" in accordance with 18 U.S.C. Section 1734 solely to indicate this fact.

‡ To whom correspondence should be addressed: Dept. of Biochemistry, College of Medicine at Urbana-Champaign, University of Illinois, 506 South Mathews Ave., Urbana, IL 61801.

[1] The abbreviations used are: LCAT, lecithin-cholesterol acyltransferase; CE, cholesterol ester; PC, phosphatidylcholine; HDL, high density lipoproteins; apoA-I, apolipoprotein A-I; rHDL, reconstituted HDL; SPM, sphingomyelin; DPPC, dipalmitoyl-PC; DMPC, dimyristoyl-PC; DPH, 1,6-diphenyl-1,3,5-hexatriene; TMA-DPH, 1-(4-trimethyl-ammonium phenyl)-6-phenyl-1,3,5-hexatriene; PRODAN, 6-propionyl-2-(dimethylamino)naphthalene.

has an altered epitope expression compared with discoidal rHDL particles, suggesting that the altered lipid composition of lymphatic HDL promotes an apoA-I conformation that may render it incapable of activating LCAT (11). Clearly, structural and compositional differences of lymphatic HDL contribute to their lower reactivity with LCAT. The phospholipid content of HDL could dramatically alter LCAT activity by interacting with and changing the conformation of apoA-I, by changing the nature of the lipid interface, by inhibiting LCAT through competition for substrate binding at the active site, or by a combination of the above. It is possible that the presence of SPM in HDL alters LCAT reactivity by several of these mechanisms.

In addition to its effects in native lipoproteins, SPM has been shown to be a poor matrix for the LCAT reaction with synthetic substrates. In fact, LCAT activity is lower with PC regardless of the acyl chain composition when the PC is presented in an SPM matrix compared with a fluid ether PC matrix (12). Research by Subbaiah and Liu (13) using proteoliposome substrates and native lipoproteins suggests that SPM competes with PC for binding to the active site of LCAT and thus participates in the regulation of the LCAT reaction. Although proteoliposomes are useful as substrates for LCAT *in vitro*, they lack the defined apoA-I structures characteristic of discoidal reconstituted HDL (rHDL) and have very different structures from native HDL. In order to clarify the role of SPM in the regulation of the LCAT reaction and its effects on the structure of apoA-I, we have prepared discoidal rHDL with egg PC, cholesterol, and apoA-I containing up to 22 mol % SPM. We have characterized these particles in terms of protein structure and properties of the lipid components and the lipid-water interface. We examined the structure of apoA-I and the binding affinity and reaction kinetics of LCAT with these particles. Our results suggest that in discoidal rHDL particles SPM introduces changes in the structure of the lipids, decreases the binding of LCAT to the substrate particles, and thus regulates the LCAT reaction. In contrast, proteoliposome substrates bind more weakly to LCAT and experience the regulatory effect of SPM not only at the binding step but also at the catalytic step.

EXPERIMENTAL PROCEDURES

Materials and Preparations—Human LCAT was purified by methods described previously (14, 15). Its average specific activity, using standard rHDL substrates, was around 100 nmol CE/hr/μg LCAT, and it remained fully active over an 8-month period. Human apoA-I was prepared using a modification of the method of Nichols *et al.* (16). Egg PC, egg SPM, cholesterol, and sodium cholate were obtained from Sigma. Radiolabeled [4-^{14}C]cholesterol and ^{3}H-labeled [2-palmitoyl-9,10-^{3}H]dipalmitoylphosphatidylcholine (^{3}H-DPPC) were purchased from DuPont NEN.

The rHDL were prepared using the sodium cholate dialysis method (17) in molar ratios of 80:8:1:80, egg PC/cholesterol/apoA-I/cholate, or in ratios ranging from 74:(4):8:1:80 to 51:(17):8:1:80 when prepared with SPM (given in parenthesis). Proteolipsome preparations contained 312:5:1:936 molar ratios of egg PC/cholesterol/apoA-I/cholate, or ratios of 275:(37):5:1:936 and 234:(78):5:1:936 when containing SPM (in parenthesis). Radiolabeled cholesterol (5,000 cpm/nmol) was incorporated only into the particle preparations that were used for the determination of reaction kinetics with LCAT. Radiolabeled ^{3}H-DPPC (20,000 cpm/nmol of cholesterol) was included in the preparation of the standard substrate for the activity inhibition measurements (18). Cholate was removed by exhaustive dialysis against 0.1 M Tris-HCl, 0.0005% EDTA, 0.15 NaCl, 1 mM NaN_3, pH 8.0 buffer at 4 °C. Diameters of rHDL were determined by nondenaturing 8–25% polyacrylamide gradient gel electrophoresis (Pharmacia PHAST gradient gel electrophoresis). Phosphatidylcholine was separated from SPM and cholesterol by TLC (Analtech Analytical) using chloroform/methanol/ammonia (65:25:4, v/v/v) and quantified using the method of Chen *et al.* (19). Protein content was determined from absorbance at 280 nm using the percentage extinction coefficient for apoA-I, 11.5×10^{-4} g^{-1} cm^{2} (20) and by the method of Lowry *et al.* (21).

Egg PC/C or SPM/C vesicles were prepared in ratios of 10:1, phospholipid/cholesterol. Preparations were dried down and dispersed in 10 ml of standard buffer. The samples were sonicated on ice (egg PC) or at 50 °C (SPM) until they cleared, alternating 3 min of sonication with 1-min rest periods. The samples were centrifuged at 15,000 rpm at 15 °C for 1 h. The phospholipid content of the supernatant (~5 mg/ml) was assessed by the method of Chen (19) and with a standard phospholipid assay kit (Wako Phospholipids B). The vesicles were used immediately following the preparation.

Activity Inhibition Assay for Determining the Binding of LCAT—LCAT affinity for the rHDL and proteoliposome particles was assessed by the activity inhibition assay previously described (18). Briefly, the activity inhibition assay uses rHDL containing ^{3}H-DPPC as substrates for the LCAT reaction. When unlabeled rHDL or proteoliposomes are present in the reaction mixture, LCAT equilibrates between labeled and unlabeled rHDL, and the total radiolabeled CE production is decreased. Lineweaver-Burke plots of reciprocal velocity *versus* reciprocal substrate apolipoprotein concentration give a family of lines that are consistent with the pattern expected for competitive inhibition. Plots of the slopes of these lines *versus* the concentration of apolipoprotein in the competing rHDL give a straight line from which the K_i (K_d, the dissociation constant) for the competing rHDL can be obtained. The substrates used were the egg PC/cholesterol/apoA-I rHDL prepared as described above including ^{3}H-DPPC. The LCAT reaction mixture consisted of rHDL or proteoliposomes with substrate apoA-I contents ranging from 2.5 to 43 μg, 2 mg of defatted bovine serum albumin, 4 mM 2-mercaptoethanol, unlabeled test rHDL or proteoliposomes with apolipoprotein contents ranging from 0 to 150 μg, and standard buffer to 0.45 ml of total volume. When vesicles were analyzed for LCAT binding, 9 μg of substrate apoA-I were included, and vesicle phospholipid contents from 0 up to 0.95 mg (egg PC) or 1.56 mg (SPM) were used as inhibitors; the remainder of the reaction mixture was unchanged. The reaction mixtures were incubated at 37 °C for 5 min, and 50 μl of a suitable LCAT dilution were added to start the reaction. The reaction proceeded 20 min and was stopped by the addition of 5 ml of chloroform/methanol (2:1, v/v). Labeled CE were separated from cholesterol and phospholipids by thin layer chromatography and were quantitated by scintillation counting as described previously (14, 17). All experiments were performed in duplicate on two separate particle preparations.

Enzymatic Reactions—LCAT reactions with rHDL or proteoliposomes containing [4-^{14}C]cholesterol were performed in standard buffer as reported previously (22). Reaction mixtures for kinetic analysis contained substrate concentrations ranging from 1×10^{-7} M (2.8 μg) to 3×10^{-6} M (84 μg) apoA-I, 2 mg of defatted bovine serum albumin, 4 mM β-mercaptoethanol, and 30–50 ng of pure LCAT. Apparent kinetic constants were obtained from Lineweaver-Burke analysis of the data. Experiments on two separate preparations were performed in duplicate, each giving similar results. A more detailed analysis of the effects of an interfacial inhibitor on the enzyme kinetics was based on the following expression derived by Verger *et al.* (23) and applied by Jonas *et al.* (24) to the inhibition of LCAT by ether PC:

$$\frac{1}{v_o} = \frac{K_m^* + K_m^*(I/K_i^*) + S}{K_{cat}E_oS} + \frac{K_m^* K_d}{K_{cat}E_o}\frac{1}{S_o}$$

In this expression, v_o is the initial velocity; K_m^* is the intrinsic Michaelis-Menten constant (in molecules/surface); I is the inhibitor concentration (in molecules/surface); K_i^* is the intrinsic inhibition constant; S is the interfacial substrate concentration (in molecules/surface); K_{cat} is the catalytic rate constant, E_o is the total enzyme concentration (in molecules/volume); K_d is the dissociation constant of the enzyme from the interface; and S_o is the bulk substrate concentration (in molecules/volume).

According to this equation, in the presence of an interfacial inhibitor, reciprocal plots of v_o *versus* bulk PC concentration should give a family of straight lines with an increasing $1/v_o$ intercept, *i.e.* decreasing apparent V_{max} values. The slope of the lines should be constant if K_d remains the same. However, changes in K_d would give increasing or decreasing slopes.

Fluorescence Characterization and Circular Dichroism—The lipid dynamics and hydration of the rHDL containing SPM were examined using fluorescent probes. The motions and polarity of the environment of the acyl chain, glycerol backbone, and head group regions were assessed using 1,3,5 diphenylhexatriene (DPH), trimethylammonium-DPH (TMA-DPH), and 6-propionyl-2-dimethylaminonaphthalene (PRODAN), respectively. All fluorescent lipophilic probes were obtained from Molecular Probes (Eugene, OR). Fluorescence measurements and analysis of the data were performed as described previously (25). Circular dichroism spectra were measured with a Jasco J-720 spectropo-

TABLE I
Characterization of the rHDL particles
rHDL particles were prepared by the sodium cholate dialysis method.

SPM[a]	Composition (A-I/C/PC/SPM)[a]	Diameter[b]	α-Helicity[c]
mol %	*mol/mol/mol/mol*	*Å*	*%*
0	1/8/75/0	97	72
3.7	1/8/74/4	97	74
11	1/8/69/10	97	72
17	1/8/60/14	97	70
22	1/8/51/17	97	71

[a] PC was separated from SPM by TLC (Analtech Analytical) using chloroform/methanol/ammonia (65:25:4, v/v/v) and quantified using the method of Chen *et al.* (19). Cholesterol content from the initial phospholipid/cholesterol ratios. Protein content from absorbance at 280 nm and extinction coefficient. The errors of measurement are approximately ±5%. A-I, apolipoprotein A-I; C, cholesterol; PC, egg phosphatidylcholine; SPM, egg sphingomyelin.

[b] From nondenaturing gradient gel electrophoresis, relative to protein standards: bovine serum albumin, lactate dehydrogenase, thyroglobulin, and ferritin. Errors are ±2 Å.

[c] Estimated from ellipticity at 222 nm from circular dichroism spectra using the method of Chen *et al.* (26). The errors of measurement are approximately ±5%.

larimeter at 24 °C between 200 and 250 nm using 0.1 mg/ml sample solutions and a 1-mm path length cuvette. The α-helical content of apo A-I in the rHDL particles containing SPM was estimated from the molar ellipticities at 222 nm using the method of Chen *et al.* (26) as previously reported (27). Two separate fluorescence experiments were performed, each giving similar results.

RESULTS

ApoA-I has been shown to combine with a variety of phospholipids, including SPM, to form stable discoidal rHDL particles (12, 28–30). Table I summarizes the properties of rHDL particles prepared in this study; their size distribution is shown in Fig. 1. The composition and size of the rHDL particles are consistent with a discoidal morphology (31). The moderate content of egg SPM, with saturated acyl chains (86% palmitoyl) (32), does not appear to alter significantly the structure of apoA-I. Circular dichroism spectra for all of the rHDL in this series were quite similar (data not shown) indicating that the α-helical content of apoA-I changes very little, as shown on Table I. It is clear that rHDL particles with similar size and total lipid contents can be prepared with apoA-I and mixtures of egg PC and SPM. The proteoliposome preparations had protein and lipid compositions very similar to those of the initial reaction mixtures and migrated on nondenaturing gradient gel electrophoresis as heterogeneous populations of particles most having diameters greater than 180 Å (data not shown).

LCAT reactivity with rHDL is highly dependent upon the phospholipid composition of the interface of the substrate particle. SPM provides a poor matrix for the LCAT reaction when it is present as 89% of the interfacial phospholipid (12). To determine the effect of SPM incorporated into discoidal rHDL or into proteoliposomes on the LCAT reaction, we used the two series of substrates containing [4-^{14}C]cholesterol. Lineweaver-Burke plots for the enzymatic reactions are shown in Fig. 2. The resulting kinetic parameters are summarized in Table II. We found (Fig. 2*B*) that increasing SPM content in the rHDL had a minimal effect on the apparent V_{max} (app V_{max}) of the LCAT reaction. The insignificant change in app V_{max} in this rHDL series suggests that SPM competition with PC for the LCAT active site is minimal in these substrates. However, the increasing slopes of the Lineweaver-Burke plots with SPM content clearly indicate, by reference to the analysis of interfacial enzyme inhibition of Verger *et al.* (23) and the work of Jonas *et al.* (24), that the major effect is on the $K_m^* K_i / K_{cat} E_o$ parameters. Because the K_m^* and the $K_{cat} E_o$ parameters of the

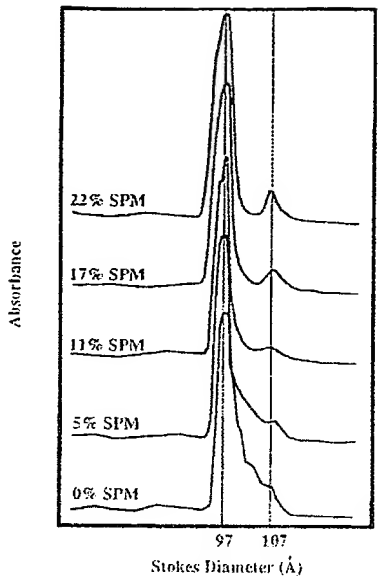

FIG. 1. **Size distribution of rHDL prepared with apoA-I, cholesterol, and mixtures of egg PC and egg SPM.** rHDL preparations were separated by 8–25% polyacrylamide gradient gel electrophoresis using Pharmacia Phast System. Bands were visualized by Coomassie staining. Gel bands were scanned with LKB UltraScan XL laser densitometer. Absorbance scales are arbitrary, and peak height has been adjusted to give peaks of comparable height. Stokes diameter was calculated using protein markers with known Stokes radii as standards: bovine serum albumin, lactate dehydrogenase, horse ferritin, and thyroglobulin.

catalytic step are in effect constants, then K_d is the likely variable that affects the slope of the Lineweaver-Burke plots shown in Fig. 2.

The proteoliposome substrates had increasing slopes for the highest SPM contents (Fig. 2*A*) consistent with increasing K_i. However, the app V_{max} values decreased with added SPM, suggesting competition of SPM for PC at the active site. These results are in complete agreement with those reported by Subbaiah and Liu (13). The apparent kinetic constants are summarized in Table II. In the absence of the SPM inhibitor, the app V_{max} is 37% higher for an rHDL than for a proteoliposome substrate, and the app K_m (in terms of PC concentration) is 4.4-fold lower for rHDL, giving an overall 5.2-fold greater catalytic efficiency (app V_{max}/app K_m) for the rHDL substrates. This is the first quantitative comparison of these two widely used synthetic substrates for LCAT.

To confirm that SPM increases the K_d for the interaction of rHDL and proteoliposomes with LCAT, we measured directly the LCAT binding affinity of a series of rHDL and proteoliposome particles without ^{14}C-cholesterol using the activity inhibition assay previously described (18). We found that the K_d for rHDL increased about 5-fold in a linear manner with increasing SPM, and the K_d for proteoliposomes increased 2-fold (see Table II). Clearly, the presence of SPM in the particles decreases LCAT affinity for the phospholipid interface. To determine if the effect of SPM on LCAT binding affinity could be observed independently of apoA-I, we prepared vesicles with cholesterol and either egg PC or SPM in a 1:10 molar ratio of cholesterol to phospholipid. The vesicles were used as test particles in competition with the standard LCAT substrate rHDL under the same conditions as the activity inhibition assay. As the amount of vesicle phospholipid increases, LCAT binds to the vesicle surface, and as a result, net production of radiolabeled cholesterol ester at the standard substrate surface decreases. Fig. 3 shows that the amount of SPM vesicle phos-

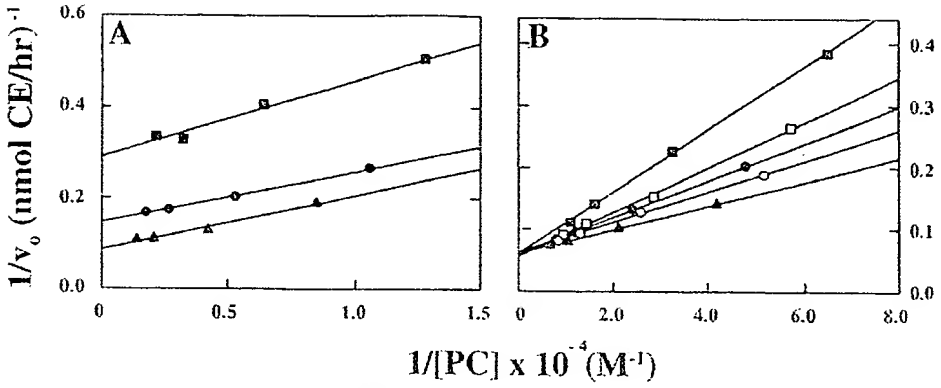

FIG. 2. **Lineweaver-Burke plots of LCAT reaction kinetics with proteoliposomes (*A*) or rHDL (*B*) containing SPM.** ■, 22 mol % SPM; □, 17 mol % SPM; ●, 11 mol % SPM; ○, 5 mol % SPM; ▲, 0 mol % SPM. Initial reaction velocities (v_o) were measured at 37 °C using reaction mixtures containing substrate concentrations ranging from 8.0×10^{-6} M to 5.0×10^{-4} M PC, 2 mg of defatted bovine serum albumin, 4 mM β-mercaptoethanol, and 30–50 ng of pure LCAT in 10 mM Tris-HCl, 0.15 M NaCl, 0.01% EDTA, 1 mM NaN_3, pH 8.0. Substrate rHDL contained 5,000 cpm [4-^{14}C]cholesterol/nmol cholesterol. Two separate experiments on two preparations were performed in duplicate; each gave similar results.

TABLE II

Apparent kinetic constants and dissociation constants (K_d) for the reaction of LCAT with rHDL and proteoliposomes containing sphingomyelin

Substrates	SPM	K_d[a]		$^{app}V_{max}$ (nmol CE/h)[b]	$^{app}K_m$ (M, PC)[b]	$^{app}V_{max}/^{app}K_m$ (nmol CE/h/M)[b]
		M, A-I	M, PC			
	mol %	$\times 10^7$	$\times 10^5$		$\times 10^5$	$\times 10^{-4}$
rHDL[c]	0	3.0	2.3	15.7	3.2	49.0
	3.7	6.0	4.4	15.0	4.0	37.5
	11	8.0	5.5	15.7	5.0	31.4
	17	11.0	6.4	17.0	6.4	26.6
	22	14.0	6.9	15.7	8.2	19.1
Proteoliposomes	0	7.9	24.0	11.5	14.0	8.2
	11	14.0	34.0	6.8	7.6	8.9
	23	19.0	41.0	3.4	5.7	6.0

[a] The dissociation constants were determined by the activity inhibition method as described under "Experimental Procedures" using the molar concentrations of apoA-I (A-I) or PC in the calculations. Average of two experiments. Errors shown on Figure 3.

[b] The apparent kinetic constants were determined from Lineweaver-Burke analysis of initial velocity versus molar PC concentrations using rHDL particles containing [4-^{14}C]cholesterol. Initial reaction velocities were measured at 37 °C in 10 mM Tris, 0.15 M NaCl, 0.01% EDTA, 1 mM NaN_3, pH 8.0. The results are expressed in terms of PC concentrations. Two separate experiments were performed in duplicate; each gave similar results.

[c] rHDL particles described in Table I.

pholipid (0.25 mg/ml) required to inhibit the LCAT reaction by 50% was nearly 5-fold higher than the amount of egg PC vesicle phospholipid (0.048 mg/ml) necessary for a similar inhibition. This result indicates that LCAT binds to the SPM/cholesterol vesicle surface in the absence of apoA-I with less affinity than it does to the egg PC/cholesterol vesicle surface. Because the K_d for LCAT binding to the egg PC rHDL particles is 2.3×10^{-5} M or 0.018 mg/ml (Table II), it follows that the affinity of LCAT for the rHDL is about 3-fold greater than for the egg PC/cholesterol vesicles. Table II also shows that the affinity of LCAT for rHDL in the absence of SPM is 10-fold greater than for comparable proteoliposomes.

To investigate the effects of the addition of SPM on the properties of the rHDL phospholipid phase, we examined the lipid dynamics and hydration of the surface of the rHDL particles using lipophilic fluorescent probes. DPH fluorescence polarization reports on the fluidity of the acyl chain region of the rHDL particles. Fig. 4 shows the temperature dependence of the polarization of DPH for the rHDL containing 22% SPM, 11% SPM, and 0% SPM. DPH polarization increases with increasing SPM content in the rHDL. As shown in Fig. 5, changes in TMA-DPH polarization with temperature indicate similar effects in the phospholipid backbone region, the region between the hydrophobic acyl chains, and the hydrophilic head group region. The higher polarization values observed with both probes indicate that the mobility of the lipids is restricted and order is increased.

The fluorescence of PRODAN was used to probe the polarity of the phospholipid head group region. The fluorescence spectra of PRODAN are quite sensitive to the polarity of the probe environment (33, 34). Fig. 6 shows the fluorescence intensity ratio for PRODAN at 440/490 nm. The probe is in a more polar environment in the egg PC control rHDL compared with the rHDL containing SPM as indicated by the blue-shift that occurs with increased SPM content in the rHDL. This suggests that the presence of SPM shields PRODAN from water molecules in the head group region. These changes are consistent with decreased hydration of egg PC/SPM interfaces as a result of altered phospholipid packing or hydrogen bonding of SPM to cholesterol or to PC, which displaces water (35) and/or allows the probe to penetrate more deeply into the head group region.

DISCUSSION

Much of what is known about the regulation of LCAT activity with lipoprotein substrates has come from kinetic studies of LCAT with substrate analogs, such as proteoliposomes or rHDL. Many factors have been shown to modulate LCAT activity *in vitro* with these substrates. Among these are substrate size and morphology (disc *versus* sphere), phospholipid composition (head group, acyl chain, and unsaturation), and apolipoprotein composition and conformation (36). It is clear that these factors are closely interrelated. As a consequence, exam-

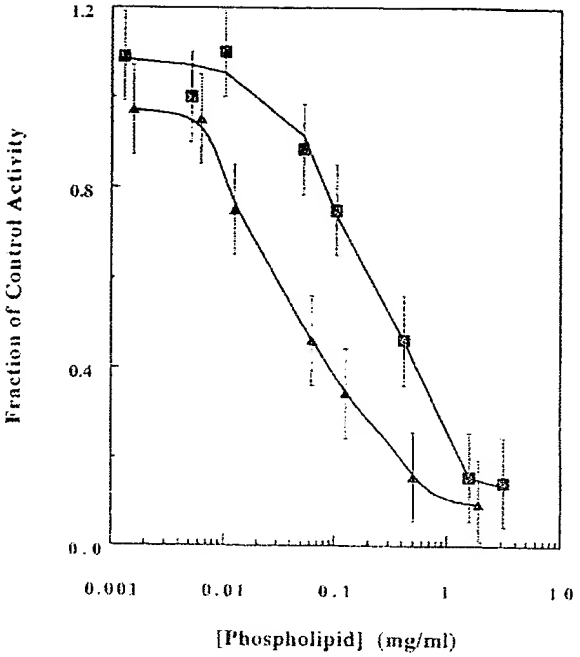

FIG. 3. **Inhibition of LCAT activity by phospholipid vesicles.** Vesicles of egg PC/cholesterol (▲) or SPM/cholesterol (▩) were prepared by sonication in ratios of 10:1, phospholipid/cholesterol. Reaction conditions were identical to those of the activity inhibition method. Concentrations of vesicle phospholipid in the assay mixture ranged from 1.3×10^{-3} to 3.2 mg/ml.

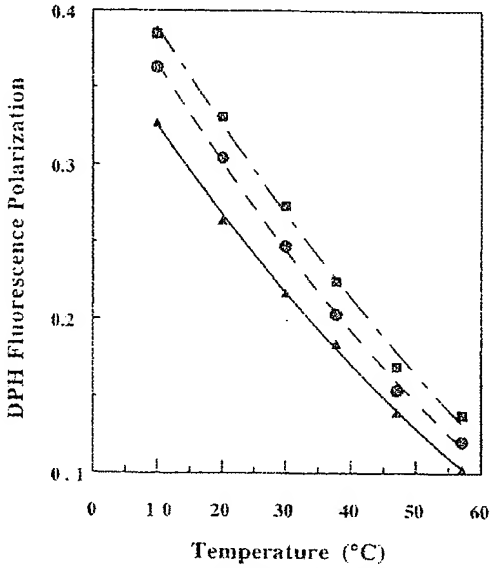

FIG. 4. **Effects of temperature on DPH fluorescence polarization in rHDL containing SPM.** ▩, 22 mol % SPM rHDL; ●, 11 mol % SPM rHDL; ▲, 0 mol % SPM rHDL. DPH was added to rHDL samples (0.1 mg/ml apoA-I) in the ratio 300:1, phospholipid/probe (mol/mol). Polarization values were obtained using a ISS GREG PC photon counting spectrophotometer using the following parameters: excitation wavelength, 366 nm; emission wavelength, 430 nm; slit width, 8 nm. Each point is the average of five measurements. Two separate experiments were performed giving similar results.

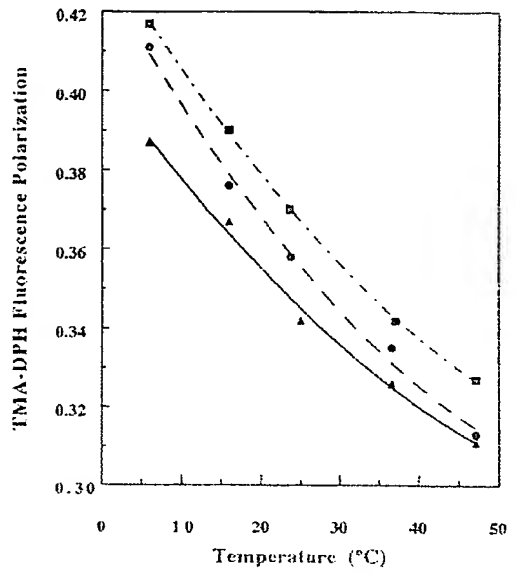

FIG. 5. **Effects of temperature on TMA-DPH fluorescence polarization in rHDL containing SPM.** ▩, 22 mol % SPM rHDL; ●, 11 mol % SPM rHDL; ▲, 0 mol % SPM rHDL. TMA-DPH was added to rHDL samples (0.1 mg/ml apoA-I) in the ratio 300:1, phospholipid/probe (mol/mol). Polarization values were obtained as described in the legend to Fig. 4, except that an emission filter at 400 nm (Corning, KV399) was used. Each point is the average of five measurements. Two separate experiments were performed giving similar results.

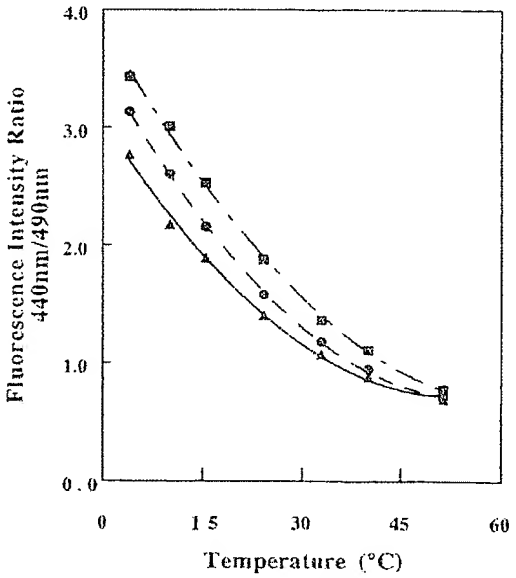

FIG. 6. **PRODAN fluorescence intensity ratio at 440/490 nm in SPM containing rHDL as a function of temperature.** ▩, 22 mol % SPM rHDL; ●, 11 mol % SPM rHDL; ▲, 0 mol % SPM rHDL. PRODAN was added to rHDL samples (0.1 mg/ml apoA-I) in the ratio 300:1, phospholipid/probe (mol/mol). Experiments were performed as described previously (26). Two separate experiments were performed giving similar results.

ining the effect of one of these parameters on LCAT activity while holding the others constant is a difficult task; however, rHDL prepared by the sodium cholate dialysis method have made possible detailed studies of the LCAT reaction with particulate substrates of defined apolipoprotein and phospholipid compositions and similar morphologies.

The conformation of apoA-I, the principal physiological activator of LCAT, is one of the key determinants of LCAT activity. ApoA-I conformation is related to the size of the particle and the phospholipid composition and content. In terms of the number of α-helices/molecule, apoA-I may adopt a conformation with six, seven, or eight α-helices, depending upon the amount of lipid complexed with the protein. But not all confor-

mations of apoA-I are equally effective in activating LCAT; the form of apoA-I with six helical segments is a poor activator of LCAT (37). rHDL prepared with DPPC and cholesterol are good substrates for LCAT if the particles are 97 Å in diameter. The same lipids, however, are 20-fold less reactive in particles that are 186 Å in diameter. Clearly, the amount of phospholipid complexed with apoA-I can profoundly influence LCAT activity through changes in apoA-I conformation and interfacial lipid properties.

Gross changes in the conformation of apoA-I can be avoided by preparing rHDL particles of nearly identical size and total phospholipid content. We have previously prepared a series of 96 Å diameter rHDL with apoA-I, cholesterol, and various mixtures of phospholipids to examine the effect of the interfacial lipid mixture on LCAT reactivity and binding affinity (18). In this study we prepared particles with apoA-I, cholesterol, and mixtures of egg PC and SPM, which are very similar in size. CD spectra for this rHDL series indicate that all have similar apoA-I α-helical contents. It is possible that subtle changes not detected by CD are introduced by the increased SPM content in the structure of apoA-I, which could alter its ability to activate LCAT, but within the resolution of our spectral methods the apoA-I structure appears identical for the series of rHDL particles used in this study.

We examined the reactivity of these rHDL particles with LCAT to investigate the effect of SPM content in discoidal substrates with similar apoA-I structure on LCAT reaction kinetics. The reaction of LCAT with aggregated lipid substrates involves multiple steps: the association of LCAT with the lipid interface, followed by activation by apolipoproteins, binding of lipid substrate(s) to the active site, and subsequent catalytic events (36). Sphingomyelin could influence the initial binding step through altered phospholipid packing as a consequence of its backbone structure or acyl chain composition, or SPM could influence subsequent steps in the LCAT reaction by acting as a competitor with PC in the LCAT phospholipase reaction or by sequestering cholesterol from LCAT on the rHDL surface. The role(s) of SPM are reflected in the kinetic parameters of the LCAT reaction.

If SPM were competing with PC in the active site of LCAT, significant changes would be expected in the app V_{max} parameter according to the Verger *et al.* analysis (23). Such changes were observed by Subbaiah and Liu (13) with SPM and palmitoyl oleoyl-PC diether inclusion in proteoliposome substrates. In this study we confirmed their results with SPM (see Fig. 2*A*). Previously, we (24) had shown that DPPC diether incorporated into rHDL particles acts as an interfacial competitive inhibitor of LCAT with a K_i^* comparable with K_m^* and little change in K_p. Similarly, Massey *et al.* (38) prepared rHDL substrates with various ratios of dimyristoyl PC (DMPC) and DMPC diether and observed that although the app K_m did not change as a function of DMPC content, the app V_{max} increased linearly with increasing DMPC. Pownall *et al.* (12) demonstrated that the app V_{max} increases with increasing sterol content. We observe no change in app V_{max} with increasing SPM content in the rHDL particles (Fig. 2*B* and Table II), suggesting that SPM is not competing with PC at the active site of LCAT nor is it sequestering cholesterol in this rHDL series as was observed for SPM in the proteoliposomes studied by Subbaiah and Liu (13). The qualitative difference between our results for rHDL and those of Subbaiah and Liu (13) for proteoliposomes can be attributed to the different structure of the substrate particles. The properties of phospholipid bilayers in liposomes depend upon liposome composition and curvature (39). Differences in the physical properties of liposomes arise from variations in phospholipid molecular packing with curvature of the liposome (39, 40). It is possible that the highly curved surface of the proteoliposomes decreases the hydrogen bonding of SPM molecules to other surface components and facilitates diffusion and binding to the active site, whereas the planar surface of the rHDL discs maximizes the intermolecular interactions of SPM. In addition, lipid phase separation of SPM or interactions with apoA-I are likely to be very different in the planar, protein-rich rHDL compared with the curved, relatively protein-poor proteoliposomes.

We observe changes in the slopes of the Lineweaver-Burke plots (Fig. 2) and app K_m with increasing SPM content, suggesting that SPM content alters the initial binding of LCAT to the rHDL surface. The changes in app K_m parallel the relationship observed between SPM content and dissociation constant for LCAT determined with these particles. Thus, it appears that SPM effects on the initial binding of LCAT are more important in discoidal substrates than SPM's role in sequestration or competition with molecular substrates. In the case of proteoliposomes, we also demonstrate an effect of SPM on the binding of LCAT to the interface. The effects of SPM on the binding of LCAT to proteoliposomes are also apparent in the results of Subbaiah and Liu (13); however, these authors do not address the change in slope of their $1/v_0$ *versus* 1/PC plot. Rather, they interpret the reversal of the effect of SPM on the activity of LCAT by sphingomyelinase treatment of the substrates, as an indication that the physical state of the lipid does not affect the enzymatic reaction. Because ceramide remains in the bilayer following the removal of the phosphocholine group, treatment of the substrates by sphingomyelinase may not affect the lipid order and motions in the acyl chain region. However, the effects of ceramide on the hydration and packing at the interface may be profound and opposite to those of SPM, considering the major differences that are known to exist between diacylglycerols and corresponding phosphatidylcholines (41).

We provide strong evidence that the interfacial lipid structure of the rHDL changes as a result of the addition of SPM. We observe significant changes in the fluorescence properties of probes in the acyl chain, backbone, and head group regions of the rHDL phospholipids containing increasing SPM. The change in DPH polarization is most likely due to the high content of saturated palmitoyl acyl chains (86%) in egg SPM (32). Saturated acyl chains restrict the mobility and increase the order of the lipids and result in higher polarization values, as has been previously observed with DPH in rHDL prepared with DPPC or palmitoyl oleoyl-PC (29).

The higher polarization values for TMA-DPH in rHDL with increasing SPM content reflect the effects of SPM in the backbone region of the bilayer. In PC, the backbone region includes carbons 1, 2, and 3 of the glycerol backbone and the two ester bonds linking the acyl chains; PC has no capacity as a hydrogen bond donor. In SPM, however, this region includes the amide bond linking the palmitoyl acyl chain and the amino group on carbon 2, the hydroxyl group on carbon 3, and possibly the trans double bond found between carbons 4 and 5 of sphingosine (42). Both the amino and hydroxyl groups of sphingosine have been suggested to participate in intra- and intermolecular hydrogen bonding, which impart important hydrogen bonding potential to SPM that is not found in PC (1, 42). The structure of SPM in the backbone region affects the packing of the acyl chains below and the orientation of the PC head group above (43), facilitating close lipid packing and a more condensed lipid organization (44). Inter- and intramolecular hydrogen bonds, as well as a compact lipid organization, would increase the order and restrict the mobility of TMA-DPH and explain the higher fluorescence polarization observed when SPM is present.

The effects of SPM on the head group region are also significant. The presence of SPM facilitates close lipid packing and condensed organization of the head group region due to its hydrogen bonding capacity. The results of ^{31}P NMR in egg PC/SPM vesicles suggest that intramolecular hydrogen bonds of SPM and close lipid packing may partially exclude water molecules from hydrating the phosphate group of PC, resulting in decreased hydration of the head group region (35). This would explain the relative blue shift of PRODAN fluorescence in rHDL with increased SPM content.

During the revision of this paper a study by Rye *et al.* (45) was published on the effects of SPM on the structure and function of spherical and discoidal rHDLs. Rye and co-workers demonstrated that SPM affects the lipid order and packing in these particles, in close agreement with our observations. They reported that SPM does not influence neutral lipid transfers involving spherical rHDL and cholesterol ester transfer protein; they also showed that SPM inhibits LCAT reaction with rHDL substrates. However, Rye *et al.* did not address the mechanism of LCAT inhibition by SPM, which is the main topic of this report.

In summary, we report that a SPM content up to 22 mol % does not alter the size of rHDL prepared with bulk egg PC, cholesterol, and apoA-I. LCAT binding affinity decreases as rHDL SPM content increases. The inhibition of LCAT by SPM at the active site has a minimal effect in the modulation of enzyme activity with these substrates. The results of our studies with lipophilic probes suggest that SPM significantly changes the properties of the phospholipid interface at the surface and also in the backbone and acyl chain regions. Furthermore, these changes in the surface properties of the rHDL correlate with decreased LCAT binding and reactivity.

REFERENCES

1. Barenholz, Y., and Gatt, S. (1982) in *Phospholipids* (Hawthorne, J. N., and Ansell, G. B., ed) pp. 129–177, Elsevier Biomedical Press, Amsterdam
2. Lund-Katz, S., Laboda, H. M., McLean, L. M., and Phillips, M. C. (1988) *Biochemistry* 27, 3416–3423
3. Slotte, J. P., and Bierman, E. L. (1988) *Biochem. J.* 250, 653–658
4. Glomset, J. (1972) in *Blood Lipids and Lipoproteins* (Nelson, G., ed) pp. 745–787, Wiley, New York
5. Fielding, C. J., Shore, V. G., and Fielding, P. E. (1972) *Biochem. Biophys. Res. Commun.* 46, 1493–1498
6. Barter, P. J., Hopkins, G. J., and Gorjatschko, L. (1985) *Atherosclerosis* 58, 97–107
7. Liu, M., Krul, E. S., and Subbaiah, P. V. (1992) *J. Biol. Chem.* 267, 5139–5147
8. Skipski, V. (1972) in *Blood Lipids and Lipoproteins: Quantitation, Composition and Metabolism* (Nelson, G. J., ed) pp. 471–583, Wiley Interscience, New York
9. Reichl, D., and Sterchi, J. M. (1992) *Biochim. Biophys. Acta* 1127, 28–32
10. Dory, L., Sloop, C. H., Boquet, L. M., Hamilton, R. L., and Roheim, P. S. (1983) *Proc. Natl. Acad. Sci. U. S. A.* 80, 3489–3493
11. Wong, L., Curtiss, L. K., Huang, J., Mann, C. J., Maldonado, B., and Roheim, P. S. (1992) *J. Clin. Invest.* 90, 2370–2375
12. Pownall, H., Pao, Q., and Massey, J. (1985) *J. Biol. Chem.* 260, 2146–2152
13. Subbaiah, P. V., and Liu, M. (1993) *J. Biol. Chem.* 268, 20156–20163
14. Matz, C. E., and Jonas, A. (1982) *J. Biol. Chem.* 257, 4541–4546
15. Jonas, A., and McHugh, H. T. (1983) *J. Biol. Chem.* 258, 10335–10340
16. Nichols, A. V., Gong, E. L., Blanche, P. J., Forte, T. M., and Anderson, D. W. (1976) *Biochim. Biophys. Acta* 446, 226–239
17. Jonas, A., and Matz, C. (1982) *Biochemistry* 21, 6867–6872
18. Bolin, D. J., and Jonas, A. (1994) *J. Biol. Chem.* 269, 7429–7434
19. Chen, P. S., Toribara, T. Y., and Warner, H. (1956) *Anal. Chem.* 28, 1756–1758
20. Gwynne, J., Brewer, B., Jr., and Edelhoch, H. (1974) *J. Biol. Chem.* 249, 2411–2416
21. Lowry, O. H., Rosebrough, N. J., Farr, A. L., and Randall, R. J. (1951) *J. Biol. Chem.* 193, 265–275
22. Jonas, A., Sweeney, S. A., and Herbert, P. N. (1984) *J. Biol. Chem.* 259, 6369–6375
23. Verger, R., Mieras, M. C. E., and deHaas, G. H. (1973) *J. Biol. Chem.* 248, 4023–4034
24. Jones, A., Daehler, J. L., and Wilson, E. R. (1985) *J. Biol. Chem.* 260, 2757–2762
25. Wald, J. H., Goormaghtigh, E., De Meutter, J., Ruysschaert, J. M., and Jonas, A. (1990) *J. Biol. Chem.* 265, 20044–20050
26. Chen, Y., Yang, J. T., and Martinez, H. M. (1972) *Biochemistry* 11, 4120–4131
27. Jonas, A., von Eckardstein, A., Churgay, L., Marsolin, W. M., and Assmann, G. (1993) *Biochim. Biophys. Acta* 1166, 202–216
28. Bonomo, E. A., and Swaney, J. B. (1990) *Biochemistry* 29, 5094–5103
29. Zorich, N., Kezdy, K. E., and Jonas, A. (1987) *Biochim. Biophys. Acta* 919, 181–189
30. Swaney, J. B. (1983) *J. Biol. Chem.* 258, 1254–1259
31. Leroy, A., Toohill, K. L. H., Fruchart, J. C., and Jonas, A. (1992) *J. Biol. Chem.* 268, 4798–4805
32. Calhoun, W. I., and Shipley, G. G. (1979) *Biochemistry* 18, 1717–1721
33. Weber, G., and Farris, F. (1979) *Biochemistry* 18, 3075–3078
34. Massey, J. B., She, H. S., and Pownall, H. J. (1985) *Biochemistry* 24, 6973–6978
35. Schmidt, C. F., Barenholz, Y., and Thompson, T. E. (1977) *Biochemistry* 16, 2649–2656
36. Jonas, A. (1991) *Biochim. Biophys. Acta* 1084, 205–220
37. Jonas, A., Kezdy, K. E., and Wald, J. H. (1989) *J. Biol. Chem.* 264, 4818–4824
38. Massey, J. B., Pao, Q., Van Winkle, W. B., and Pownall, H. J. (1985) *J. Biol. Chem.* 260, 11719–11723
39. Sheetz, M. P., and Chan, S. I. (1972) *Biochemistry* 11, 4573–4581
40. Lichtenberg, D., Freire, E., Schmidt, C. F., Barenholz, Y., Felgner, P. L., and Thompson, T. E. (1981) *Biochemistry* 20, 3462–3467
41. Small, D. M. (1986) in *The Physical Chemistry of Lipids*, pp. 382–386, 481–515, Plenum Press, New York
42. Barenholz, Y., and Thompson, T. E. (1980) *Biochim. Biophys. Acta* 604, 129–158
43. Barenholz, Y. (1984) in *Physiology of Membrane Fluidity* (Shinitzky, M., ed) pp. 131–173, CRC Press, Boca Raton, FL
44. Abrahamsson, S., Dahlen, B., Lofgren, H., Pascher, I., and Sundell, S. (1977) in *Structure of Biological Membranes* (Abrahamsson, S. and Pascher, I. ed) pp. 1–24, Plenum Press, New York
45. Rye, K. A., Hime, N. J., and Barter, P. J. (1996) *J. Biol. Chem.* 271, 4243–4250

THE JOURNAL OF BIOLOGICAL CHEMISTRY
© 1996 by The American Society for Biochemistry and Molecular Biology, Inc.

Vol. 271, No. 8, Issue of February 23, pp. 4243–4250, 1996
Printed in U.S.A.

The Influence of Sphingomyelin on the Structure and Function of Reconstituted High Density Lipoproteins*

(Received for publication, July 18, 1995, and in revised form, October 30, 1995)

Kerry-Anne Rye‡§, Neil J. Hime¶, and Philip J. Barter¶

From the ‡Division of Cardiovascular Services and ¶University of Adelaide, Department of Medicine, Royal Adelaide Hospital, Adelaide, South Australia, Australia 5000

The effect of sphingomyelin (SPM) on the structure and function of discoidal and spherical reconstituted high density lipoproteins (rHDL) has been studied. Three preparations of discoidal rHDL with 1-palmitoyl-2-oleoyl phosphatidylcholine (POPC)/SPM/unesterified cholesterol (UC)/apolipoprotein (apo)A-I molar ratios of 99.6/0.0/10.2/1.0, 86.0/13.6/10.8/1.0, and 72.5/26.3/11.4/1.0 were prepared by cholate dialysis. SPM did not affect discoidal rHDL size or surface charge. Esterification of cholesterol by lecithin:cholesterol acyltransferase (LCAT) was inhibited in the SPM-containing discoidal rHDL. When the discoidal rHDL of POPC/SPM/UC/apoA-I molar ratio 99.6/0.0/10.2/1.0 were incubated with low density lipoproteins (LDL) and LCAT, SPM transferred spontaneously from the LDL to the rHDL ($t_{1/2}$ = 0.8 h) and spherical particles with a POPC/SPM/UC/CE/apoA-I molar ratio of 24.6/4.9/3.6/24.9/1.0 were formed. Depleting the spherical rHDL of SPM head groups by incubation with sphingomyelinase increased the negative charge on the surface, but did not change their size. Cholesteryl ester transfer protein (CETP)-mediated transfers of cholesteryl esters and triglyceride between spherical rHDL and Intralipid were not affected by SPM head group depletion. The effect of SPM on rHDL structure was assessed spectroscopically. SPM increased POPC acyl chain and head group packing in the discoidal rHDL. When the spherical rHDL were depleted of SPM head groups, POPC acyl chain packing order decreased, but head group packing order was not affected. SPM inhibited the lipid-water interfacial hydration of discoidal rHDL. This parameter was not affected when the spherical rHDL were depleted of SPM head groups. The SPM molecule and the SPM head group, respectively, inhibited the unfolding of apoA-I in discoidal and spherical rHDL. It is concluded that (i) SPM influences the structure of discoidal and spherical rHDL, (ii) SPM inhibits the LCAT reaction in discoidal rHDL, and (iii) the SPM head group does not affect CETP-mediated lipid transfers into or out of spherical rHDL.

Sphingomyelin (SPM)[1] is a glycosphingolipid which is present in cell membranes and plasma lipoproteins. For many years SPM was thought only to maintain the structural integrity of membranes, but recent studies have shown that it is also involved in a wide range of metabolic events (1, 2). The SPM molecule comprises a phosphocholine head group and a ceramide backbone with a sphingosine base and an amide-linked acyl chain. The ceramide backbone of SPM plays a regulatory role in cell growth, differentiation, and apoptosis (1, 2). Ceramide also modulates protein phosphorylation and has been implicated as a tumor-suppressor lipid (3). The influence of SPM on lipoprotein metabolism is poorly understood. It has been reported that the concentration of SPM in the artery wall increases with aging and that it comprises 70–80% of the phospholipids in atherosclerotic lesions (4). These observations suggest that SPM may be involved in the development of atherosclerosis. The additional finding that the SPM in atherosclerotic lesions is derived from plasma lipoproteins (4) emphasizes the importance of understanding how this molecule influences lipoprotein metabolism.

At present little is known about the origin of SPM in lipoproteins. SPM reportedly transfers from cell membranes to pre-β-migrating high density lipoproteins (HDL) (5). SPM is also present in discoidal, nascent HDL which are secreted from the rat liver (6). However, it is not known whether the SPM, which enters the plasma compartment as a component of pre-β-migrating HDL and nascent HDL, is subsequently incorporated into mature, spherical HDL. Similarly, little is known of the origins of SPM in low density lipoproteins (LDL) and very low density lipoproteins. It has been reported that the lipoproteins in peripheral lymph are enriched in SPM relative to their plasma counterparts (7), suggesting that SPM from cell membranes may be incorporated into lipoproteins before they enter the plasma compartment.

Given that there are strong Van der Waals interactions between SPM and unesterified cholesterol (UC) (8, 9) and that the concentrations of UC and SPM in membranes and lipoproteins change in a coordinated manner (10), it follows that SPM may participate in the regulation of cholesterol transport and the maintenance of cell cholesterol homeostasis. Evidence for this comes from studies which show that SPM regulates the uptake and intracellular processing of LDL (11, 12). The additional finding that SPM-containing lipid/apolipoprotein complexes are excellent acceptors of cellular cholesterol (13) suggests that SPM may also be involved in the initial step of the reverse cholesterol transport process. Further support for the involvement of SPM in reverse cholesterol transport comes

* This work was supported by the National Health and Medical Research Council of Australia and the Ramaciotti Foundation. The costs of publication of this article were defrayed in part by the payment of page charges. This article must therefore be hereby marked "*advertisement*" in accordance with 18 U.S.C. Section 1734 solely to indicate this fact.

§ To whom correspondence should be addressed: Lipid Research Laboratory, Level 1, Hanson Centre, Frome Road, Adelaide, South Australia, Australia 5000. Tel.: 61-8-222-3448; Fax: 61-8-223-3870.

[1] The abbreviations used are: SPM, sphingomyelin; HDL, high density lipoprotein(s); LDL, low density lipoprotein(s); rHDL, reconstituted high density lipoproteins; PC, phosphatidylcholine; POPC, 1-palmitoyl-2-oleoyl phosphatidylcholine; UC, unesterified cholesterol; CE, cholesteryl ester(s); apo, apolipoprotein; LCAT, lecithin:cholesterol acyltransferase; CETP, cholesteryl ester transfer protein; TBS, Tris-buffered saline; TG, triglyceride; DPH, 1,6-diphenyl-1,3,5-hexatriene; TMA-DPH 1-(4-trimethylammoniumphenyl)-6-phenyl-1,3,5-hexatriene *p*-toluene sulfonate; PRODAN, 6-propionyl-2-(dimethylamino)-naphthalene; GdnHCl, guanidine hydrochloride.

from the observation that [^{3}H]cholesterol efflux from fibroblasts to HDL increases if the cells have been incubated with sphingomyelinase (10).

The aim of the present study is to better understand the influence of SPM on HDL metabolism. In order to overcome the problems of interpretation which may occur due to the heterogeneity of native HDL, the study has been carried out with well characterized preparations of discoidal and spherical reconstituted HDL (rHDL) (14, 15). The results show that SPM influences both the structure and function of rHDL.

EXPERIMENTAL PROCEDURES

Isolation of HDL, LDL, and Apolipoprotein (Apo) A-I—Plasma samples for the isolation of LDL, HDL and apoA-I were donated by the Transfusion Service, Royal Adelaide Hospital. LDL and HDL were isolated in the $1.019 < d < 1.055$ and $1.07 < d < 1.21$ g/ml density range, respectively (16). ApoA-I was prepared by delipidating HDL (17) and anion exchange chromatography of the resulting apoHDL on Q Sepharose Fast Flow (Pharmacia Biotechnology AB, Uppsala, Sweden) (18).

Preparation of Discoidal and Spherical rHDL—UC, 1-palmitoyl-2-oleoyl phosphatidylcholine (POPC), egg yolk SPM, and sodium cholate were purchased from Sigma. Discoidal rHDL were prepared by the cholate dialysis method (19). Discs containing SPM were prepared by drying POPC, SPM, and UC onto the walls of glass test tubes, then proceeding as previously described (19). When the discoidal rHDL were used as substrates for the lecithin:cholesterol acyltransferase (LCAT) reaction, [^{3}H]UC (48 Ci/mmol) (Amersham International, Buckinghamshire, UK) was added to the lipids before drying. The resulting particles contained approximately 48,000 cpm/nmol UC. Lipid-free apoA-I was not present in the discoidal rHDL preparations as judged by nondenaturing gradient gel electrophoresis and staining with Coomassie Blue. Spherical rHDL were prepared by incubating discoidal rHDL with LDL and LCAT as described previously (20). Before use, all of the rHDL preparations were dialyzed extensively against 0.01 M Tris-buffered saline (TBS) (pH 7.4) containing 0.15 M NaCl, 0.005% (w/v) EDTA-Na_2, and 0.006% (w/v) NaN_3.

Purification of LCAT—LCAT was isolated from 2 liters of human plasma (Transfusion Service, Royal Adelaide Hospital) by precipitation with ammonium sulfate and citric acid followed by ultracentrifugation at a density of 1.25 g/ml (21). The $d > 1.25$ g/ml fraction was applied to an XK 50/60 column containing phenyl-Sepharose 6 Fast Flow (high substitution) (Pharmacia) which had been preequilibrated with 3 M NaCl. LCAT was eluted from the column with Milli Q water at a flow rate of 10 ml/min. The active fractions were pooled, dialyzed against 20 mM Tris (pH 7.4), and applied to a preequilibrated XK 26/40 column packed with DEAE Sepharose Fast Flow (Pharmacia). LCAT was eluted from the column with 20 mM Tris, 160 mM NaCl (pH 7.4) at a flow rate of 10 ml/min, and the active fractions were pooled. These steps were carried out at room temperature on a fast protein liquid chromatography system (Pharmacia). The purified LCAT appeared as a single band following electrophoresis on a 20% homogeneous SDS-gel and staining with Coomassie Blue. Activity was assessed as described by Piran and Morin (22) using [^{3}H]UC-labeled POPC/UC/apoA-I discoidal rHDL as a substrate. The assay was linear if less than 30% of the [^{3}H]UC was esterified. The preparation used in this study generated 227 nmol of cholesteryl esters (CE)/ml LCAT/h.

Purification of Cholesteryl Ester Transfer Protein (CETP)—CETP was prepared as described previously (23). Transfer activity was assessed as the transfer of [^{3}H]CE from [^{3}H]CE-HDL_3 to LDL (24, 25). The assay was linear if less than 30% of the [^{3}H]CE transferred from HDL_3 to LDL. Activity is expressed in units, with 1 unit being the transfer activity of 1 ml of a preparation of pooled, human lipoprotein-deficient plasma. The preparation of CETP used for this study had 6 units of activity/ml.

Incubations—Unless stated otherwise, all incubations were carried out in stoppered plastic tubes in a shaking water bath maintained at 37 °C. Nonincubated controls were stored at 4 °C. Details of individual incubations are described in the legend to the figures. Incubations with sphingomyelinase from *Bacillus cereus* (Boehringer Mannheim) were carried out for 1 h at 37 °C using 1.4 units of sphingomyelinase/mg apoA-I (26). As EDTA-Na_2 inhibits sphingomyelinase (26), the rHDL were dialyzed against TBS without EDTA-Na_2 before incubation. When the incubations were complete the rHDL were dialyzed extensively against TBS with EDTA-Na_2.

The rHDL were isolated from incubation mixtures by ultracentrifugation at 100,000 rpm in the $1.07 < d < 1.25$ g/ml density range using a TLA-100.4 rotor or in the $1.063 < d < 1.25$ g/ml density range using a TLA-100.2 rotor. Two 16-h spins at the lower density and one 16-h spin at the higher density were performed. These procedures were carried out at 4 °C in a Beckman TL-100 tabletop ultracentrifuge. The rHDL were dialyzed extensively against TBS before use.

Electrophoresis—Agarose-gel electrophoresis was carried out as described previously (15). Electrophoretic mobilities were calculated by dividing electrophoretic velocity (migration distance (μm)/time (s)) by the electrophoretic potential (voltage (V)/length of gel (cm)) (27). Mobilities were corrected for pI-dependent retardation as follows (27).

$$\text{Mobility}_{\text{corrected}} = \frac{\text{Mobility}_{\text{agarose}} - 0.136}{1.211} \quad \text{(Eq. 1)}$$

Nondenaturing gradient gel electrophoresis on 3/35% gels (Gradipore, Sydney, Australia) was carried out as described previously (28).

Spectroscopic Studies—These studies were carried out with a Perkin-Elmer LS-50 luminescence spectrometer fitted with a thermostatted cell holder and polarizers. Sample temperatures were controlled by a Lauda RM6T recirculating water bath (Lauda-Königshofen, Germany) and monitored with a digital temperature probe (Baker Medical Research Institute, Melbourne, Australia).

Packing of rHDL phospholipid head groups and acyl chains was monitored by labeling with 1-(4-trimethylammoniumphenyl)-6-phenyl-1,3,5-hexatriene *p*-toluene sulfonate (TMA-DPH) and 1,6-diphenyl-1,3,5-hexatriene (DPH), respectively (29, 30). Polarity of rHDL lipid-water interfacial regions was assessed with 6-propionyl-2-(dimethylamino)-naphthalene (PRODAN) (31). In all cases the molar ratio of phospholipid/probe was 500/1, and the phospholipid concentration was 0.5 mM. The labeling procedures and spectroscopic conditions are described in detail elsewhere (15).

The unfolding of apoA-I was assessed from the wavelength of maximum fluorescence of samples following incubation at 25 °C for 0, 2, 5, 7, and 24 h with 0–8 M guanidine hydrochloride (GdnHCl). Data from the 24-h time points were used for the calculations described below. All calculations are based on the assumption that the unfolding of apoA-I is represented by a two-state process such that, at a given time, the only species present at significant concentrations are either completely folded or completely unfolded (32). The central, linear regions of the unfolding curves were used for the calculations. For a given concentration of GdnHCl, the fraction of unfolded apoA-I was calculated as

$$f_u = \frac{y_f - y}{y_f - y_u} \quad \text{(Eq. 2)}$$

where y_f, y_u, and y represent the respective wavelengths of maximum fluorescence in the folded, unfolded, and transition states.

The equilibrium constant (K) for unfolding was calculated as

$$K = \frac{f_u}{1 - f_u} \quad \text{(Eq. 3)}$$

and the free energy change was calculated as

$$\Delta G = -RT\ln K \quad \text{(Eq. 4)}$$

where R is the gas constant (1.987 cal/degree/mol) and T is the absolute temperature (198.15 K). The concentration of GdnHCl at the midpoint of the denaturation curve was calculated from plots of ΔG *versus* the concentration of GdnHCl using values of ΔG between −1.5 and +1.5 kcal/mol. ΔG_{H_2O}, the conformational stability of apoA-I in the absence of GdnHCl, was determined from the following equation using the denaturant binding model of unfolding described by Pace (32).

$$\Delta G = \Delta G_{H_2O} - \Delta nRT\ln(1 + k_a) \quad \text{(Eq. 5)}$$

where Δn is the difference in the number of binding sites between the folded and unfolded states, k is the equilibrium constant for binding at each site (0.6), and a, the activity of GdnHCl, is calculated from the molarity (M) of GdnHCl as follows

$$a = 0.6761(M) - 0.1468(M)^2 + 0.02475(M)^3 - 0.00132(M)^4 \quad \text{(Eq. 6)}$$

Chemical Analyses—All assays were carried out on a Cobas Para Centrifugal Analyser (Roche Diagnostics, Zurich, Switzerland). Boehringer Mannheim kits were used for phospholipid, UC, and total cholesterol assays. Esterified cholesterol concentrations were calculated as the difference between the total and UC concentrations. The concentration of apoA-I was measured by an immunoturbidometric assay (33).

TABLE I

Influence of SPM on the physical properties of discoidal and spherical rHDL

Discoidal rHDL were prepared by cholate dialysis. Spherical rHDL (SPM/apoA-I molar ratio = 4.9/1) were prepared by incubating discoidal rHDL (SPM/apoA-I molar ratio = 0/1) with LDL and LCAT. The spherical rHDL were depleted of SPM headgroups by incubation at 37 °C for 1 h with sphingomyelinase. These procedures are described under "Experimental Procedures."

Sample	Incubation conditions	Stoichiometry[a] POPC/SPM/UC/CE/apoA-I	λ_{max}[b]	Polarization[c]	Electrophoretic mobility[d]
		mol/mol	*nm*	*P*	$\mu m \cdot s^{-1}/V \cdot cm^{-1}$
Disc		99.6/0.0/10.2/0.0/1.0	332.9 ± 0.2	0.147 ± 0.003	−0.56
Disc		86.0/13.6/10.8/0.0/1.0	332.6 ± 0.2	0.146 ± 0.003	−0.56
Disc		72.5/26.3/11.4/0.0/1.0	332.7 ± 0.3	0.143 ± 0.003	−0.56
Sphere	+Sphingomyelinase	24.5/0.0/4.3/24.8/1.0	332.8 ± 0.8	0.140 ± 0.003*	−0.65
Sphere	−Sphingomyelinase	24.6/4.9/3.6/24.9/1.0	333.3 ± 1.0	0.147 ± 0.002	−0.59
ApoA-I			334.9 ± 0.4	0.194 ± 0.003**	−0.48
Native HDL					−0.65

[a] Means of triplicate determinations which varied by less than 10% were used to calculate concentrations of individual components.
[b] Wavelength of maximum fluorescence. Values represent the mean ± S.D. of four determinations.
[c] Intrinsic steady state fluorescence polarization. Values represent the mean ± S.D. of five determinations.
[d] Determined by agarose gel electrophoresis as described under "Experimental Procedures."
* $p < 0.01$ compared to other spherical rHDL.
** $p < 0.001$ compared to all other values.

SPM concentrations were determined as described by Bradley *et al.* (34).

Statistical Analyses—The Student's *t* test for paired samples was used to determine whether differences between values were significant.

RESULTS

Effect of SPM on the Physical and Spectroscopic Properties of Discoidal and Spherical rHDL (Figs. 1, 2, and 3, and Table I)—Discoidal rHDL containing apoA-I, UC, and varying amounts of POPC and SPM were prepared as described under "Experimental Procedures." The resulting particles had SPM/apoA-I molar ratios of 0/1, 13.6/1, and 26.3/1. The corresponding POPC/apoA-I molar ratios were 99.6/1, 86.0/1, and 72.5/1 (Table I). SPM had little effect on rHDL size, with all the preparations containing a major population of particles 10.0 nm in diameter (Fig. 1). The discs with SPM/apo A-I molar ratios of 0/1 and 13.6/1 also contained minor populations of larger particles. The larger particles were less apparent in the rHDL which had an SPM/apo A-I molar ratio of 26.3/1.

When these discoidal rHDL preparations were incubated with LDL and LCAT, the resulting spherical rHDL all had SPM/apoA-I molar ratios of approximately 5/1 (result not shown). This was consistent with SPM transferring spontaneously between LDL and rHDL. The kinetics of the transfer of SPM from LDL to rHDL was investigated by incubating discoidal rHDL with a POPC/SPM/UC/apoA-I molar ratio of 99.6/0.0/10.2/1.0 in the presence of LDL and LCAT for 0–24 h. The rHDL were then isolated by ultracentrifugation and the molar ratio of SPM/apoA-I was determined (Fig. 2). The SPM/apoA-I molar ratio increased rapidly during the first hour of incubation. Equilibrium was achieved between 6 and 12 h, with a $t_{1/2}$ for the transfer of 0.8 h. After 24 h of incubation, the POPC/SPM/UC/CE/apoA-I molar ratio of the spherical rHDL was 24.6/4.9/3.6/24.9/1.0. In molar terms, SPM accounted for 17% of the phospholipid in the spherical rHDL (Table I).

When the spherical rHDL were depleted of SPM head groups by incubation with sphingomyelinase, the concentrations of the other constituents and the size of the particles did not change (Fig. 1 and Table I). This was not the case for the SPM-containing discoidal rHDL, which were converted quantitatively to larger and smaller particles by incubation with sphingomyelinase (result not shown). These larger and smaller particles were not further characterized.

Various spectroscopic techniques were used to assess the effect of SPM on rHDL structure. The discoidal and spherical rHDL had comparable wavelengths of maximum fluorescence (Table I). This is consistent with the environment of apoA-I Trp residues not being affected by (i) the shape of the rHDL, (ii) the presence of SPM in discoidal rHDL, or (iii) removal of SPM head groups from spherical rHDL by incubation with sphingomyelinase. The wavelengths of maximum fluorescence for the apoA-I in the rHDL were blue-shifted relative to lipid-free apoA-I. In other words, the apoA-I Trp residues in the rHDL are in a more hydrophobic environment than those in lipid-free

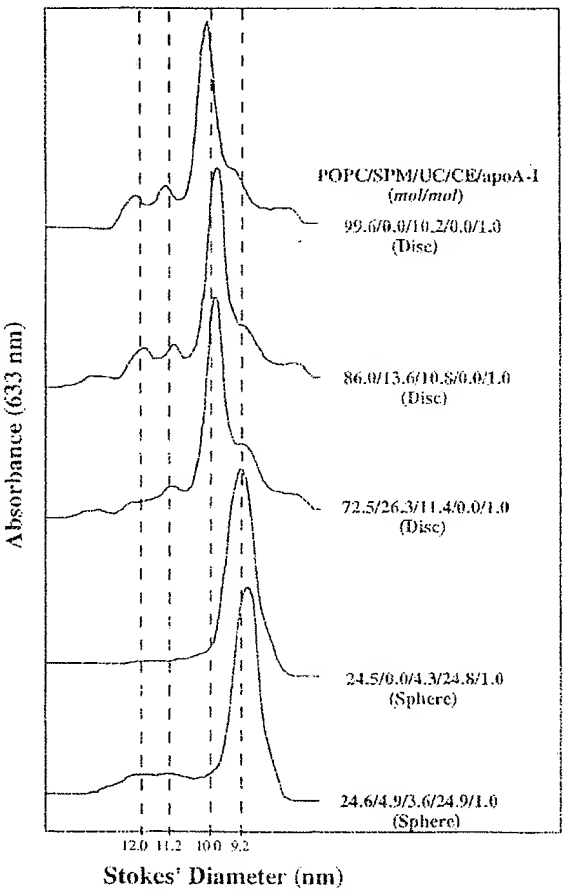

FIG. 1. **Influence of SPM on the size of discoidal and spherical rHDL.** Discoidal and spherical rHDL with varying amounts of SPM were prepared as described under "Experimental Procedures," electrophoresed on 3/35% polyacrylamide nondenaturing gradient gels, and stained with Coomassie Blue G-250. Laser densitometric scans of the stained gels are shown.

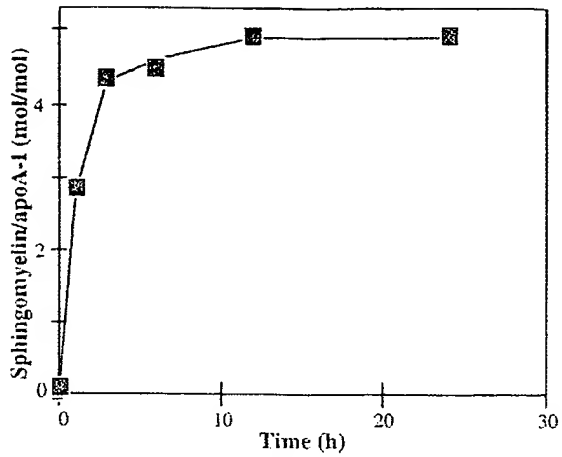

FIG. 2. **Kinetics of the transfer of SPM from LDL to rHDL.** Discoidal rHDL (SPM/apoA-I molar ratio = 0/1; final apoA-I concentration, 0.4 mg/ml) were incubated at 37 °C for 0, 1, 3, 6, 12, or 24 h with LDL (final apoB concentration, 1.5 mg/ml) and LCAT (1.9 nM). The incubation mixtures also contained bovine serum albumin (final concentration, 60 mg/ml) and β-mercaptoethanol (final concentration, 4.0 mM). The final volume of the incubation mixtures was 5.0 ml. When the incubations were complete, the rHDL were isolated by ultracentrifugation in the $1.07 < d < 1.25$ g/ml density range. Concentrations of SPM and apoA-I were determined as described under "Experimental Procedures." Molar ratios were calculated from means of triplicate determinations which varied by less than 10%. The values in the figure represent the mean of two separate experiments.

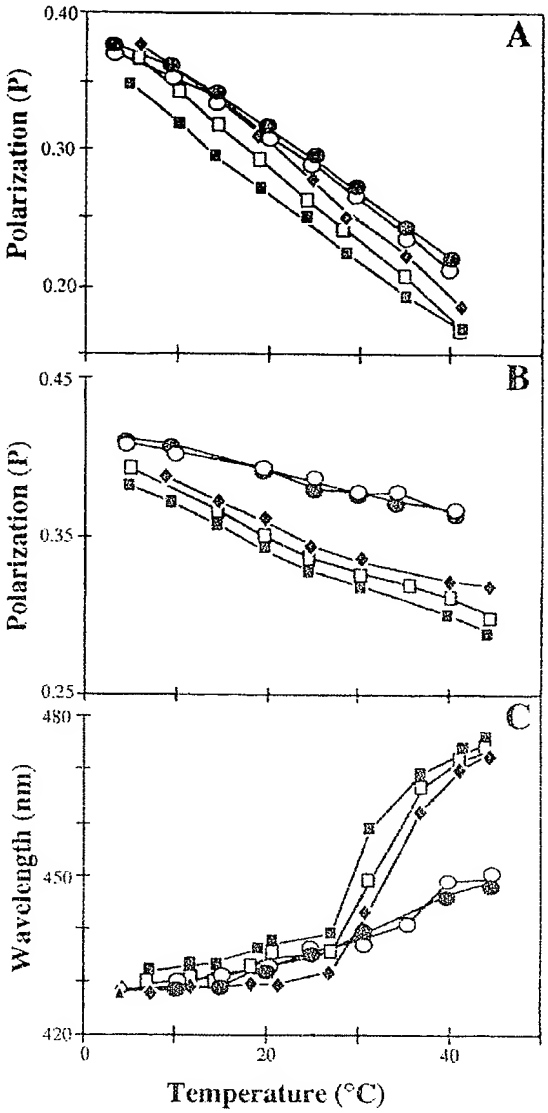

FIG. 3. **Influence of SPM on the structure of discoidal and spherical rHDL.** Discoidal rHDL with SPM/apoA-I molar ratios of 0/1 (■), 13.6/1 (□), and 26.3/1 (♦) and spherical rHDL with SPM/apoA-I molar ratios of 0/1 (○) and 4.9/1 (●) were labeled with DPH (*Panel A*), TMA-DPH (*Panel B*), and PRODAN (*Panel C*). Steady state fluorescence polarization of the DPH- and TMA-DPH-labeled samples and the wavelength of maximum fluorescence of the PRODAN-labeled samples are shown. Values represent the mean of at least three determinations. Experimental errors for the polarization values are ±0.003 and ±1.0 nm for the wavelength of maximum fluorescence.

apoA-I. This is in agreement with what has been reported elsewhere (23, 35).

The local rotational motions of the rHDL apoA-I Trp residues were determined by steady state fluorescence polarization (Table I). Although the discoidal rHDL polarization values decreased as the SPM content of the particles increased, the differences were not statistically significant. This is consistent with SPM having little effect on the local rotational motions of the apoA-I Trp residues in discoidal rHDL. The polarization of the spherical rHDL which contained SPM was comparable to that of the discoidal rHDL, suggesting that particle shape does not affect the rotation of apoA-I Trp residues. However, the polarization decreased when the spherical rHDL were depleted of SPM head groups ($p < 0.01$). This is consistent with the SPM head group restricting the rotation of apoA-I Trp residues in spherical rHDL. In all cases the polarization of lipid-associated apoA-I was significantly lower than that of lipid-free apoA-I ($p < 0.001$). In other words, lipid association enhances local rotational motions of apoA-I Trp residues. This confirms what has been reported previously (23, 35).

The effect of SPM on rHDL surface charge was assessed by agarose gel electrophoresis. The electrophoretic mobilities of the discoidal rHDL were intermediate between lipid free apoA-I and native HDL and were not affected by SPM (Table I). This demonstrates that the SPM molecule does not influence the surface charge of discoidal rHDL. The spherical rHDL with intact SPM migrated slightly slower than native HDL, but more rapidly than discoidal rHDL. After incubation with sphingomyelinase, their electrophoretic mobility increased and was indistinguishable from that of native HDL. This is consistent with the SPM head group decreasing the negative charge on the spherical rHDL surface.

The influence of SPM on phospholipid acyl chain packing order was assessed from the polarization of DPH-labeled spherical and discoidal rHDL (Fig. 3*A*). The SPM molecule increased discoidal rHDL acyl chain packing order as evidenced by the increase in polarization values with increasing SPM/apoA-I molar ratios. The polarization of the spherical rHDL which had been incubated with sphingomyelinase (*open circles*) was slightly lower than that of the spherical rHDL which had been incubated with TBS (*closed circles*). This is consistent with the SPM head group having a minor ordering effect on spherical rHDL phospholipid acyl chains. The additional finding that spherical rHDL have higher polarization values than discoidal rHDL demonstrates that phospholipid acyl chains are more ordered in spheres than in discs. This is in agreement with what has been reported by Jonas *et al.* (35).

Phospholipid head group packing order was assessed from the polarization of TMA-DPH-labeled discoidal and spherical rHDL (Fig. 3*B*). The order of the discoidal rHDL phospholipid head groups increased as the SPM/apoA-I molar ratio in-

creased from 0/1 (*closed squares*) to 13.6/1 (*open squares*) to 26.3/1 (diamonds). The values for the spherical rHDL with (*closed circles*) and without (*open circles*) SPM head groups were comparable. The additional finding that spherical rHDL have more ordered phospholipid head groups than discoidal rHDL confirms what has been reported elsewhere (35).

The rHDL were also labeled with PRODAN, a polarity sensitive fluorescent probe (Fig. 3*C*). The wavelength of maximum fluorescence of the discoidal rHDL increased rapidly at temperatures above 25 °C. The increase was greatest for the discs without SPM (SPM/apoA-I molar ratio = 0/1) (*closed squares*), intermediate when the SPM/apoA-I molar ratio was 13.6/1 (*open squares*) and least when the SPM/apoA-I molar ratio was 26.3/1 (*diamonds*). In other words, SPM inhibits the hydration of discoidal rHDL lipid-water interfacial regions. The wavelength of maximum fluorescence of PRODAN in the spherical rHDL was comparable after incubation in the presence (*open circles*) and absence (*closed circles*) of sphingomyelinase. This demonstrates that SPM head groups do not influence the hydration of the spherical rHDL lipid-water interface. As the increase in the wavelength of maximum fluorescence of the spherical rHDL was small, it seems that the lipid-water interface of these particles is resistant to hydration.

Effect of SPM on the Unfolding and Conformational Stability of ApoA-I in rHDL (Figs. 4 and 5, and Table II)—The influence of SPM on the unfolding of apoA-I was assessed by incubating aliquots of discoidal and spherical rHDL for varying times with increasing concentrations of GdnHCl. The wavelength of maximum fluorescence of apoA-I was determined at 0, 2, 5, 7, and 24 h. For clarity, only the values for 0 (*squares*), 2 (*closed circles*), and 24 h (*open circles*) are shown (Fig. 4). *Panels A*, *B*, and *C*, respectively, show the results for discoidal rHDL with SPM/apoA-I molar ratios of 0/1, 13.6/1, and 26.3/1. The results for spherical rHDL with SPM/apoA-I molar ratios of 0/1 and 4.9/1 are in *Panels D* and *E*, respectively. The unfolding of lipid-free apoA-I is shown in *Panel F*.

Lipid-free apoA-I unfolded rapidly and completely, as evidenced by the comparable wavelengths of maximum fluorescence at 0, 2, and 24 h (Fig. 4*F*). The wavelengths of maximum fluorescence for the discoidal and spherical rHDL (Fig. 4, *A*–*E*) were blue-shifted at 0 and 2 h relative to 24 h, confirming that unfolding of apoA-I is inhibited by lipid association (23, 35). Fig. 5 shows the kinetics of the unfolding of apoA-I at 2.5 M GdnHCl. The apoA-I in the spherical rHDL which had been incubated with sphingomyelinase (*closed circles*) unfolded more rapidly than the apoA-I in the spherical rHDL which had been incubated with TBS (*open circles*). The rate of unfolding of apoA-I in discoidal rHDL decreased as the molar ratio of SPM/apoA-I increased from 0/1 (*open squares*) to 13.6/1 (*closed diamonds*) to 26.3/1 (*open diamonds*). Taken together, these results suggest that the SPM head group may be partly responsible for inhibiting the unfolding of apoA-I in discoidal rHDL. It should also be noted that, irrespective of the SPM content of the particles, the apoA-I in spherical rHDL unfolds more rapidly than the apoA-I in discoidal rHDL.

The influence of SPM on apoA-I stability was assessed from the concentration of GdnHCl required for 50% unfolding of apoA-I ($[GdnHCl]_{1/2}$). Values for $[GdnHCl]_{1/2}$ were determined directly from the 24-h denaturation curves in Fig. 4 and calculated as described under "Experimental Procedures." The results in Table II show good agreement between the two approaches. $[Gdn\text{-}HCl]_{1/2}$ for lipid-free apoA-I was 1.0 M, confirming what has been reported elsewhere (36). $[GdnHCl]_{1/2}$ for the discoidal rHDL increased with the molar ratio of SPM/apoA-I, suggesting that the stability of apoA-I is enhanced by the SPM molecule. When the spherical rHDL were incubated with sphingomyelinase, $[GdnHCl]_{1/2}$ was not affected. In other words, SPM head groups do not influence the stability of apoA-I in spherical rHDL. Although $[GdnHCl]_{1/2}$ increased when the apoA-I was associated with lipid, this change does not necessarily translate into an increase in the stability of apoA-I. For example, although $[GdnHCl]_{1/2}$ for apoA-I in spherical rHDL is

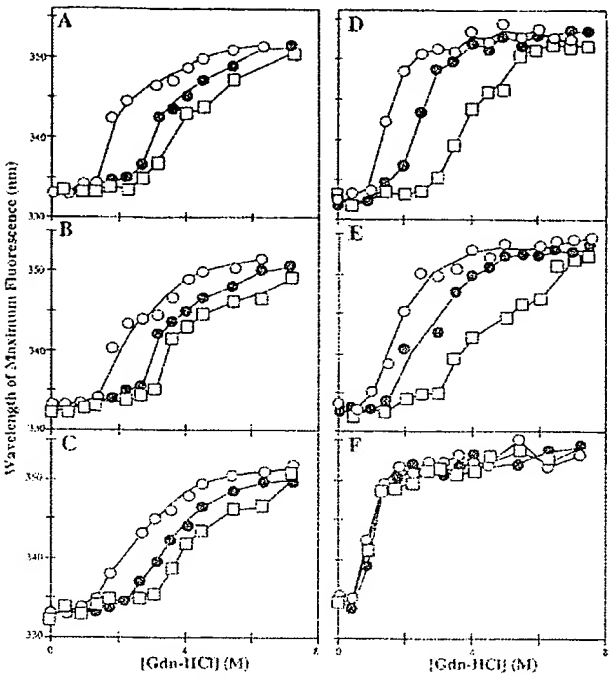

FIG. 4. **Influence of SPM on the GdnHCl-mediated unfolding of apoA-I in discoidal and spherical rHDL.** Discoidal and spherical rHDL and lipid-free apoA-I were incubated with increasing concentrations of GdnHCl for 0 (□), 2 (●), and 24 (○) h as described under "Experimental Procedures." Results for discoidal rHDL with SPM/apoA-I molar ratios of 0/1, 13.6/1, and 26.3/1 are shown in *Panels A*, *B*, and *C*, respectively. Results for spherical rHDL with SPM/apoA-I molar ratios of 0/1 and 4.9/1 are shown in *Panels D* and *E*, respectively. The data in *Panel F* represents lipid-free apoA-I. Each data point represents the mean of triplicate determinations. Experimental errors for the wavelength of maximum fluorescence are ± 1.0 nm.

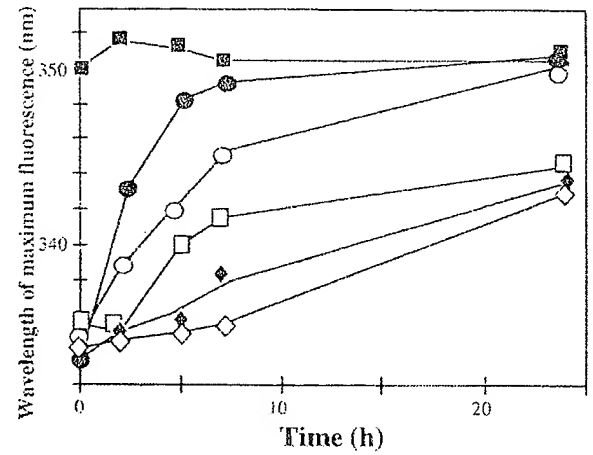

FIG. 5. **Influence of SPM on the kinetics of unfolding of apoA-I in discoidal and spherical rHDL.** Discoidal rHDL with SPM/apoA-I molar ratios of 0/1 (□), 13.6/1 (◆), and 26.3/1 (◇), spherical rHDL with SPM/apoA-I molar ratios of 0/1 (●) and 4.9/1 (○) and lipid-free apoA-I (■) were incubated for 0–24 h with 2.5 M GdnHCl. Values for the wavelength of maximum fluorescence represent the mean of triplicate determinations. Experimental errors are ±1.0 nm.

TABLE II

Effect of SPM on the conformational stability of apoA-I in discoidal rHDL, spherical rHDL, and lipid-free apoA-I

Lipid-free apo A-I and discoidal and spherical rHDL were incubated for 24 h at 25 °C with varying concentrations of GdnHCl as described under "Experimental Procedures."

rHDL	SPM/apoA-I	$[GdnHCl]_{1/2}$[a]	$[GdnHCl]_{1/2}$[b]	ΔG_{H_2O}[c]	Δn[d]
	mol/mol	*M*	*M*	*kcal/mol*	
Disc	0/1	1.8	2.0	1.6	6.5
Disc	13.6/1	2.1	2.2	1.3	4.4
Disc	26.3/1	2.7	2.7	1.7	4.9
Sphere	0/1	1.5	1.6	4.0	17.7
Sphere	4.9/1	1.8	1.8	3.5	13.9
Lipid-free apoA-I		1.0	1.0	3.7	22.6

[a] Concentration of GdnHCl required to achieve 50% unfolding of apoA-I. Determined directly from Fig. 4.

[b] Concentration of GdnHCl required to achieve 50% unfolding of apoA-I. Calculated from the linear region of the 24-h curve in Fig. 4 as described under "Experimental Procedures."

[c] Conformational stability of apoA-I. Calculated as described under "Experimental Procedures."

[d] Difference in the number of GdnHCl binding sites on apoA-I in the folded and unfolded states. Calculated as described under "Experimental Procedures."

greater than that of lipid-free apoA-I, the two preparations have similar conformational stabilities (ΔG_{H_2O}). In addition, although ΔG_{H_2O} for discoidal rHDL is lower than that of lipid-free apoA-I, $[GdnHCl]_{1/2}$ is higher. These discrepancies, which have also been reported by Sparks *et al.* (36) and Davidson *et al.* (13), highlight the fact that $[GdnHCl]_{1/2}$ is influenced by the number of GdnHCl binding sites on apoA-I (Δn) and that this number depends on whether the protein is associated with lipid.

Influence of SPM on the Lipid Transfers Mediated by CETP (Fig. 6) To determine whether SPM influences CETP-mediated transfers of CE and triglyceride (TG), spherical rHDL were preincubated with TBS (Fig. 6, *open symbols*) or sphingomyelinase (*closed symbols*), reisolated by ultracentrifugation, then incubated with CETP and Intralipid for 0–24 h. *Panels A* and *B*, respectively, show the concentrations of CE and TG in the rHDL. *Panel C* shows the total core lipid concentration (*CE + TG*) of the rHDL. CETP mediated the transfer of CE from rHDL to Intralipid as evidenced by the time-dependent decrease in the concentration of rHDL CE (*Panel A*). The concentration of rHDL TG increased during the first 3 h of incubation and decreased thereafter, as reported previously (23) (*Panel B*). The net result of these transfers was a progressive decrease in the concentration of rHDL core lipids (*Panel C*). During the incubation the diameter of the rHDL decreased from 8.6 to 8.0 nm, and lipid-free apoA-I dissociated from the particles (results not shown). The reduction in rHDL size and dissociation of apoA-I, which have been described elsewhere (23), were not influenced by preincubation with sphingomyelinase.

Influence of SPM on the LCAT Reaction (Fig. 7)—Aliquots of discoidal rHDL with POPC/SPM/UC/apoA-I molar ratios of 97.7/0.0/9.6/1.0 and 69.8/26.2/9.8/1.0 were incubated with purified LCAT for 5, 10, 15, 20, and 30 min. The nanomoles of CE generated in the discoidal rHDL with (Fig. 7, *open symbols*) and without SPM (*closed symbols*) is shown. At each time point there was less cholesterol esterification in the SPM-containing rHDL. This confirms what has been reported elsewhere (26). Comparable results were obtained when the experiment was repeated using discoidal rHDL with SPM/apoA-I molar ratios of 0/1 and 26/1 and UC/apoA-I molar ratios of 2/1, 4/1, and 6/1 (results not shown).

DISCUSSION

SPM, a glycosphingolipid consisting of a ceramide backbone and phosphocholine head group, is present in most cell membranes. SPM is transported in the plasma as a component of lipoproteins, but its impact on lipoprotein metabolism, and on HDL metabolism in particular, is poorly understood. This issue is addressed in the present study. Specifically we have determined how the SPM molecule and its head group influence the structure and function of discoidal and spherical rHDL.

To assess the influence of the SPM head group on rHDL metabolism, the rHDL were incubated with sphingomyelinase. Interpretation of these studies was dependent on sphingomyelinase affecting neither rHDL size nor the concentrations of other rHDL constituents. This was achieved for spherical rHDL (Fig. 1 and Table I). The discoidal rHDL, by contrast, were converted into larger and smaller particles during incubation with sphingomyelinase (data not shown). This is not consistent with what has been reported by Subbaiah and Lui (26), who found that the size of discoidal rHDL was not affected by incubation with sphingomyelinase. Given that the rHDL described by Subbaiah and Lui contained egg PC, as opposed to POPC in the present studies, it is possible that this discrepancy may be due to the structural differences between the two phospholipids. As egg PC has a higher proportion of unsaturated acyl chains than POPC (37), it follows that egg PC-containing discoidal rHDL will have less ordered phospholipid acyl chains and more hydrated interfacial regions than POPC-containing discoidal rHDL (38). Given that electrostatic repulsions between phospholipid head groups decrease as hydration of lipid bilayers increases (39), it is possible that rHDL which contain egg PC may be more stable, and resistant to size changes, than rHDL which contain POPC. Regardless of the mechanism, the fact that sphingomyelinase altered the size of the POPC-containing discoidal rHDL precluded investigation of the influence of SPM head groups on their structure.

The problem of sphingomyelinase-mediated changes to the size of discoidal rHDL was circumvented by investigating the influence of the entire SPM molecule on their structure and function. To this end discoidal rHDL were prepared with a range of concentrations of SPM. The phospholipid/apoA-I molar ratio in these rHDL was maintained at approximately 100/1 by appropriate reductions in the concentration of POPC (Table I). The rHDL size was not affected as the SPM/POPC molar ratio increased from 0/1 to 0.4/1 (Fig. 1). This differs from what has been reported by Subbaiah and Lui (26), who found that the diameter of discoidal rHDL with egg PC increased from 10.0 to 16.8 nm when the SPM/egg PC molar ratio increased from 0/1 to 0.5/1. This discrepancy can be explained if the concentration of egg PC was not decreased when SPM was introduced into the rHDL. Under these circumstances the phospholipid/apoA-I molar ratio of the rHDL would increase and the particles would increase in size (40). It is also possible that the increase in rHDL size was due to the somewhat disordered egg PC acyl chains being unable to accommodate the asymmetric SPM molecule. Under these circumstances the rHDL may undergo a

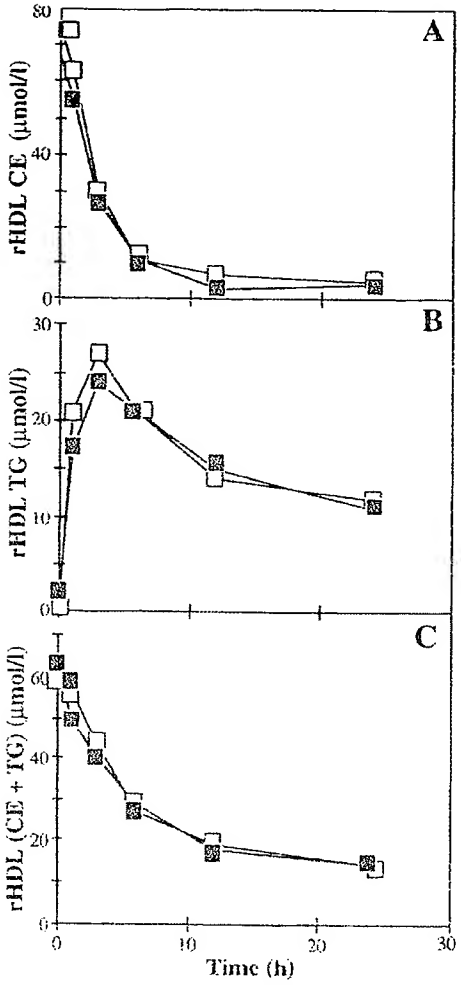

FIG. 6. **Influence of SPM on the CETP-mediated transfer of core lipids between spherical rHDL and Intralipid.** Spherical rHDL were incubated with sphingomyelinase or TBS and reisolated by ultracentrifugation as described under "Experimental Procedures." Their composition is shown in Table I. They were then incubated with TBS, TBS and Intralipid, or TBS, Intralipid, and CETP for 0, 1, 3, 6, 12, or 24 h. The final concentrations of rHDL CE and Intralipid TG (if present) in the incubation mixtures were 0.1 and 3.9 mmol/liter, respectively. The final activity of CETP (if present) was 2.6 units/ml. The final volume of the incubation mixtures was 2.0 ml. When the incubations were complete, the rHDL were isolated by ultracentrifugation in the $1.063 < d < 1.25$ g/ml density range as described under "Experimental Procedures." Concentrations of rHDL CE (*Panel A*), rHDL TG (*Panel B*), and rHDL CE + TG (*Panel C*) are shown. Values in *Panels A* and *B* represent the mean of triplicate determinations which varied by 10% or less.

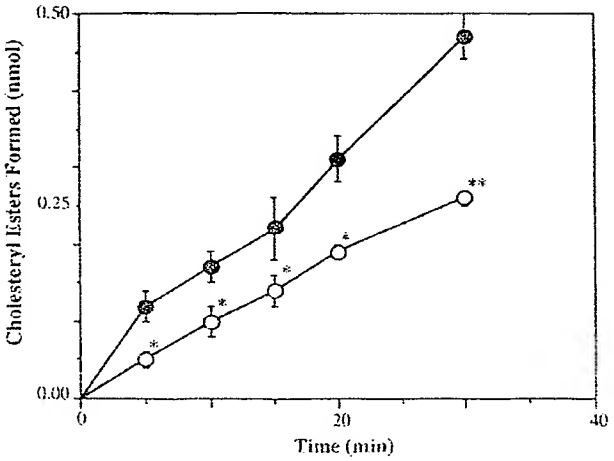

FIG. 7. **Influence of SPM on the LCAT reaction in discoidal rHDL.** Discoidal rHDL with POPC/SPM/UC/apoA-I molar ratios of 97.7/0.0/0.6/1.0 and 69.8/26.2/0.8/1.0 were prepared by cholate dialysis. Both preparations were radiolabeled with [^{3}H]UC as described under "Experimental Procedures." Aliquots of each preparation which contained 3.25 nmol UC were incubated at 37 °C for 5, 10, 15, 20, or 30 min with purified LCAT. Esterification of cholesterol in the rHDL with (○) and without (●) SPM is shown. The data points represent the mean ± S.D. of triplicate determinations. $^*p < 0.05$, $^{**}p < 0.005$

structural reorganization to form larger, more stable particles.

The polarization results in Fig. 3 show that SPM increases the packing order of phospholipid acyl chains and head groups in discoidal rHDL. This is probably because the SPM interfacial region contains a C4–C5 *trans* double bond which has been reported to increase acyl chain packing order (4). The results in Fig. 3 also show that the SPM head group has a slight ordering effect on the acyl chains in spherical rHDL. When these results are taken together it is tempting to speculate that the SPM head group is partly responsible for increasing the acyl chain packing order in discoidal rHDL. However, this is not necessarily the case as DPH partitions differently in discoidal and spherical rHDL. In spherical HDL, DPH is located at the interface of the phospholipid acyl chains and neutral lipid core (41). In discoidal rHDL, DPH intercalates between phospholipid acyl chains (42).

The results of the PRODAN studies (Fig. 3*C*) show that neither the SPM molecule nor its head group affect the hydration of rHDL lipid-water interfacial regions at temperatures less than 25 °C. This is in agreement with the report of Jonas *et al.* (35). Above 25 °C, by contrast, there is a pronounced increase in discoidal rHDL lipid-water interfacial hydration which becomes less apparent as the concentration of SPM increases. This suggests that SPM limits the access of water to the discoidal rHDL lipid-water interface and is consistent with the observation that SPM-containing lipid bilayers have a low permeability to water (43). The additional finding, that above 25 °C, spherical rHDL have less hydrated lipid-water interfaces than discoidal rHDL, suggests that access of water to the surface of spherical rHDL is restricted. This may occur if a proportion of the phospholipid head groups on the surface of spherical rHDL is masked by apoA-I. Finally, as incubation of spherical rHDL with sphingomyelinase does not affect the wavelength of maximum fluorescence of PRODAN, it follows that the SPM head group does not influence the interfacial hydration of these particles.

One of the most unexpected findings to emerge from the present study is that SPM transfers rapidly and spontaneously between LDL and rHDL with a $t_{1/2}$ = 0.8 h. The $t_{1/2}$ for the spontaneous transfer of phosphatidylcholine mass between discoidal rHDL and LDL, by contrast, ranges from 5.8 to 6.9 h (44). This marked difference in half-times probably reflects structural differences between SPM and phosphatidylcholine. The interfacial region of SPM is polar and contains a *trans* double bond, a free hydroxyl group, and an amide bond (4). This region interacts strongly with water and is probably responsible for the rapid transfer of SPM. The corresponding region of phosphatidylcholine, by contrast, comprises a glycerol backbone and possibly the carbonyl portion of the ester bonds. These regions neither interact with water nor facilitate the spontaneous transfer of phosphatidylcholines.

A primary aim of the present study was to determine how SPM influences the metabolism of HDL. The finding that SPM inhibits the LCAT-mediated esterification of UC in discoidal

rHDL (Fig. 7) confirms what has been reported elsewhere (26). This reduction in cholesterol esterification has been attributed to competition between SPM and phospholipids for binding to the active site of LCAT (26). Our results also show that CETP-mediated transfers of CE and TG between spherical rHDL and Intralipid are not affected when the rHDL are depleted of SPM head groups (Fig. 6). As CETP reportedly binds to phospholipid head groups on the surface of HDL (45), this result suggests that the concentration of phospholipids is not rate-limiting for CETP-mediated transfers of core lipids.

When spherical rHDL are subjected to agarose gel electrophoresis they migrate slower than native HDL (Table I). This difference in mobility, which reflects the different surface charges of the preparations, is most likely due to variations in apolipoprotein and phospholipid composition. Native HDL contain several classes of apolipoproteins (46), whereas the rHDL used in the present study contain only apoA-I. Davidson *et al.* (13) have also shown that phospholipid acyl chain composition affects HDL surface charge. As native HDL contain a range of phospholipids (47), it is to be expected that their surface charge differs from that of rHDL which contain only POPC. When spherical rHDL are depleted of SPM head groups, their mobility is indistinguishable from that of native HDL. In other words, removing the SPM head group increases the negative charge on the surface of rHDL. One explanation for this observation is that removing the SPM head group exposes the polar, interfacial region of the molecule and that this region influences the surface charge of rHDL. Alternatively, it is possible that the conformation of apoA-I changes when spherical rHDL are depleted of SPM head groups. However, given that rHDL size is not affected by incubation with sphingomyelinase (Fig. 1), and the conformation of apoA-I is dependent on rHDL size (48), this is not likely.

The finding that SPM decreases the GdnHCl-mediated unfolding of apoA-I in discoidal rHDL (Fig. 5) confirms what has been reported by Swaney (49). This decrease may be due to the hydrogen bonds in the SPM interfacial region enhancing apoA-I-phospholipid interactions and stabilizing the particles. The additional finding that incubation with sphingomyelinase increases the unfolding of apoA-I in spherical rHDL suggests that SPM head groups also enhance phospholipid-apoA-I interactions. An alternative explanation for the increased unfolding of apoA-I in spherical rHDL is that removal of SPM head groups alters the orientation of phosphocholine head groups. Scherer and Seelig have shown that the orientation of these head groups is sensitive to surface charge (50). As the negative charge on the surface of spherical rHDL increases after incubation with sphingomyelinase (Table I), it follows that phosphocholine head group orientation may be altered such that phospholipid-apoA-I interactions decrease and the rHDL are destabilized.

In summary, this study provides an insight into the effect of SPM on the structure and function of discoidal and spherical rHDL. We have shown that the SPM molecule, and its head group, influence the structure and stability of both types of rHDL. When these results are considered, together with the observation that SPM inhibits cholesterol esterification in discoidal rHDL, it follows that factors which regulate the concentration of SPM in HDL may have a significant impact on plasma cholesterol transport.

REFERENCES

1. Hannun, Y. A., and Obeid, L. M. (1995) *Trends Biochem. Sci.* 20, 73–77
2. Hannun, Y. A., and Linardic, C. M. (1993) *Biochim. Biophys. Acta* 1154, 223–226
3. Hannun, Y. A. (1994) *J. Biol. Chem.* 269, 3125–3128
4. Barenholz, Y., and Gatt, S. (1982) in *Phospholipids* (Hawthorn, J. N., and Ansell, G. B., eds) pp. 129–177, Elsevier Biomedical Press, Amsterdam
5. Kawano, M., Miida, T., Fielding, C. J., and Fielding, P. E. (1993) *Biochemistry* 32, 5025–5028
6. Winkler, K. E., and Marsh, J. B. (1989) *J. Lipid Res.* 30, 979–987
7. Reichl, D., and Sterchi, J. M. (1992) *Biochim. Biophys. Acta* 1127, 28–32
8. Kan, C.-C., Ruan, Z.-s., and Bittman, R. (1991) *Biochemistry* 30, 7759–7766
9. McIntosh, T. J., Simon, S. A., Needham, D., and Huang, C.-h. (1992) *Biochemistry* 31, 2012–2020
10. Pons, M. L., Ares, M. P. S., and Slotte, J. P. (1993) *J. Lipid Res.* 34, 1385–1392
11. Xu, X.-X., and Tabas, I. (1991) *J. Biol. Chem.* 266, 24849–24858
12. Gupta, A. K., and Rudney, H. (1992) *J. Lipid Res.* 33, 1741–1752
13. Davidson, W. S., Gillotte, K. L., Lund-Katz, S., Johnson, W. J., Rothblat, G. H., and Phillips, M. C. (1995) *J. Biol. Chem.* 270, 5882–5890
14. Rye, K.-A. (1990) *Biochim. Biophys. Acta* 1042, 227–236
15. Rye, K.-A., and Barter, P. J. (1994) *J. Biol. Chem.* 269, 10298–10303
16. Rye, K.-A., Garrety, K. H., and Barter, P. J. (1992) *J. Lipid Res.* 33, 215–224
17. Osborne, J. C., Jr. (1986) *Methods Enzymol.* 128A, 213–222
18. Weisweiler, P. (1987) *Clin. Chim. Acta* 169, 249–254
19. Matz, C. E., and Jonas, A. (1982) *J. Biol. Chem.* 257, 4535–4540
20. Rye, K.-A., Garrety, K. H., and Barter, P. J. (1993) *Biochim. Biophys. Acta* 1167, 316–325
21. Mahadevan, V., and Soloff, L. A. (1983) *Biochim. Biophys. Acta* 752, 89–97
22. Piran, U., and Morin, R. J. (1979) *J. Lipid Res.* 20, 1040–1043
23. Rye, K.-A., Hime, N. J., and Barter, P. J. (1995) *J. Biol. Chem.* 270, 189–196
24. Tollefson, J. H., Lui, A., and Albers, J. J. (1988) *Am. J. Physiol.* 255, E894–E902
25. Barenholz, M., Scholnick, H. R., and Morfin, R. (1970) *J. Lipid Res.* 11, 583–595
26. Subbaiah, P., and Lui, M. (1993) *J. Biol. Chem.* 268, 20156–20163
27. Sparks, D. L., and Phillips, M. C. (1992) *J. Lipid Res.* 33, 123–130
28. Rye, K.-A. (1989) *J. Lipid Res.* 30, 335–346
29. Lentz, B. R., Barenholz, Y., and Thompson, T. E. (1976) *Biochemistry* 15, 4521–4528
30. Precechtegast, F. G., Haugland, R. P., and Callahan, P. J. (1981) *Biochemistry* 20, 7335–7338
31. Weber, C., and Farris, F. J. (1979) *Biochemistry* 18, 3075–3078
32. Pace, N. C. (1986) *Methods Enzymol.* 131, 266–280
33. Hopkins, G. J., and Barter, P. J. (1989) *Atherosclerosis* 75, 73–82
34. Bradley, C. A., Salhany, K. E., Eritman, S. S., Aleshire, S. L., and Pari, F. F. (1987) *Clin. Chem.* 33, 81–86
35. Jonas, A., Wald, J. H., Toohill, K. L. H., Krul, E. S., and Kezdy, K. E. (1990) *J. Biol. Chem.* 265, 22123–22129
36. Sparks, D. L., Davidson, W. S., Lund-Katz, S., and Phillips, M. C. (1993) *J. Biol. Chem.* 268, 23250–23257
37. Kuksis, A. (1992) *Biochim. Biophys. Acta* 1124, 205–222
38. Stramme, M., and Litman, B. J. (1987) *Biochemistry* 26, 5113–5120
39. Slater, S. J., Ho, C., Taddeo, F. J., Kelly, M. B., and Stubbs, C. D. (1993) *Biochemistry* 32, 3714–3721
40. Wetterau, J. R., and Jonas, A. (1983) *J. Biol. Chem.* 258, 2637–2643
41. Ben-Yashar, V., and Barenholz, Y. (1991) *Chem. Phys. Lipids* 60, 1–14
42. Lentz, B. R. (1989) *Chem. Phys. Lipids* 50, 171–190
43. Barenholz, Y., and Thompson, T. E. (1980) *Biochim. Biophys. Acta* 604, 129–158
44. Jonas, A., Kézdy, K. E., Williams, M. L., and Rye, K.-A. (1988) *J. Lipid Res.* 29, 1349–1357
45. Pattnaik, N. M., and Zilversmit, D. B. (1979) *J. Biol. Chem.* 254, 2782–2786
46. Eisenberg, S. (1984) *J. Lipid Res.* 25, 1017–1058
47. Scanu, A. M. (1979) in *The Biochemistry of Atherosclerosis* (Scanu, A. M., ed) pp. 3–8, Marcel Dekker, New York
48. Jonas, A., Kézdy, K. E., and Wald, J. H. (1989) *J. Biol. Chem.* 264, 4818–4824
49. Swaney, J. B. (1983) *J. Biol. Chem.* 258, 1254–1259
50. Scherer, P. G., and Seelig, J. (1989) *Biochemistry* 28, 7720–7728

INFECTION AND IMMUNITY, Jan. 1995, p. 253–258
0019-9567/95/$04.00+0

Vol. 63, No. 1

Reconstituted High-Density Lipoprotein Neutralizes Gram-Negative Bacterial Lipopolysaccharides in Human Whole Blood

THOMAS S. PARKER,[1] DANIEL M. LEVINE,[1]* JENNIE C. C. CHANG,[2] JULIE LAXER,[2] CHRIS C. COFFIN,[2] AND ALBERT L. RUBIN[1,3]

The Rogosin Institute[1] and Departments of Biochemistry and Surgery,[3] The New York Hospital-Cornell Medical Center, New York, New York 10021, and The Immune Response Corporation, Carlsbad, California 92008[2]

Received 21 March 1994/Returned for modification 18 July 1994/Accepted 11 October 1994

We have tested hypotheses relating lipoprotein structure to function as measured by the relative ability to neutralize endotoxin by comparing natural human lipoproteins, a chemically defined form of reconstituted high-density lipoprotein (R-HDL), and a lipid emulsion (Intralipid). The human whole-blood system was used as an in vitro model of lipopolysaccharide (LPS) binding protein and CD14-dependent activation of cytokine production. When lipoproteins were compared on the basis of protein content, R-HDL was most effective in reducing tumor necrosis factor alpha (TNF-α) production followed in order by very low density lipoprotein, low-density lipoprotein, Intralipid, and natural HDL. However, when these particles were compared by protein, phospholipid, cholesterol, or triglyceride content by stepwise linear regression analysis, only phospholipid was correlated to effectiveness ($r^2 = 0.873$; $P < 0.0001$). Anti-CD14 monoclonal antibodies MY4 and 3C10 inhibited LPS binding protein and CD14-dependent activation of TNF-α production by LPS at LPS concentrations up to ~1.0 ng/ml. R-HDL (2 mg of protein per ml) blocked TNF-α production by LPS from both smooth- and rough-type gram-negative bacteria at concentrations up to 100 ng of LPS per ml but had little effect on heat-killed gram-positive *Staphylococcus aureus* and no effect on other LPS-independent stimuli tested. These results support our hypothesis that LPS is neutralized by binding to phospholipid on the surface of R-HDL and demonstrate that R-HDL is a potent inhibitor of the induction of TNF-α by LPS from both rough- and smooth-form gram-negative bacteria in whole human blood.

Endotoxin is a lipopolysaccharide (LPS) that is anchored by a phospholipid-like lipid A domain in the outer monolayer of the outer membrane of gram-negative bacteria (28). When bacteria are exposed to blood or serum, LPS is released from the bacterial surface as membrane fragments, membrane blebs, or mixed vesicles of bacterial phospholipid and LPS (4, 32). In vivo, these extended molecular complexes of LPS are rapidly cleared from the circulation by the phagocytic system (22). In vitro and in vivo, they are only weakly toxic in the absence of a 60-kDa plasma glycoprotein named LPS binding protein (LBP) (13, 33). LPS is transferred from a single high-affinity binding site on LBP (34) to the CD14 antigen expressed by monocytes (42) and activated neutrophils (41). By "solubilizing" vesicular LPS and transferring it to CD14, LBP lowers the threshold for triggering production and release of a cascade of cytokines, including tumor necrosis factor alpha (TNF-α), interleukin 1, and interleukin 6 (31), from ~100 to <0.1 ng of LPS per ml.

LPS can also bind to plasma lipoproteins: high-density lipoprotein (HDL) (35), low-density lipoprotein (LDL), very low density lipoprotein (VLDL) (11, 12, 16, 36), and chylomicron remnants (17). Binding to any of these lipoproteins greatly reduces the ability of LPS to induce production and release of TNF-α, and interleukins 1 and 6 (1, 6, 24). Although normal plasma lipoprotein concentrations provide a vast excess (>1,000-fold) of LPS binding sites, we and others have recently shown that resistance to endotoxemia is increased in vivo by relatively modest increases in plasma HDL or chylomicron remnant concentrations (8, 16, 18, 21). Further in vivo studies of a chemically defined form of HDL, made by reconstituting apo-HDL protein (R-HDL) or a synthetic peptide with pure phosphatidylcholine (PC), led us to propose a model of the LPS-HDL complex (21). In this leaflet insertion model, the fatty acyl chains of lipid A are anchored in the monolayer of phospholipid that covers the surface of lipoproteins in the same orientation that LPS assumes on the outer membrane of gram-negative bacteria, phospholipid monolayers, liposomes (29, 40), and LDL (38). Binding in this orientation would effectively mask the lipid A domain which carries the biological activity of LPS (28).

The leaflet insertion model predicts that the different capacities of VLDL, LDL, and HDL to neutralize LPS should be proportional to the amount of phospholipid surface available for insertion of the lipid A domain rather than the amount of protein, cholesterol, or triglyceride. The model also predicts that HDL or R-HDL will neutralize endotoxins from both rough (*Escherichia coli* O111:B4) and smooth (*Salmonella minnesota* Re595) gram-negative bacteria that contain complete lipid A domains and either truncated or fully developed polysaccharide domains, respectively. These hypotheses were tested in an in vitro human whole-blood system that preserves the integrity of interactions between plasma proteins and the cellular elements of blood, including those between LBP and CD14.

MATERIALS AND METHODS

LPS. Smooth-strain LPS from *E. coli* O111:B4, *Salmonella typhimurium*, and *Serratia marcescens* and rough-strain LPS from *S. minnesota* R595 (Re) were purchased from List Biological Laboratories, Inc. (Cambell, Calif.). An additional rough-strain LPS, Re595, extracted from *S. minnesota* according to a method described previously (24), was kindly provided by J. C. Mathison and R. J. Ulevitch (Scripps Clinic, La Jolla, Calif.). Stock solutions of LPS (5 mg/ml) were prepared by sonication in 200 mM EDTA, pH 7.0.

Reagents. Heat-killed *Staphylococcus aureus* (HKSA), at 10^{11} cells per ml in saline and monoclonal mouse anti-human antibodies 3C10 (anti-CD14 [37])

* Corresponding author. Phone: (212) 746-1557. Fax: (212) 288-8370.

hybridoma line from the American Type Culture Collection (TIB 228) and IB4 (anti-CD18 [23, 43]) were kindly provided by J. C. Mathison and R. J. Ulevitch. Monoclonal anti-CD14 antibody MY4 (14) was obtained from Coulter Cytometry (Hialeah, Fla.); monoclonal anti-prolactin was obtained from Zymed Laboratories (South San Francisco, Calif.). All antibodies were immunoglobulins and were purified on a protein A column.

Natural lipoproteins. Fresh plasma was drawn from healthy, fasting human volunteers. Lipoproteins were purified by sequential density flotation in a Beckman Ti60 rotor (30), with EDTA (1 mg/ml) used as an anticoagulant and an antioxidant.

R-HDL. HDL was purified from human plasma. Beta lipoproteins were removed, and an HDL-rich concentrate was prepared by the two-stage phosphotungstic acid precipitation method of Burstein and Scolnick (5) as modified by Koizumi et al. (19). HDL was isolated by isopycnic focusing in a Beckman V Ti50 vertical rotor by a modification of the procedure described by Chung et al. (7). The purified HDL was washed by density flotation through a layer of 1.21 g of sodium bromide per ml in a Beckman Ti60 rotor (30). The final HDL preparation contained ~85% apolipoprotein A-I, 15% apolipoprotein A-II, and apolipoprotein CI-III and less than 0.5% albumin when estimated by scanning of sodium dodecyl sulfate gradient polyacrylamide (3 to 30%) gels or by direct measurement of protein in fractions separated by chromatography through columns of Superose 6 and 12 in series.

Purified HDL (5-g lots) was dialyzed against 1 mg of EDTA per ml, lyophilized, and extracted three times with 2 liters of cold chloroform-methanol (2:1, vol/vol) and twice with 500 ml of anhydrous diethyl ether. Apo-HDL was collected by filtration through Whatman no. 4 paper, dried under vacuum, and stored at −70°C.

Apo-HDL was reconstituted (R-HDL) with 99% pure egg phosphatidylcholine (PC) (2:1, wt/wt; Avanti Polar Lipids, Alabaster, Ala.) as described by Matz and Jonas (25), except that the last traces of detergent (cholic acid) were removed by adsorption to Bio-Rad SM2 beads as described by Bonomo and Swaney (3). The molar ratio of protein (as A-I) to PC in the final R-HDL preparation was 1:100, with <0.02 mol% cholic acid and ≤0.1 endotoxin unit per mg of protein (~20 pg of LPS per mg of protein).

Whole-blood TNF-α induction assays. Blood was collected in a heparinized tube, diluted with Hank's balanced salt solution (HBSS) or R-HDL, and transferred to Sarstedt tubes (250 μl per tube) (Hayward, Calif.). LPS or HKSA was added (2.5 μl) at various concentrations in pyrogen-free saline containing 10 mM HEPES (*N*-2-hydroxyethylpiperazine-*N'*-2-ethanesulfonic acid). After incubation for 4 h at 37°C, the tubes were chilled to 4°C and centrifuged at 10,000 × *g* for 5 min. The supernatant was collected for determination of TNF-α.

A two-way dose-response experiment was carried out in the whole-blood system by mixing a 4-mg/ml solution of R-HDL with whole blood at 6.25, 12.5, 25, 33, 50, and 75% (vol/vol) to obtain 0.25, 0.5, 1.0, 1.25, 2.0, and 3.0 mg of R-HDL (as protein) per ml, respectively. Controls contained HBSS in the place of R-HDL. HBSS controls and R-HDL were incubated with *E. coli* O111:B4 LPS at concentrations of 0, 0.1, 0.3, 1, 10, and 100 ng/ml. A total of 72 (2 × 6 × 6) incubations were run in three batches, using blood from a single donor. A 50% HBSS control was included in each run. TNF-α concentrations from incubations at various dilutions (6.25%, 12.5%, etc.) were adjusted by an appropriate factor to normalize them to 50% whole blood. Adjustment for dilution was unnecessary in all subsequent experiments, which were carried out in 50% mixtures.

Comparison of R-HDL to natural lipoproteins and Intralipid. Fresh whole human blood was supplemented with lipoprotein-free human serum or lipoproteins (VLDL, LDL, and HDL), Intralipid, or R-HDL and incubated with 10 ng of *E. coli* O111:B4 LPS per ml for 4 h. Cell-free supernatants were collected for measurement of TNF-α.

TNF-α production in PBM. Blood mononuclear cells were isolated from fresh human plasma or after preincubation with R-HDL by Ficoll-Paque density gradient centrifugation, as previously described (20). Washed human peripheral blood mononuclear cells (PBM) were suspended in RPMI containing 5% fetal calf serum (10^6 cells per ml), and 200,000 cells were added to each well of a 96-well round-bottom plate. The cells were incubated with phytohemagglutinin (2 μg/ml), anti-CD3 (100 ng/ml), *Staphylococcus aureus* enterotoxin B (1 μg/ml; Sigma Chemical Co., St. Louis, Mo.), or LPS (*E. coli* O111:B4; 10 ng/ml) for 64 h (last 16 h in the presence of [^{3}H]thymidine, 1 μCi per well). The cells were harvested and [^{3}H]thymidine uptake was measured as described previously (20). Incubations of PBM with LPS were supplemented with 10% autologous plasma as a source of LBP. The media were collected after a 48-h incubation. TNF-α was measured by immunoassay (Genzyme, Cambridge, Mass.).

Cytolytic assay for TNF-α. TNF-α was measured by using a cytolytic assay with actinomycin D-treated WEHI-13 cells (10). WEHI cells were maintained in tissue culture medium containing RPMI 1640 supplemented with 10% fetal bovine serum (not heated), 10 mM HEPES, 2 mM L-glutamine, 50 U of penicillin per ml, and 50 μg of streptomycin per ml. WEHI cells were plated in 96-well, flat-bottomed microtiter plates at 20,000 cells per well in a 100-μl volume. The cells were allowed to adhere for 2 to 3 h. Samples for measurement were added at 50 μl per well, and serial threefold dilutions were then made. Plates were incubated for 18 to 20 h. MTT [3-(4,5-dimethylthiazol-2-yl)-2,5-diphenyltetrazolium bromide] (Sigma) was added (10 μl of 5 mg/ml in 0.01 M phosphate-buffered saline, pH 7.5), and the plates were incubated for an additional 4 h. Isopropanol containing 40 mM HCl was added to each well (100 μl) to dissolve crystals formed as a product of the metabolism of MTT by the live cells. The degree of cytolysis was directly proportional to the amount of formazan produced and was determined by the optical density at 570 nm corrected for that at 650 nm due to cell debris.

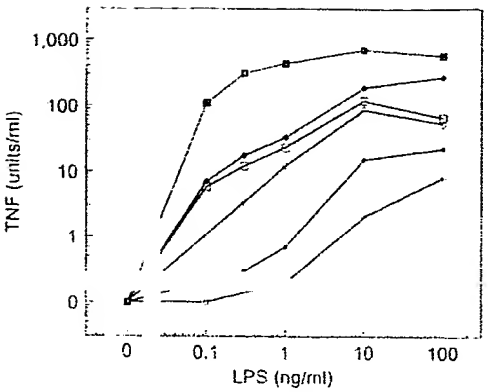

FIG. 1. LPS-dependent TNF-α production in the whole human blood system. Shown is the amount of TNF-α produced by whole human blood in response to *E. coli* O111:B4 LPS. Symbols: control (■) versus R-HDL at 0.5 (◆), 1 (□), 1.3 (◇), 2 (●), and 3 (○) mg/ml.

Each assay contained WEHI cells incubated with no TNF-α (minimum lysis) and cells incubated with a standard (conditioned medium from LPS-treated RAW 264.7 cells), which gave rise to maximum lysis. One unit of TNF-α was defined as the amount of TNF-α resulting in lysis of 50% of the WEHI cells. Samples measured to be below the sensitivity of the assay were assigned a value equal to the lowest standard.

Lipid, lipoprotein, and LPS measurements. Lipid and lipoprotein measurements were carried out using a Roche COBAS FARA II (Roche Diagnostic Systems, Branchburg, N.J.). Total cholesterol and triglycerides were measured by enzymatic methods (Boehringer Mannheim Diagnostics, Indianapolis, Ind.), as described previously (9). Cholic acid was measured with an enzymatic test kit (Sigma). Phospholipid was measured by using an enzymatic method based on measurement of the choline content of PC, sphingomyelin, and lysophosphatidylcholine (Wako Chemical USA, Dallas, Tex.); these phospholipids make up approximately 95% of total serum phospholipids (39). LPS was measured in lipoprotein preparations after dilution and heating at 75°C (15) by the *Limulus* amebocyte lysate method, using the E-Toxate kit (Sigma).

Data analysis and statistics. Results are expressed as mean TNF-α units; the standard deviation was always less than 10% of the mean and is not shown. Lipoprotein concentrations are expressed as milligrams of protein per milliliter unless otherwise stated. Regardless of the units, lipoprotein concentrations in whole-blood incubations refer to the concentration of added lipoprotein. We estimate that endogenous VLDL, LDL, and HDL concentrations, respectively, were less than 0.1, 0.2, and 0.1 mg of protein per ml in incubations containing 50% (vol/vol) whole blood. Stepwise linear regression of TNF-α against lipoprotein protein, PC, TC, and triglycerides was carried out after transformation of the independent variables to $\log_{10}$: $\log(\text{TNF}) = K_{\text{PC}}\log(\text{PC}) + K_{\text{protein}}\log(\text{protein}) + K_{\text{TC}}\log(\text{TC}) + K_{\text{TG}}\log(\text{TG}) + K_{\text{intercept}}$, where K_{PC}, K_{protein}, K_{TC}, K_{TG}, and $K_{\text{intercept}}$ are constants derived from the stepwise regression analysis, TC is total cholesterol, and TG is triglycerides. Mathematical models that included the independent variables protein, cholesterol, and/or triglyceride concentration did not "fit" the data better than the simple model that uses only PC: $\log(\text{TNF}) = K_{\text{PC}}\log(\text{PC}) + K_{\text{intercept}}$.

RESULTS

Dose-response of R-HDL on TNF-α induction by LPS in whole blood. A two-way dose-response experiment was carried out to determine the relationship between TNF-α production in whole blood and the concentrations of *E. coli* O111:B4 LPS and R-HDL. Substantial dose-response relationships, extending over more than 3 $\log_{10}$ units of TNF-α production, were observed between TNF-α production and both LPS and R-HDL concentrations (Fig. 1 and 2). Production of TNF-α decreased steadily with increasing concentrations of R-HDL at LPS concentrations ranging from 0.01 to 100 ng/ml (Fig. 2). The effect of R-HDL was clearly apparent at 0.5 mg/ml and optimal at 2 mg/ml or from approximately half- to twice the concentration of HDL protein in normal human plasma (~1

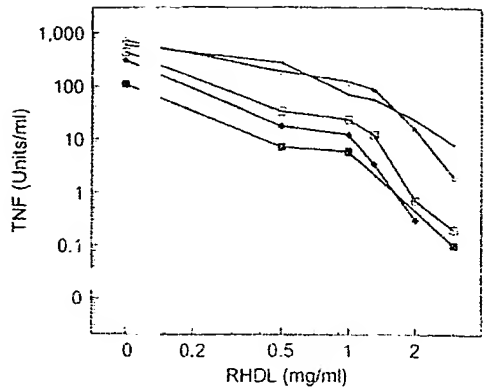

FIG. 2. Effect of R-HDL on LPS-dependent TNF-α production in whole human blood. Shown is the amount of TNF-α produced by whole human blood in response to *E. coli* O111:B4 LPS at 0.1 (■), 0.3 (◆), 1.0 (□), 10 (◇), and 100 (●) mg/ml as affected by increasing R-HDL concentrations.

TABLE 1. Lipoprotein composition

Lipoprotein[a]	% of total lipoprotein mass			
	Protein	PC	TC[b]	TG[c]
VLDL	8.7	14.2	10.2	66.9
LDL	13.8	20.2	32.7	33.3
HDL	52.9	27.4	17.2	2.5
R-HDL	21.1	78.9	ND[d]	ND
LPDS	97.9	2.1	ND	ND
Intralipid	ND	5.6	0.7	93.7

[a] The phospholipid concentrations (milligrams per milliliter) in these stock solutions of purified lipoproteins were as follows: VLDL, 3.62; LDL, 9.51; HDL, 15.17; R-HDL, 38.51; lipoprotein-deficient serum (LPDS), 2.17; and Intralipid, 12.03.
[b] TC, total cholesterol.
[c] TG, triglycerides.
[d] ND, not detectable.

mg/ml). Optimal concentrations of R-HDL (2 mg/ml) reduced TNF-α production to <5% of the control at LPS concentrations up to 100 ng/ml. All subsequent experiments were carried out with R-HDL at 2 mg/ml.

Comparison of R-HDL with natural lipoproteins and Intralipid. The effect of natural lipoproteins, R-HDL, or 20% Intralipid on LPS-mediated TNF-α production is shown in Fig. 3. Lipoprotein concentrations are expressed as milligrams of lipoprotein protein per milliliter. The compositions of the purified lipoproteins are shown in Table 1. As previously reported by others (11, 12, 16), VLDL and LDL more effectively reduced TNF-α production per unit of lipoprotein protein than did natural HDL (Fig. 3, left panel). In contrast, R-HDL was more effective than either VLDL or LDL and substantially more effective than natural HDL, confirming previous findings (9a). Stepwise regression analysis of the data identified a strong inverse correlation between TNF-α production and the concentration of added phospholipid (Fig. 3, right panel; $r^2 = 0.873$; $P < 0.0001$). The correlation was not improved significantly by including terms for protein, cholesterol, and/or triglyceride concentration in the linear regression analysis.

R-HDL inhibits induction of TNF-α production by LPS from rough and smooth gram-negative bacteria. Two rough types (Re595 and *S. minnesota*) and three smooth types (*E. coli*, *S. typhimurium*, and *Serratia marcescens*) of LPS were used to stimulate TNF-α production in the presence or absence of R-HDL (Fig. 4). Virtually complete inhibition of TNF-α production was observed in incubations of whole blood with LPS from smooth types of gram-negative bacteria. LPS from rough-type gram-negative bacteria induced comparatively more TNF-α production in control incubations when compared on an LPS weight basis (nanograms per milliliter) with smooth-type LPS, but R-HDL inhibited TNF-α production by 90% at LPS concentrations of 100 ng/ml.

Anti-CD14 antibodies inhibit TNF-α production by LPS stimulation. Blocking the LBP-CD14 membrane receptor pathway with anti-CD14 monoclonal antibodies (MY4 and 3C10) essentially abolished TNF-α production at low concentrations of LPS up to 0.3 ng/ml (Fig. 5). Antibodies against prolactin (APA) and CD18 (IB4), used as negative controls, had no effect on TNF-α production. R-HDL so completely inhibited TNF-α production in these studies that it was not possible to draw conclusions regarding complementary or competitive interactions between R-HDL and the anti-CD14 monoclonal antibodies.

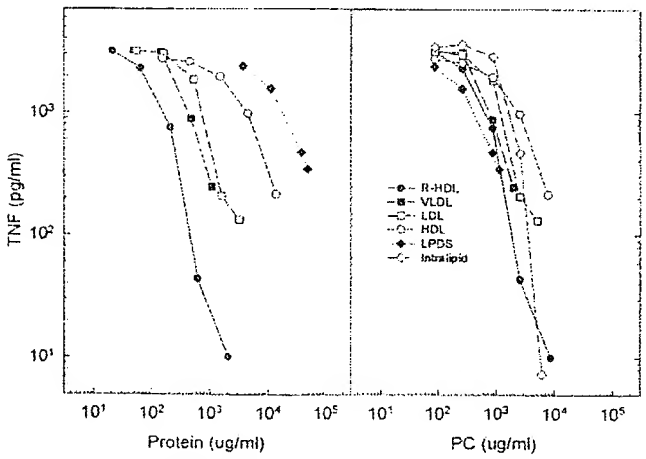

FIG. 3. Inhibition of LPS-dependent TNF-α production is inversely correlated to lipoprotein protein and phospholipid concentration. TNF-α concentration is plotted against protein (left) and phospholipid (right) concentration in whole-blood incubations containing 10 ng of *E. coli* O111:B4 LPS per ml supplemented with R-HDL, VLDL, LDL, HDL, lipoprotein-deficient serum (LPDS), and Intralipid.

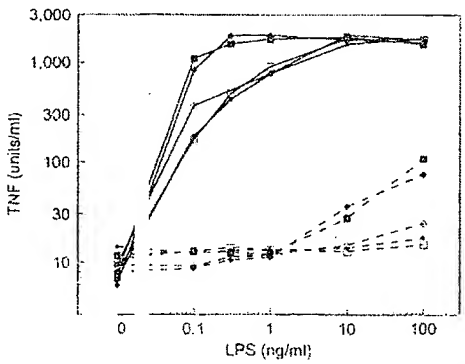

FIG. 4. TNF-α production in response to LPS from rough- and smooth-type gram-negative bacteria: rough types, Re595 (■) and *S. minnesota* (◆); smooth types, *E. coli* (□), *S. typhimurium* (◇), and *Serratia marcescens* (●). Solid lines are incubations without R-HDL; dashed lines are incubations with LPS from the same source in the presence of 2 mg of R-HDL per ml.

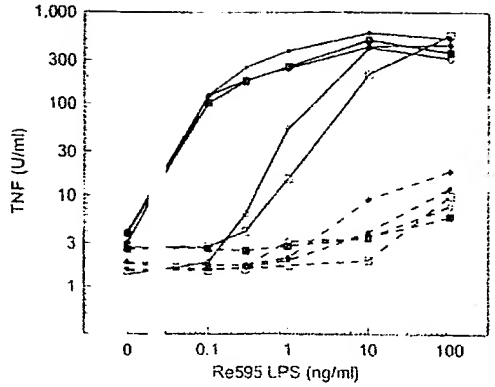

FIG. 5. Comparative inhibition of LPS-stimulated TNF-α production by R-HDL and selected monoclonal antibodies (10 μg/ml). Solid lines are incubations with HBSS; dashed lines are incubations with 2 mg of R-HDL per ml. Symbols: HBSS or R-HDL alone (▣); APA (◆); MY4 (□); 3C10 (◇); TB4 (●).

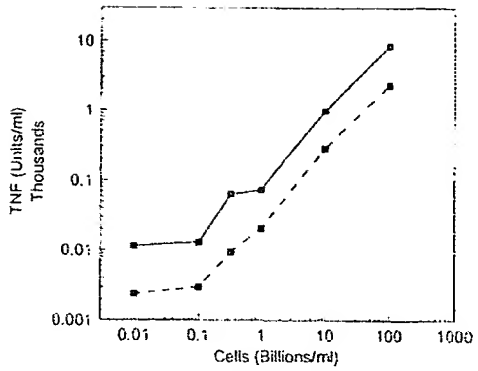

FIG. 6. Induction of TNF-α production by HKSA alone (solid line) and in the presence of 2 mg of R-HDL (dashed line) per ml.

Effect of R-HDL on non-LPS induction of TNF-α. To demonstrate that the effect of R-HDL on cells was not caused by a nonspecific cytotoxicity or immune suppression, we studied the effect of R-HDL on LPS-independent signaling pathways. HKSA activates cells by several pathways, all of which are independent of the LPS signaling pathway. Although R-HDL was not expected to block TNF-α production stimulated by HKSA, we observed a shift in the dose-response curve to the right toward higher concentrations of HKSA (Fig. 6). This could be due to a nonspecific effect of R-HDL on TNF-α production or to neutralization of unidentified gram-positive toxins that meet the structural requirements for binding to R-HDL. To rule out nonspecific effects, whole human blood was incubated with R-HDL (0.5, 1.0, and 2.0 mg/ml) for 4 h as described in Materials and Methods. R-HDL was washed out during preparation of PBM from whole blood. Preincubation with R-HDL had no effect either on the yield of PBM or the percent viable cells as determined by exclusion of trypan blue. The data shown in Table 2 indicate that washed PBM responded normally to LPS and the three non-LPS mitogens (phytohemagglutinin, anti-CD3, and staphylococcal enterotoxin B) tested.

DISCUSSION

Our working hypotheses are that R-HDL and other lipoproteins block the activation of cytokine production by competing successfully with cellular receptors for LPS, that LPS binds to lipoproteins by insertion of the lipid A domain into the phospholipid leaflet that covers the surface of lipoproteins, and that insertion masks the lipid A domain, preventing interactions between LPS and LPS receptors that are necessary for activation of cytokine production. Because LBP and CD14 recognize the lipid A domain of LPS and play an essential role in the cellular response to low (<1 ng/ml) concentrations of LPS in vitro and in vivo, it was important to study lipoprotein-mediated neutralization of LPS in a system that models these interactions.

The studies with anti-CD14 monoclonal antibodies MY4 and 3C10 demonstrated that activation of TNF-α production by LPS was dependent on LBP and CD14 in the human whole-blood system that was used in these experiments. Our finding that R-HDL blocked TNF-α production at low concentrations of LPS supports the hypothesis that R-HDL competed successfully with LBP and CD14 for binding LPS. Activation by higher concentrations of LPS, which can occur through CD14-independent pathways, was also blocked. This suggests that virtually all of the LPS was bound to R-HDL. If nearly all of the added LPS in this system was indeed bound, it would amount to ~18 ng of LPS per mg of phospholipid or <1 molecule of LPS per 3,000 R-HDL disks. (The molar ratio of LPS to PC was estimated by assuming average molecular sizes of LPS [*E. coli* O111:B4] and egg PC molecules to be 12,000 and 786 g/mol, respectively, and the weight ratio of PC to protein measured in the R-HDL to be 2.8 g/g.) Others have pointed to this apparent excess of binding capacity and argued that further increases should be without effect, but neutralization of LPS remains clearly dependent on HDL concentration both in vivo and in vitro (21; this paper). The continued relationship between plasma HDL concentration and inhibition of TNF-α production in response to LPS may be explained by data that indicate that LPS does not dissociate from preformed LPS-lipoprotein complexes while they remain circulating in the vascular compartment (12, 22, 26, 27).

In the whole-blood system used in these experiments, LPS is present initially as free vesicles and LPS-LBP complexes that can interact with cell membranes directly or through receptors, but the concentration of "exchangeable" LPS decreases rapidly with time as the fraction bound to lipoproteins increases. (Wurfel et al. [44] have recently reported the transient presence of exchangeable LPS on LBP and LBP-dependent transfer to R-HDL.) In our system LPS was still present as LPS-lipoprotein complexes, but TNF-α production was 5% or less of that in control incubations when R-HDL and other lipoproteins were added. This would not be the case if LPS readily dissociated from LPS-lipoprotein complexes. Under these conditions, competition among LBP, CD14, and lipoproteins occurs primarily during the first encounter between LPS (or LPS bound to LBP) and lipoproteins or cellular LPS receptors, and the probability of encountering a lipoprotein would be determined by lipoprotein concentration.

Previous studies (11, 12, 16) have compared HDL with the other lipoproteins and concluded that chylomicron remnants and VLDL are as good as or better than HDL at neutralizing LPS. These studies compared lipoproteins by protein content and therefore made the implicit assumption that the protein portion of the lipoprotein particle is the active component that governs binding of LPS. Our model of the LPS-HDL complex predicts that the phospholipid surface of the lipoproteins is the active component. Stepwise regression analysis of the data comparing natural lipoproteins and R-HDL in whole blood showed a strong inverse correlation between TNF-α production and phospholipid concentration. After allowing for the

TABLE 2. Response of PBM to LPS and non-LPS mitogens after R-HDL washout[a]

R-HDL (mg/ml)	TNF-α with LPS (pg/ml)	[^{3}H]thymidine uptake (dpm/10^6 cells)			
		Control	PHA	Anti-CD3	SEB
0	888 ± 211	263 ± 69	32,699 ± 1,401	21,470 ± 1,520	17,462 ± 174
0.5	606 ± 164	301 ± 182	34,476 ± 1,852	16,747 ± 2,317	18,611 ± 2,246
1	872 ± 292	368 ± 163	29,832 ± 4,513	16,242 ± 3,902	17,611 ± 1,343
2	752 ± 66	178 ± 54	30,608 ± 3,938	23,718 ± 654	20,038 ± 3,260

[a] R-HDL was present at the indicated concentrations during a 4-h preincubation in whole blood. R-HDL was removed during the isolation of PBM. Subsequent incubations with LPS and mitogens were carried out in the absence of R-HDL as described in Materials and Methods. TNF-α concentrations in control incubations without LPS averaged 14 pg/ml. Values are given as means ± standard deviations. PHA, phytohemagglutinin; SEB, staphylococcal enterotoxin B.

contribution of phospholipid, no other component, lipoprotein protein, cholesterol, or triglyceride, was significantly correlated with TNF production. Phospholipid content accounted for 94% of the activity of lipoproteins as measured by change in TNF-α production.

Additional support for the role of phospholipid comes from the observations that protein-free Intralipid and cholesterol- and triglyceride-free R-HDL were active. The weak inhibition of TNF-α production by lipoprotein-deficient serum appears to be due to very high density lipoprotein in this fraction as indicated by the presence of phospholipid and by the good correlation of inhibition with phospholipid concentration (Fig. 3, left panel). We conclude that R-HDL was more effective than the natural lipoproteins because it delivered more phospholipid per unit of protein. The small differences in effectiveness between preparations that remained after adjustment in phospholipid could be explained by the presence on the surface of components other than phospholipid that were not measured in this study. Thus, we speculate that the ability of R-HDL to present a clean, unhindered phospholipid surface favors insertion and inactivation of LPS.

The comparative study of LPS from both smooth and rough gram-negative bacteria also supports the hypothesis that the phospholipid leaflet covering lipoproteins provides a surface for insertion and neutralization of LPS. R-HDL neutralized LPS from both groups of bacteria independently of the size and structure of their polysaccharide domains. However, the difference in TNF-α production curves of LPS from both smooth and rough gram-negative bacteria was not expected. LPS isolated from the rough-form bacteria activated TNF-α production at lower concentrations (nanograms per milliliter) than did high-molecular-weight LPS from smooth-form bacteria (Fig. 4). We speculate that this is explained by the difference in molecular weight (the higher molar concentration of the low-molecular-weight forms at the same nanogram-per-milliliter level). Tobias et al. (34) found similar differences in the mass of LPS required to inhibit LBP binding to an LPS-coated surface: 13 versus 50 ng/ml for LPS from *S. minnesota* Re595 compared with *E. coli* O111:B4. Nevertheless, it remains possible that the polysaccharide domains affect association of LPS with LBP or transfer of LPS in LPS-LBP complexes to CD14 and/or R-HDL.

Several lines of evidence argue that inhibition of TNF-α production was not due to a nonspecific inactivation of the cellular immune response. Preincubation with R-HDL had no effect of recovery of viable PBM from whole blood. Moreover, washed PBM responded normally to LPS and mitogens in the absence of R-HDL. However, the modest inhibition of TNF-α production in response to HKSA was unexpected. Gram-positive bacteria do not contain LPS but may contain other membrane-anchored toxins which could in theory be neutralized by R-HDL. Examples include lipoteichoic acid from *Staphylococcus aureus* and the lipoarabinomannans of mycobacteria. At least one pore-forming alpha-toxin of *Staphylococcus aureus* is known to be neutralized by LDL (2). Although natural HDL does not inactivate this alpha-toxin, the effect of R-HDL remains to be determined.

Overall, these results from the human whole-blood system extend our previous data showing increased survival in the mouse endotoxemia model and demonstrate that R-HDL is a potent inhibitor of the induction by LPS of TNF-α production in human whole blood.

ACKNOWLEDGMENTS

We thank J. C. Mathison and R. J. Ulevitch (Scripps Clinic, La Jolla, Calif.) for suggesting the use of the human whole-blood system. We thank Ashwani Khanna and Manikkam Suthanthiran for helpful discussions and assistance with experiments with PBM. We thank Sandra Santos Vizcaino, Ruth Vega, and Evelyne Ribary for technical assistance and for the preparation of apo-HDL, along with summer research students Joanna Tracey and Eliott Silverman, who were supported by the Clark Foundation. We thank Jocelyn Robles and Earla Williams for diagnostic testing and Roche Diagnostic Systems, Branchburg, N.J., for the use of the COBAS FARA II.

This work was supported in part by the Louis Calder Foundation and the Starr Foundation.

REFERENCES

1. Baumberger, C., R. J. Ulevitch, and J. M. Dayer. 1991. Modulation of endotoxic activity of lipopolysaccharide by high-density lipoprotein. Pathobiology 59:378–383.
2. Bhakdi, S., J. Tranum-Jensen, G. Utermann, and R. Fussle. 1983. Binding and partial inactivation of Staphylococcus aureus alpha-toxin by human plasma low density lipoprotein. J. Biol. Chem. 258:5899–5904.
3. Bonomo, E. A., and J. B. Swaney. 1988. A rapid method for the synthesis of protein-lipid complexes using adsorption chromatography. J. Lipid Res. 29: 380–384.
4. Brandtzaeg, P., K. Bryn, P. Kierulf, R. Ovstebo, E. Namork, B. Aase, and E. Jantzen. 1992. Meningococcal endotoxin in lethal septic shock plasma studied by gas chromatography, mass-spectrometry, ultracentrifugation, and electron microscopy. J. Clin. Invest. 89:816–823.
5. Burstein, M., and H. R. Scolnick. 1973. Lipoprotein-polyanion-metal interactions. Adv. Lipid Res. 11:67–108.
6. Cavaillon, J. M., C. Fitting, N. Haeffner-Cavaillon, S. J. Kirsch, and H. S. Warren. 1990. Cytokine response by monocytes and macrophages to free and lipoprotein-bound lipopolysaccharide. Infect. Immun. 58:2375–2382.
7. Chung, B. H., J. P. Segrest, M. J. Ray, J. D. Brunzell, J. E. Hokanson, R. M. Krauss, K. Beaudrie, and J. T. Cone. 1986. Single vertical spin density gradient ultracentrifugation. Methods Enzymol. 128:181–209.
8. Cue, J. I., J. T. DiPiro, L. J. Brunner, J. E. Doran, M. E. Blankenship, A. R. Mansberger, and M. L. Hawkins. 1994. Reconstituted high density lipoprotein inhibits physiologic and tumor necrosis factor alpha responses to lipopolysaccharide in rabbits. Arch. Surg. 129:193–197.
9. Donnelly, T. M., S. F. Kelsey, D. M. Levine, and T. S. Parker. 1990. Control of variance in experimental studies of hyperlipidemia using the WHHL rabbit. J. Lipid Res. 32:1089–1098.
9a. Doran, J. E. Personal communication.
10. Espevik, T., and J. Nissen-Meyer. 1986. A highly sensitive cell line, WEHI 164 clone 13, for measuring cytotoxic factor/tumor necrosis factor from human monocytes. J. Immunol. Methods 95:99–105.

11. Flegel, W. A., A. Wolpl, D. N. Mannel, and H. Northoff. 1989. Inhibition of endotoxin-induced activation of human monocytes by human lipoproteins. Infect. Immun. 57:2237–2245.
12. Freudenberg, M., T. Bog-Hausen, U. Back, and C. Galano. 1980. Interaction of lipopolysaccharides with plasma high-density lipoprotein in rats. Infect. Immun. 28:373–380.
13. Galley, P., D. Heumann, D. Le Roy, C. Barras, and M. Glauser. 1993. Lipopolysaccharide-binding protein as a major plasma protein responsible for endotoxic shock. Proc. Natl. Acad. Sci. USA 90:9935–9938.
14. Griffin, J. D., J. Ritz, L. M. Nadler, and S. F. Schlossman. 1983. Expression of myeloid differentiation antigens on normal and malignant myeloid cells. J. Clin. Invest. 68:932–941.
15. Harris, H. W., E. B. Eichbaum, J. P. Kane, and J. H. Rapp. 1991. Detection of endotoxin in triglyceride-rich lipoproteins in vitro. J. Lab. Clin. Med. 118: 186–193.
16. Harris, H. W., C. Grunfeld, K. R. Feingold, and J. H. Rapp. 1990. Human very low density lipoproteins and chylomicrons can protect against endotoxin-induced death in mice. J. Clin. Invest. 86:696–702.
17. Harris, H. W., C. Grunfeld, K. R. Feingold, T. E. Read, J. P. Kane, A. L. Jones, E. B. Eichbaum, G. F. Bland, and J. H. Rapp. 1993. Chylomicrons alter the fate of endotoxin, decreasing tumor necrosis factor release and preventing death. J. Clin. Invest. 91:1028–1034.
18. Hubsch, A., F. Powell, P. Lerch, and J. Doran. 1993. A reconstituted, apolipoprotein A-I containing lipoprotein reduces tumor necrosis factor release and attenuates shock in endotoxemic rabbits. Circ. Shock 40:14–23.
19. Koizumi, J., M. Kano, K. Okabayashi, A. Jadhav, and G. R. Thompson. 1989. Behavior of human apolipoprotein A-I:phospholipid and apoHDL: phospholipid complexes in vitro and after injection into rabbits. J. Lipid Res. 29:1405–1415.
20. Lander, H. M., P. Sehajpal, D. M. Levine, and A. Novogrodsky. 1993. Activation of human peripheral blood mononuclear cells by nitric oxide-generating compounds. J. Immunol. 150:1509–1516.
21. Levine, D., T. Parker, T. Donnelly, A. Walsh, and A. Rubin. 1993. In vivo protection against endotoxin by plasma high density lipoprotein. Proc. Natl. Acad. Sci. USA 90:12040–12044.
22. Mathison, J., and R. Ulevitch. 1979. The clearance, tissue distribution, and cellular localization of intravenously injected lipopolysaccharide in rabbits. J. Immunol. 123:2133–2143.
23. Mathison, J., E. Wolfson, S. Steinmann, P. Tobias, and R. Ulevitch. 1993. Lipopolysaccharide (LPS) recognition in macrophages. Participation of LPS-binding protein and CD14 in LPS-induced adaptation in rabbit peritoneal exudate macrophages. J. Clin. Invest. 92:2053–2059.
24. Mathison, J. C., E. Wolfson, and R. J. Ulevitch. 1988. Participation of tumor necrosis factor in the mediation of gram negative bacterial lipopolysaccharide-induced injury in rabbits. J. Clin. Invest. 81:1925–1937.
25. Matz, C. E., and A. Jonas. 1982. Reaction of human lecithin cholesterol acyltransferase with synthetic micellar complexes: of apolipoprotein A-I, phosphatidylcholine, and cholesterol. J. Biol. Chem. 257:4541–4546.
26. Munford, R. S., J. M. Anderson, and J. M. Dietschy. 1981. Sites of tissue binding and uptake *in vivo* of bacterial lipopolysaccharide-high density lipoprotein complexes: studies in the rat and squirrel monkey. J. Clin. Invest. 68:1503–1513.
27. Munford, R. S., and J. M. Dietschy. 1985. Effects of specific antibodies, hormones, and lipoproteins on bacterial lipopolysaccharides injected into the rat. J. Infect. Dis. 152:177–184.
28. Raetz, C. R., R. I. Ulevitch, S. D. Wright, C. H. Sibley, A. Ding, and C. F. Nathan. 1991. Gram-negative endotoxin: an extraordinary lipid with profound effects on eukaryotic signal transduction. FASEB J. 5:2652–2660.
29. Romeo, D., A. Hinckley, and L. Rothfield. 1970. Reconstitution of a functional membrane enzyme system in a monomolecular film. II. Formation of a functional ternary film of lipopolysaccharide, phospholipid and transferase enzyme. J. Mol. Biol. 53:491–501.
30. Schumaker, V. N., and D. L. Puppione. 1986. Sequential flotation ultracentrifugation. Methods Enzymol. 128:155–170.
31. Schumann, R. R., S. R. Leong, G. W. Flaggs, P. W. Gray, S. D. Wright, J. C. Mathison, P. S. Tobias, and R. J. Ulevitch. 1990. Structure and function of lipopolysaccharide binding protein. Science 249:1429–1431.
32. Seydel, U., H. Labischinski, M. Kastowsky, and K. Brandenburg. 1993. Phase behavior, supramolecular structure, and molecular conformation of lipopolysaccharide. Immunobiology 187:191–211.
33. Tobias, P. S., J. C. Mathison, and R. J. Ulevitch. 1988. A family of lipopolysaccharide binding proteins involved in responses to gram-negative sepsis. J. Biol. Chem. 263:13479–13481.
34. Tobias, P. S., K. Soldau, and R. Ulevitch. 1989. Identification of a lipid A binding site in the acute phase reactant lipopolysaccharide binding protein. J. Biol. Chem. 264:10867–10871.
35. Ulevitch, R. J., and A. R. Johnston. 1978. The modification of biophysical and endotoxic properties of bacterial lipopolysaccharides by serum. J. Clin. Invest. 62:1313–1324.
36. Van Lenten, B. J., A. M. Fogelman, M. E. Haberland, and P. A. Edwards. 1986. The role of lipoproteins and receptor-mediated endocytosis in the transport of bacterial lipopolysaccharide. Proc. Natl. Acad. Sci. USA 83: 2704–2708.
37. Van Voorhis, W. C., R. M. Steinman, L. S. Hair, J. Luban, M. D. Witmer, S. Koide, and Z. A. Cohn. 1983. Specific antimononuclear phagocyte monoclonal antibodies. Application to the purification of dendritic cells and the tissue localization of macrophages. J. Exp. Med. 158:126–145.
38. Victorov, A. V., N. V. Medvedeva, E. M. Gladkaya, A. D. Morozkin, E. A. Podrez, V. A. Kosykh, and V. A. Yurkiv. 1989. Composition and structure of lipopolysaccharide-human plasma low density lipoprotein complex. Analytical ultracentrifugation, 31P-NMR, ESR and fluorescence spectroscopy studies. Biochim. Biophys. Acta 984:119–127.
39. Warnick, G. R. 1986. Enzymatic methods for quantification of lipoprotein lipids. Methods Enzymol. 129:101–123.
40. Weiser, M. M., and L. Rothfield. 1968. The reassociation of lipopolysaccharide, phospholipid, and transferase enzymes of the bacterial cell envelope. Isolation of binary and ternary complexes. J. Biol. Chem. 243:1320–1328.
41. Wright, S. D., R. A. Ramos, A. Hermanowski-Vosatska, P. Rockwell, and P. A. Detmers. 1991. Activation of the adhesive capacity of CR3 on neutrophils by endotoxin: dependence on lipopolysaccharide binding protein and CD14. J. Exp. Med. 173:1281–1286.
42. Wright, S. D., R. A. Ramos, P. S. Tobias, R. J. Ulevitch, and J. C. Mathison. 1990. CD14, a receptor for complexes of lipopolysaccharide (LPS) and LPS binding protein. Science 249:1431–1433.
43. Wright, S. D., P. E. Rao, W. C. Van Voorhis, L. S. Craigmyle, K. Iida, M. A. Talle, E. F. Westberg, G. Goldstein, and S. C. Silverstein. 1983. Identification of the C3bi receptor of human monocytes and macrophages by using monoclonal antibodies. Proc. Natl. Acad. Sci. USA 80:5699–5703.
44. Wurfel, M. M., S. T. Kunitake, H. Lichenstein, J. P. Kane, and S. D. Wright. 1994. Lipopolysaccharide (LPS)-binding protein is carried on lipoproteins and acts as a cofactor in neutralization of LPS. J. Exp. Med. 180:1025–1035.

Synthesis of the Dioleoyl Derivative of Iododeoxyuridine and Its Incorporation into Reconstituted High Density Lipoprotein Particles

Martin K. Bijsterbosch,* Donald Schouten, and Theo J. C. van Berkel

Division of Biopharmaceutics, Leiden/Amsterdam Center for Drug Research, University of Leiden, P.O. Box 9503, 2300 RA Leiden, The Netherlands

Received June 30, 1994; Revised Manuscript Received September 19, 1994[⊗]

ABSTRACT: We investigated the potential use of reconstituted HDL particles (NeoHDL) as a carrier for lipophilic (pro)drugs. The antiviral drug iododeoxyuridine (IDU) was used as model compound. [^{3}H]-IDU was derivatized with two oleoyl residues to dioleoyl[^{3}H]iododeoxyuridine ([^{3}H]IDU-Ol$_2$), and the lipophilic prodrug was incorporated into NeoHDL by cosonication of [^{3}H]IDU-Ol$_2$ with lipids and HDL apoproteins. NeoHDL particles with the same density, size, and electrophoretic mobility as native HDL were obtained, which contained 7.3 ± 0.8% (w/w) [^{3}H]IDU-Ol$_2$ (about 30 molecules of prodrug per particle). NeoHDL-associated [^{3}H]IDU-Ol$_2$ was stable during 2 h of incubation with human plasma; the prodrug was not appreciably hydrolyzed, nor exchanged with LDL. After intravenous injection of [^{3}H]-IDU-Ol$_2$-loaded ^{125}I-NeoHDL into rats, [^{3}H]IDU-Ol$_2$ disappeared more rapidly from the circulation than the ^{125}I-apoproteins (78.0 ± 8.0% vs 30.1 ± 4.5% of the dose cleared from plasma in 60 min, respectively). The hepatic association of the prodrug was higher than that of the apoproteins (21.6 ± 0.5 vs 5.2 ± 1.0% of the dose at 10 min after injection, respectively). As selective clearance and uptake of lipid esters is also observed with native HDL, this suggests that, *in vivo*, prodrug-loaded NeoHDL may be subject to physiological HDL-specific processing. Lactosylated [^{3}H]IDU-Ol$_2$-loaded ^{125}I-NeoHDL, which contains galactose residues that can be recognized by galactose receptors on parenchymal liver cells, was rapidly cleared from plasma. At 10 min after injection, only about 10% of the injected ^{125}I-apoprotein and ^{3}H-prodrug was left in plasma, and approximately 75% of the injected amount of both labels was recovered in the liver. We conclude that it is possible to convert a hydrophilic drug, like IDU, into a lipophilic prodrug that can be efficiently incorporated into a reconstituted HDL particle with similar properties as native HDL. The same approach may be applied for other water-soluble drugs. In particular, with lactosylated NeoHDL, an efficient delivery system to the liver can be achieved, which allows a more effective treatment of diseases like hepatitis B.

The selective delivery of drugs to their specific cellular targets increases their therapeutic effectivity and reduces undesired interactions with nontarget tissues. A number of soluble molecules, like antibodies and lectins, and particulate systems, such as liposomes and nanoparticles, have been proposed as carriers for drugs (Poznansky & Juliano, 1984; Tomlinson, 1987). Furthermore, in the past decade it has become clear that lipoproteins are also attractive potential carriers (Counsell & Pohland, 1982; Shaw et al., 1987; Bijsterbosch & van Berkel, 1990; Firestone, 1994).

Lipoproteins are spherical lipid/protein complexes responsible for the transport of lipids in the circulation. As endogenous carriers, they are not immunogenic and escape recognition by the reticuloendothelial system ("stealth behavior"). Structurally, they consist of an apolar core, composed of cholesteryl oleate and/or triglycerides, surrounded by a monolayer of phospholipids in which cholesterol and specific apoproteins are embedded. A variety of lipophilic compounds can be incorporated in the lipid moiety of lipoproteins and thus be transported, hidden inside these particles (Counsell & Pohland, 1982; Shaw et al., 1987; Bijsterbosch & van Berkel, 1990; Firestone, 1994). Lipoproteins may therefore be utilized as carriers for lipophilic (pro)drugs. The distribution of a drug associated with a lipoprotein will depend on the metabolic fate of its lipoprotein carrier. Lipoproteins are removed from the circulation by specific receptors that recognize their apoproteins (Bijsterbosch & van Berkel, 1990). In addition, lipoproteins can be directed to nonlipoprotein receptors by chemical modification of the apoproteins. We have shown, for example, that by reductive lactosamination low density lipoprotein (LDL)[1] and high denstity lipoprotein (HDL) can be directed to galactose receptors present on Kupffer cells and liver parenchymal cells, respectively (Bijsterbosch et al., 1989; Bijsterbosch & van Berkel, 1992).

A possible limitation for the use of lipoproteins as drug carriers may be their limited availability. In a recent study we therefore investigated the possibility to synthesize, from commercially available lipids and isolated apoproteins, lipoprotein-like lipid particles. We succeeded in preparing

* Correspondence should be addressed to this author at the Division of Biopharmaceutics, Leiden/Amsterdam Center for Drug Research, P.O. Box 9503, 2300 RA Leiden, The Netherlands. Telephone: (071)-276038; Telefax: (071)-276032.

[⊗] Abstract published in *Advance ACS Abstracts*, November 1, 1994.

[1] Abbreviations: DMAC, dimethylacetamide; EDTA, ethylenediaminetetraacetic acid; HDL, high density lipoprotein; HPLC, high performance liquid chromatography; IDU, 5-iodo-2′-deoxyuridine; IDU-Ol$_1$, 5′-oleoyl-5-iodo-2′-deoxyuridine; IDU-Ol$_2$, 3′,5′-dioleoyl-5-iodo-2′-deoxyuridine; LDL, low density lipoprotein; PBS, phosphate-buffered saline; TLC, thin layer chromatography.

0006-2960/94/0433-14073$04.50/0

particles with properties very similar to the naturally occuring human HDL (Schouten et al., 1993).

In the present study, we extended this earlier work and investigated whether such a reconstituted HDL particle, denoted NeoHDL, can actually be used to transport lipophilic drugs. A number of drugs, for instance, cyclosporin A and some porphyrin derivatives, incorporate spontaneously into lipoproteins (Mraz et al., 1986; De Smidt et al., 1993). Most drugs, however, are not sufficiently lipophilic for incorporation into (neo)lipoproteins. To be incorporated, these drugs have to be converted to a lipophilic prodrug. It has been shown earlier that antineoplastic drugs can be incorporated in LDL after derivatization with lipophilic residues (Firestone et al., 1984; Vitols et al., 1985; De Smidt & van Berkel, 1990). In the present study, we used 5-iodo-2′-deoxyuridine (IDU) as a model compound. IDU is a drug with antiviral activity, and it may also be used as radiosentisizer in the radiotherapy of tumors (Prusoff & Goz, 1974; Santos et al., 1992). IDU is not very lipophilic, and we therefore synthesized a lipophilic prodrug by derivatizing IDU with two oleoyl residues. The resulting lipophilic compound, 3′,5′-dioleoyl-5-iodo-2′-deoxyuridine (IDU-Ol_2), was incorporated into NeoHDL, and the physicochemical properties and biological fate of the prodrug-loaded particles were investigated. By using ^{3}H-labeled IDU-Ol_2 and radioiodination of apoproteins, the incorporated prodrug and apoprotein moiety could be monitored simultaneously.

EXPERIMENTAL PROCEDURES

Reagents and Materials. 2′-Deoxy[6-^{3}H]uridine (25.5 Ci/mmol) was obtained from New England Nuclear Research Products, Boston, Ma. Na^{125}I (carrier free) was supplied by Amersham International, Amersham, Bucks, U.K. Oleoyl chloride, 2′-deoxyuridine, 5-iodo-2′-deoxyuridine, cholesteryl oleate, and Dowex 1 X8 (200−400 mesh) were from Janssen, Beerse, Belgium. Egg yolk phosphatidylcholine was from Fluka, Buchs, Switzerland. Cholesterol and bovine serum albumin (fraction V) were obtained from Sigma, St. Louis, Mo. Lactose was supplied by Merck, Darmstadt, Germany. Sodium cyanoborohydride was from Aldrich, Brussels, Belgium. Emulsifier Safe and Hionic Fluor scintillation cocktails and Soluene-350 were from Packard, Downers Grove, IL. All other reagents were of analytical grade. Thin layer chromatography (TLC) plates (silica 60-F_{254} preformed 0.2-mm-thick layers on aluminium sheets) were obtained from Merck, Darmstadt, Germany.

Synthesis of 5-Iodo-2′-deoxy[6-^{3}H]uridine ([^{3}H]IDU). ^{3}H-Labeled and unlabeled 2′-deoxyuridines were dissolved in 1 N HNO_3 and mixed to a final concentration of 25 mM (5.7 mg/mL; specific radioacticity 50 mCi/mmol). An aliquot of 0.6 mL of this solution was refluxed for 3 h at 70 °C under continuous stirring with 30 mg of I_2 and 0.3 mL of $CHCl_3$. Then, $CHCl_3$ and unreacted iodide were removed by extraction with diethyl ether. The aqueous phase was mixed with 10 mL of 90 mM NaOH and applied to a column of 2 mL of Dowex-1 (X8; 200−400 mesh) in the formate form. The column was subsequently washed with 10 mL of 10 mM NaOH. Fractions were collected and assayed for the presence of (modified) pyrimidine base by measuring radioactivity and absorbance at 288 nm. Less than 5% of the applied radioactivity and UV-absorbing material eluted from the column during application of the diluted aqueous phase and subsequent washing of the column. Virtually all of the applied radioactivity and UV-absorbing material were subsequently eluted from the column by 0.1 M formic acid (total recoveries >90%). The eluted material showed a number of spots upon TLC (solvent: ethyl acetate saturated with 50 mM sodium phosphate buffer, pH 6.0). The major spot, which contained approximately 65% of the applied radioactivity, was at the same position (R_f 0.25) as the 5-iodo-2′deoxyuridine marker (2′-deoxyuridine: R_f 0.06). The column fractions were lyophilized and further purified by preparative TLC on silica gel 60 using the solvent system described above. Material at the same postion as 5-iodo-2′-deoxyuridine marker was scraped off and extracted with methanol. The (radiochemical) purity was >95% as judged by TLC (solvent: methanol/water/ammonia, 80:40:8) and HPLC (column: Nucleosil 120 7C_{18}; eluent: 10% acetonitrile in 0.1 M sodium acetate buffer, pH = 5.45).

Synthesis of 3′,5′-Dioleoyl-5-iodo-2′-deoxyuridine (IDU-Ol_2). To 71 mg of 5-iodo-2′-deoxyuridine (0.2 mmol), dissolved in 8 mL of dry dimethylacetamide (DMAC), were added 1.67 mL of dry pyridine and 0.33 mL of oleoyl chloride (1.0 mmol). After standing for 24 h at 65 °C, the reaction mixture was transferred to a separatory funnel containing 80 mL of H_2O and 40 mL of $CHCl_3$. The organic phase was washed once with 80 mL of 10% (w/v) $NaHCO_3$ and twice with 80 mL of H_2O, and subsequently the solvent was evaporated. The resulting yellowish oil showed two spots upon analysis by TLC (solvent: methanol/dichloromethane, 5:95): a major spot with R_f = 0.75 and a minor spot with R_f = 0.20 (iododeoxyuridine marker: R_f < 0.05). The material was further purified by column chromatography over silica gel 60 (230−400 mesh; column dimensions 0.8 × 12.0 cm) by applying a gradient of 0−5% (v/v) methanol in dichloromethane. Fractions containing the major and the minor product were pooled and analyzed by NMR and mass spectroscopy. The major product was identified as 3′,5′-dioleoyl-5-iodo-2′-deoxyuridine (IDU-Ol_2), and the minor product as 5′-oleoyl-5-iodo-2′-deoxyuridine (IDU-Ol_1).

IDU-Ol_2: yield 79 mg (45%); ^{1}H-NMR (200 MHz, $CDCl_3$): δ 7.96 (s, 1H: C*H*-6), 6.26 (t, 1H: C*H*-1′), 5.32 (t, 4H: C*H* C_9/C_{10}-oleoyl), 5.20 (m, 1H: C*H*-3′), 4.50−4.26 (m, 3H: C*H*-4′, CH_2-5′), 2.52−2.24 (m, 6H: CH_2-2′, CH_2 C_2-oleoyl), 2.00 (d, 8H: CH_2 C_8/C_{11}-oleoyl), 1.61 (m, 4H: CH_2 C_{17}-oleoyl), 1.28 (m, 40H: CH_2 C_5-C_7/C_{12}-C_{16}-oleoyl), 0.86 (t, 6H: CH_3-oleoyl). Mass: 882.5 (calculated: 883.0).

IDU-Ol_1: yield 19 mg (15%); ^{1}H-NMR (200 MHz, $CDCl_3$): δ 7.96 (s, 1H: C*H*-6), 6.23 (t, 1H: C*H*-1′), 5.32 (t, 2H: C*H* C_9/C_{10}-oleoyl), 4.46−4.14 (m, 4H: C*H*-3′, C*H*-4′, CH_2-5′), 2.52−2.28 (m, 4H: CH_2-2′, CH_2 C_2-oleoyl), 2.00 (d, 4H: CH_2 C_8/C_{11}-oleoyl), 1.64 (m, 2H: CH_2 C_{17}-oleoyl), 1.26 (m, 20H: CH_2 C_3-C_7/C_{12}-C_{16}-oleoyl), 0.86 (t, 3H: CH_3-oleoyl). Mass: 618.2 (calculated: 618.6).

NMR spectra were measured at 200 MHz using a JEOL JNM-FX 200 spectrometer. ^{1}H chemical shifts are given in ppm (δ) relative to tetramethylsilane as internal standard. Mass spectra were measured by plasma desorption mass spectrometry in positive ionization mode.

Synthesis of 3′,5′-Dioleoyl-5-iodo-2′-deoxy[6-^{3}H]uridine ([^{3}H]IDU-Ol_2). To 1 mg of [^{3}H]IDU (2.8 μmol; specific radioactivity 13.5 mCi/mmol), dissolved in 0.11 mL of dry DMAC, were added 9 μl of oleoyl chloride (28 μmol) and 23 μl of dry pyridine. After standing for 20 h at 65 °C, the reaction mixture was transferred to a glass vial containing

0.6 mL of $CHCl_3$. The organic phase was washed once with 1.2 mL of 10% (w/v) $NaHCO_3$ and thrice with 1.2 mL of H_2O, and subsequently the solvent was evaporated. The resulting yellowish oil was further purified by TLC on silica gel 60 (dichloromethane/methanol, 95:5). Material at the same position as the IDU-Ol_2 marker (approximately 80% of the applied radioactivity) was scraped off and extracted with dichloromethane/methanol (95:5). The radiochemical purity of the product was >96% as judged by TLC using the solvent systems dichloromethane/methanol (95:5) and ethyl acetate saturated with 50 mM sodium phosphate buffer, pH 6.0.

Determination of Partition Coefficients. Aliquots of 100 nmol of [^{3}H]IDU or [^{3}H]IDU-Ol_2 were dried in 4 mL stoppered glass vials. Then, 1.0 mL of 1-octanol and 1 mL of 50 mM sodium phosphate buffer (pH 7.4) were added, and the mixtures were shaken for 16 h at 37 °C. Samples of the octanol and the aqueous phase were then assayed for radioactivity, and the partition coefficients P (amount in octanol/amount in aqueous phase) were calculated.

Preparation and HDL and HDL Apoproteins. Human HDL (density 1.063−1.210 g/mL) was isolated by two repetitive centrifugations as described earlier (Redgrave et al., 1975). HDL was subsequently depleted of apoE-containing material using a Sepharose−heparin column (Weisgraber & Mahley, 1980). To isolate apoproteins, HDL was dialyzed against water and freeze-dried. The lyophilized material was extracted with ethanol/diethyl ether (3:1) for 16 h at 4 °C and, subsequently, centrifuged for 5 min at 2000g. The supernatant was aspirated, and the pellet was subjected to two similar extractions for 4 h each. The final pellet was washed with ether, dried, and stored under nitrogen at −20 °C.

Preparation of [^{3}H]IDU-Ol_2-Loaded NeoHDL. The following lipids, dissolved in $CHCl_3$, were mixed in a 20 mL glass scintillation counting vial: 3.6 mg of phosphatidylcholine, 1.8 mg of cholesteryl oleate, 0.9 mg of cholesterol, and 0.9 mg of [^{3}H]IDU-Ol_2. The solvent was evaporated under a stream of nitrogen. Subsequently, 10 mL of sonication buffer (10 mM Tris-HCl buffer, pH 8.0, containing 0.1 M KCl, 1 mM EDTA, and 0.025% NaN_3), degassed and saturated with nitrogen, was added, and the contents of the vial was sonicated with a macrotip (14-μm output) under a stream of nitrogen. The temperature was maintained at 49−52 °C. The sonication was stopped after 60 min, and the temperature was lowered to 42−44 °C. Sonication was continued, and 20 mg of HDL apoproteins, dissolved in 1 mL of 4 M urea, were added in 10 equal portions over a period of 10 min. After all protein was added, the mixture was sonicated for a further 20 min. The sonication mixture was then centrifuged at 12000g for 5 min to remove large particles. Subsequently, the preparation was subjected to density gradient ultracentrifugation as described earlier (Redgrave et al., 1975). Particles with a density ranging from 1.08 to 1.18 g/mL (50−75% of the applied radioactivity) were pooled and concentrated. The NeoHDL was further purified by FPLC using a Superose-6 column (Pharmacia, Uppsala, Sweden). The column (60 × 1.8 cm) was eluted with 0.1 M sodium phosphate buffer, pH 7.0, containing 0.5 M NaCl and 10 mM EDTA (flow rate 24 mL/h). Fractions eluting at the the same position as native HDL (60−90% of the applied radioactivity) were collected, pooled, and concentrated.

Physicochemical Characterization of [^{3}H]IDU-Ol_2-Loaded NeoHDL. The chemical composition of [^{3}H]IDU-Ol_2-loaded NeoHDL was determined as follows. Protein was measured by the method of Lowry et al. (1951), using bovine serum albumin as a standard. Cholesterol and cholesteryl oleate were determined by an enzymatic method as described earlier (Nagelkerke et al., 1986). Phosphatidylcholine was determined using a colorometric test kit provided by Boehringer Mannheim, Mannheim, Germany. [^{3}H]IDU-Ol_2 was assayed by measuring its radioactivity.

The size of [^{3}H]IDU-Ol_2-loaded NeoHDL was determined by FPLC (Superose-6 column) and by photon correlation spectroscopy, using a Malvern 4700c submicron particle analyzer, at an angle of 90°.

Radioiodination of [^{3}H]IDU-Ol_2-Loaded NeoHDL. [^{3}H]-IDU-Ol_2-loaded NeoHDL was labeled with ^{125}I using iodine monochloride as described earlier (Bijsterbosch & van Berkel, 1992). The resulting double-labeled preparations contained approximately equal amounts of ^{125}I and ^{3}H. The distribution of ^{125}I over apoproteins and lipids in [^{3}H]IDU-Ol_2-loaded ^{125}I-NeoHDL was determined by extraction as described by Folch et al. (1957). The apoprotein moiety contained 98.9 ± 0.2% of the ^{125}I, and 0.5 ± 0.1% was present in the lipids. The remaining 0.6 ± 0.1% was free ^{125}I (means ± SEM of 3 determinations).

Lactosylation of [^{3}H]IDU-Ol_2-Loaded NeoHDL. [^{3}H]IDU-Ol_2-loaded NeoHDL (1 mg/mL in 0.1 M sodium phosphate buffer, pH 7.0, containing 1 mM EDTA) was incubated under sterile conditions at 37 °C with lactose and sodium cyanoborohydride to final concentrations of 100 and 50 mg/mL, respectively. After 60 h, the reaction was stopped by the addition of 0.2 volume of 0.6 M NH_4HCO_3. Subsequently, sodium cyanoborohydride and unbound lactose were removed by exhaustive dialysis against PBS (10 mM sodium phoshate buffer, containing 0.15 M NaCl and 1 mM EDTA).

In Vivo Plasma Clearance and Liver Association. Male Wistar rats (225−325 g) were used. The animals were anesthesized by intraperitoneal injection of 15−20 mg of sodium pentobarbital, and the abdomen was opened. Radiolabeled ligands were injected via the vena penis. At the indicated times, blood samples of 0.2−0.3 mL were taken from the inferior vena cava and collected in heparinized tubes. The samples were centrifuged for 2 min at 16000g and assayed for radioactivity. The total amount of radioactivity in plasma was calculated using the equation: plasma volume (mL) = [0.0219 × body weight (g)] + 2.66 (Bijsterbosch et al., 1989). At the indicated times, liver lobules were tied off and excised. At the end of the experiment the remainder of the liver was removed. The amount of liver tissue tied off successively did not exceed 15% of the total liver mass. Radioactivity in the liver at each time point was calculated from the radioactivities and weights of the liver samples and corrected for radioactivity in plasma present in the tissue at the time of sampling (85 μL/g fresh weight; Caster et al., 1955).

Determination of Radioactivity. Samples containing ^{3}H were counted in a Packard Tri-Carb 1500 liquid scintillation counter, using Emulsifier Safe or Hionic Fluor scintillation cocktails. Liver samples, TLC scrapings, and gel slices were first digested with Soluene-350. In samples containing both ^{125}I and ^{3}H, the ^{125}I-radioactivity was counted in a Packard Auto-Gamma 5000 counter, and the ^{3}H-activity was mea-

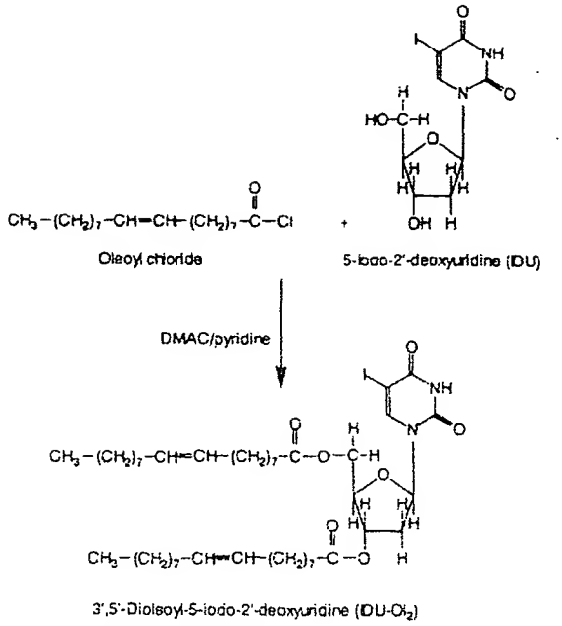

FIGURE 1: Synthesis of IDU-Ol_2.

sured as described above and corrected for the contribution of ^{125}I.

Assay of the Stability of NeoHDL-Associated IDU-Ol_2. [^{3}H]IDU-Ol_2-loaded NeoHDL (10 μg of protein/mL) was incubated with serum or phosphate-buffered saline at 37 °C in aliquots of 0.16 mL. After 2 h, the incubation was terminated by the addition of 0.6 mL of chloroform/methanol (1:2). Phases were separated by adding 0.2 mL of chloroform and 0.2 mL of 0.28 N HCl. The upper (aqueous) phase was taken off, and the lower (organic) phase was washed thrice with 0.5 mL of 0.1 N HCl. The aqueous phase was combined with the wash fluids and counted for radioactivity. The organic phase was subjected to TLC (solvent: methanol/dichloromethane, 5:95). Approximately 10 μg of IDU-Ol_2 and IDU-Ol_1 were added as carrier and to enable detection. The IDU-Ol_2 and IDU-Ol_1 spots were scraped off and counted for radioactivity.

RESULTS

Synthesis of and Characterization of (^{3}H-Labeled) IDU-Ol_2. The synthesis of IDU-Ol_2 was based on a previously described procedure for the preparation of dioleoylfluorodeoxyuridine (Nishizawa et al., 1965). In short, oleoyl chloride was allowed to react with IDU in a mixture of dimethylacetamide and pyridine (Figure 1). IDU-Ol_2 was subsequently purified from the reaction mixture by extraction and silica column chromatography. The identity of IDU-Ol_2 was confirmed by ^{1}H-NMR and mass spectroscopy. To be able to monitor the biological fate of the (pro)drug, a ^{3}H-labeled derivative was synthesized. First, [^{3}H]IDU was synthesized from 2'-deoxy[6-^{3}H]uridine by electrophilic substitution, essentially as described by Prusoff (1959). The UV spectrum of the product was identical to that of reference IDU (a maximum at 279 nm and a minimum at 254 nm), but clearly different from that of 2'-deoxyuridine (Figure 2). The radiochemical purity was >95%, as estimated by thin layer chromatography and HPLC. [^{3}H]IDU was subsequently derivatized with oleoyl chloride as described above.

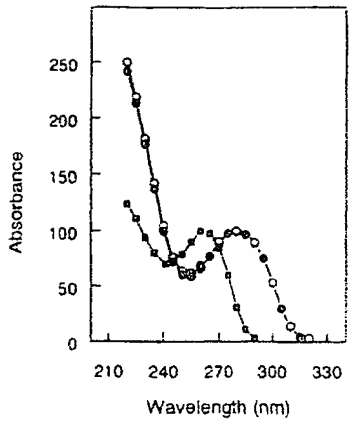

FIGURE 2: Spectral properties of [^{3}H]iododeoxyuridine and deoxyuridine. Iododeoxyuridine (●), [^{3}H]iododeoxyurine (○), and deoxyuridine (■) were dissolved in 0.1 M NH_4OH, and their absorption in the ultraviolet region was determined spectrophotometrically. The results are expressed as % of the maxima at 262 nm (■) and 279 nm (○, ●).

Table 1: Chemical Composition of [^{3}H]IDU-Ol_2-Loaded NeoHDL; Comparison with Native ApoE-Depeleted HDL[a]

	% of total wt	
	[^{3}H]IDU-Ol_2-loaded NeoHDL	native apoE-free HDL
protein	52.3 ± 0.2	48.9 ± 3.9
phosphatidylcholine	26.5 ± 0.9	28.9 ± 1.4
cholesterol	3.6 ± 0.4	2.9 ± 0.5
cholesteryl oleate	10.3 ± 0.6	19.4 ± 0.6
[^{3}H]IDU-Ol_2	7.3 ± 0.8	

[a] The chemical compositions of [^{3}H]IDU-Ol_2-loaded NeoHDL and native apoE-depleted HDL were analyzed as described in the Experimental Procedures. Values given are means ± SEM of 3 different preparations.

[^{3}H]IDU-Ol_2 was identical to unlabeled IDU-Ol_2 as judged by its chromatographic behavior in two TLC systems. Measurement of the partition coefficients of [^{3}H]IDU-Ol_2 and [^{3}H]IDU confirmed that the prodrug was much more lipophilic than the parent compound: log P values were found to be 4.07 ± 0.01 and −0.65 ± 0.01, respectively (means ± SEM of 3 determinations).

Preparation of [^{3}H]IDU-Ol_2-Loaded NeoHDL. The procedure used to prepare [^{3}H]IDU-Ol_2-loaded NeoHDL was based on previously described methods for the preparation HDL-like particles (Atkinson & Small, 1986; Pittman et al., 1987; Jonas et al., 1989; Schouten et al., 1993). In brief, a lipid emulsion was obtained by cosonication of phophatidylcholine, cholesterol, cholesteryl oleate, and [^{3}H]IDU-Ol_2. Subsequently, HDL apoproteins were added to the emulsion, and sonication was continued for another 30 min. The resulting [^{3}H]IDU-Ol_2-loaded NeoHDL was purified by density gradient centrifugation and FPLC.

Physicochemical Characterization of [^{3}H]IDU-Ol_2-Loaded NeoHDL. The chemical composition of [^{3}H]IDU-Ol_2-loaded NeoHDL is given in Table 1, and is compared with the composition of native apoE-depleted HDL. The formation of the prodrug-loaded particles was very reproducible; only small variations were found in the compositions of different preparations. The particles contained a substantial amount of IDU-Ol_2: 7.3 ± 0.8% of the total weight (15.4 ± 1.6% of the lipid moiety). From the size, density, and composition

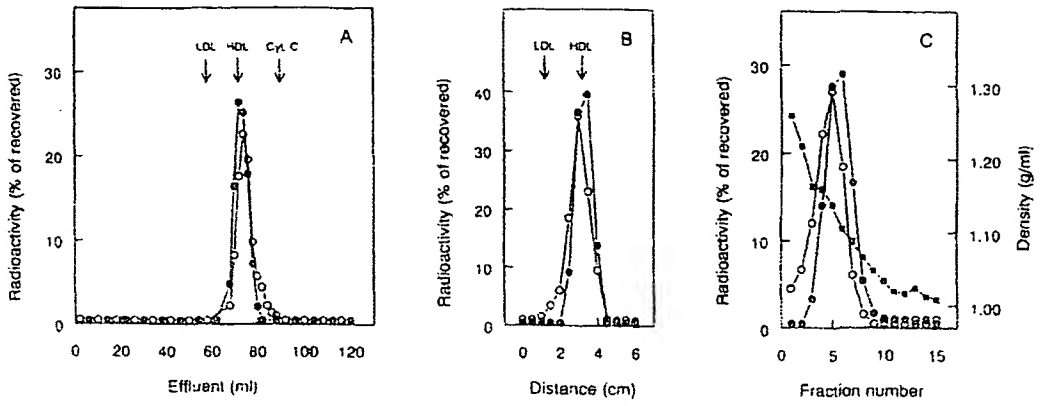

FIGURE 3: Analysis of the physical properties of [^{3}H]IDU-Ol$_2$-loaded ^{125}I-NeoHDL by gel chromatography (A), gel electrophoresis (B), and density gradient centrifugation (C). (A) [^{3}H]IDU-Ol$_2$-loaded ^{125}I-NeoHDL (0.25 mg of protein) was injected onto a Superose-6 column (60 × 1.8 cm), and the column was eluted with 0.1 M sodium phosphate buffer, pH 7.0, containing 0.5 M NaCl and 10 mM EDTA (flow rate 6 mL/h). Fractions of 2.0 mL were collected and assayed for ^{3}H (●) and ^{125}I (○). The results are expressed as % of the recovered radioactivity (recoveries >96%). The elution volumes of LDL, HDL, and cytochrome *c*, which were used to calibrate the column, are indicated by arrows. (B) [^{3}H]IDU-Ol$_2$-loaded ^{125}I-NeoHDL (0.025 mg of protein) was subjected to electrophoresis in a 0.75% (w/v) agarose gel at pH 8.8 (75 mM Tris−hippuric acid buffer). The gel was cut in slices that were assayed for ^{3}H (●) and ^{125}I (○). The radioactivity in each slice is given as % of the recovered radioactivity (recoveries >97%). Arrows indicate the positions of LDL and HDL markers. (C) [^{3}H]IDU-Ol$_2$-loaded ^{125}I-NeoHDL (0.25 mg of protein) was subjected to density gradient centrifugation (Redgrave et al., 1975). The gradient (12.0 mL) was fractionated in fractions of 0.8 mL. The fractions were assayed for ^{3}H (●) and ^{125}I (○), and their densities (■) were measured. The results are expressed as % of the recovered radioactivity (recoveries >97%).

of the prodrug-loaded NeoHDL, it can be calculated that each particle contains about 30 IDU-Ol$_2$ molecules. The results further show a remarkable similarity with the composition of native HDL.

The size of the prodrug-loaded particles was studied using photon correlation spectroscopy, and compared to that of native HDL. The mean sizes of [^{3}H]IDU-Ol$_2$-loaded NeoHDL and native apoE-depleted HDL were found to be 9.7 ± 0.6 and 9.4 ± 0.7 nm, respectively (means ± SEM of 3 preparations). The physical properties of [^{3}H]IDU-Ol$_2$-loaded NeoHDL were further studied by size exclusion chromatography, agarose gel electrophoresis, and density gradient centrifugation. For these studies, the apoproteins of the particles were also labeled with ^{125}I. This allowed the monitoring of both the incorporated ^{3}H-labeled prodrug and the ^{125}I-labeled apoproteins. Figure 3A shows the elution profile of [^{3}H]IDU-Ol$_2$-loaded ^{125}I-NeoHDL on a calibrated Superose-6 FPLC column. Both ^{125}I and ^{3}H eluted at the same position as native HDL. This finding indicates that the size of [^{3}H]IDU-Ol$_2$-loaded NeoHDL is similar to that of native HDL, which corroborates the results of the analysis by photon correlation spectroscopy. Figure 3B shows the result of agarose electrophoresis of [^{3}H]IDU-Ol$_2$-loaded ^{125}I-NeoHDL. Lipoproteins subjected to this type of electrophoresis are separated mainly according to their electric charge. Both ^{125}I and ^{3}H were recovered at the same position as the native HDL marker. The results of density gradient centrifugation of [^{3}H]IDU-Ol$_2$-loaded ^{125}I-NeoHDL are shown in Figure 3C. More than 90% of both ^{125}I and ^{3}H radioactivity was recovered at a density between 1.088 and 1.218 g/mL, which corresponds to the density of native HDL. Thus, our findings indicate that size, density, and charge of IDU-Ol$_2$-loaded NeoHDL are very similar to those of native HDL. Moreover, because in all experiments ^{125}I and ^{3}H behaved similarly, the results further indicate that under the conditions employed the particles are stable.

Stability of IDU-Ol$_2$-Loaded NeoHDL in Serum in Vitro. The stability of NeoHDL-associated IDU-Ol$_2$ in serum was tested by incubating prodrug-loaded NeoHDL in rat serum at 37 °C. After 2 h of incubation, the amounts of [^{3}H]IDU-Ol$_2$, [^{3}H]IDU-Ol$_1$, and water-soluble [^{3}H]metabolites were determined. Table 2 shows that during incubation the amount of IDU-Ol$_2$ decreased only slightly, with a concomittant small increase in the amount of water-soluble metabolites.

Exchange of NeoHDL-associated IDU-Ol$_2$ with other serum proteins was studied by incubating the prodrug-loaded particle with human serum for 1 h at 37 °C. After incubation, the distribution of IDU-Ol$_2$ over serum proteins was determined by density gradient centrifugation. Human serum was used in this experiment to be able to detect possible exchange with LDL (rat serum contains mainly HDL and very little LDL). Figure 4 shows that, although a high amount of LDL was present in the incubation mixture, hardly any exchange of the prodrug from NeoHDL to LDL had occurred.

In Vivo Fate of [^{3}H]IDU-Ol$_2$-Loaded NeoHDL: Effect of Lactosylation. To investigate the biological fate of the prodrug-loaded particles, rats were injected with [^{3}H]IDU-Ol$_2$-loaded ^{125}I-NeoHDL. The plasma clearance of both labels was monitored. Because of the major role of the liver in the metabolism of native HDL (Glass et al., 1985), we also measured the association of radioactivity with the liver. The results are shown in Figure 5A. As judged by the behavior of the ^{125}I-labeled apoproteins, the particles were slowly cleared from the circulation, just as native ^{125}I-labeled HDL (Schouten et al., 1988). Only a small proportion of the ^{125}I became associated with the liver (5.2 ± 1.0% of the dose at 10 min after injection). The ^{3}H-radioactivity disappeared more rapidly from plasma, and it associated to a higher extent with the liver.

For comparison, Figure 5B shows the fate of underivatized [^{3}H]IDU after intravenous injection into rats. The labeled drug is very rapidly cleared from the circulation, and a relatively small amount was recovered in the liver. The remainder of the dose, as has been shown previously, was

Table 2: Stability of NeoHDL-Associated IDU-Ol_2 in Phosphate-Buffered Saline and Rat Serum *in Vitro*[a]

	% of total radioactivity		
incubation	IDU-Ol_2	IDU-Ol_1	water-soluble metabolites
control	97.9 ± 0.2	2.1 ± 0.2	0.0 ± 0.0
PBS, 2 h	97.3 ± 0.2	1.8 ± 0.2	0.9 ± 0.3
serum, 2 h	95.7 ± 0.4	0.8 ± 0.3	3.5 ± 0.2

[a] [^{3}H]IDU-Ol_2-loaded NeoHDL (10 μg of protein/mL) was incubated with rat serum or phosphate-buffered saline (PBS) at 37 °C. After 2 h, the amounts of [^{3}H]IDU-Ol_2, [^{3}H]IDU-Ol_1, and water-soluble [^{3}H]metabolites were determined by extraction and thin layer chromatography. Controls were extracted immediately after mixing prodrug-loaded NeoHDL with serum or PBS. The results are expressed as % of the total radioactivity and are means ± SEM of 3 incubations.

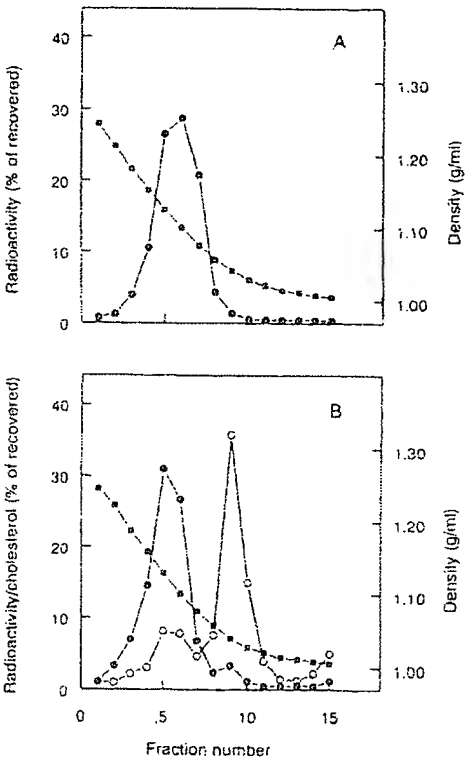

FIGURE 4: Density gradient centrifugation of [^{3}H]IDU-Ol_2-loaded NeoHDL incubated with saline (A) or serum (B). [^{3}H]IDU-Ol_2-loaded NeoHDL (0.05 mg of protein/mL) was incubated for 1 h at 37 °C with phosphate-buffered saline (A) or human serum (B). Aliquots of 2 mL of the incubation mixtures were subjected to density gradient centrifugation (Redgrave et al., 1975). The gradients (12.0 mL) were fractionated in fractions of 0.8 mL. The fractions were assayed for ^{3}H (●) and cholesterol (○; only B), and their densities (■) were measured. The results are expressed as % of the recovered amounts of radioactivity and cholesterol (recoveries >98%).

nonspecifically distributed over the total body (Biessen et al., 1994).

We showed in previous studies that lactosylation of native HDL and NeoHDL, a procedure by which the particles are provided with terminal galactose residues, leads to very rapid uptake of the particles by galactose-specific receptors on parenchymal liver cells (Bijsterbosch & van Berkel, 1992; Schouten et al., 1994). To investigate whether a high liver uptake of the prodrug can be induced via this pathway, [^{3}H]-IDU-Ol_2-loaded ^{125}I-NeoHDL was lactosylated and injected into rats. Figure 6 shows that lactosylation of the prodrug-loaded particle dramatically alters its biological fate. After injection of lactosylated [^{3}H]IDU-Ol_2-loaded ^{125}I-NeoHDL, both labels were equally rapidly cleared from the circulation. At 10 min after injection, only 11.5 ± 1.0% and 7.5 ± 2.1% of the injected ^{3}H- and ^{125}I-activity were left in plasma, respectively. At that time, the liver contained 74.9 ± 9.2% and 75.3 ± 6.6% of the injected amounts of ^{3}H and ^{125}I, respectively.

DISCUSSION

To enable incorporation of IDU into NeoHDL, we synthesized a lipophilic prodrug of IDU. The approach to prepare a lipophilic prodrug from a water-soluble parent compound by the coupling of lipophilic residues was applied in a number of earlier studies (De Smidt & van Berkel, 1990; Firestone et al., 1984; Vitols et al., 1985). In these studies, lipophilic prodrugs of antineoplastic compounds like nitrogen mustard, doxorubicin, methotrexate, and floxuridine were incorporated in LDL, and it was found that the resulting prodrug−LDL complexes can be recognized by LDL receptors on cultured cells. In the present study, IDU was derivatized with two oleoyl residues. Oleyl residues were chosen as lipophilic "anchor" as they are natural components of lipoproteins. The residues were attached via an ester linkage. As esterases are ubiquitous, this type of linkage ensures release of the original, pharmacologically active drug at the site of delivery (Sinkula & Yalowski, 1975). In previous studies, a series of 5′-mono esters of IDU were synthesized, and it was found that the lipophilicity of the prodrug is determined by the choice of side chain (Narurkar & Mitra, 1988; Ghosh & Mitra, 1991). In these earlier studies, relatively short aliphatic chains were used, which resulted in a moderate degree of lipophilicity (log P < 1.4). The oleoyl 3′,5′-diester prepared in the present study was much more lipophilic (log P > 4.0).

The lipophilic prodrug was incorporated into neoHDL by including it in the lipid mixture used to prepare the particles. This procedure resulted in the reproducible formation of particles containing a substantial amount of IDU-Ol_2. The prodrug accounted for 7.3 ± 0.8% of the total weight, which corresponds to approximately 15% of the lipid moiety. It was calculated that each particle contains about 30 prodrug molecules. Higher loads have not been tested, but may very well be possible. The composition further shows a remarkable similarity with that of native HDL. In the present study, the particles were prepared from commercially available components and isolated apoproteins. In the future, recombinant apoproteins may be used to prepare fully artificial particles. Various physical properties of [^{3}H]IDU-Ol_2-loaded NeoHDL were studied and compared with those of native HDL. To allow the simultaneous monitoring of both the incorporated prodrug and the apoproteins of the particles, the apoproteins of the [^{3}H]prodrug-loaded NeoHDL were labeled with ^{125}I. We demonstrate by two different methods that the size of [^{3}H]IDU-Ol_2-loaded NeoHDL is very similar to that of native HDL. Photon correlation spectroscopy indicated sizes for the prodrug-loaded particle and native HDL of 9.7 ± 0.6 and 9.4 ± 0.7 nm, respectively. Furthermore, [^{3}H]IDU-Ol_2-loaded ^{125}I-NeoHDL eluted at the same position as native HDL on a Superose-6 FPLC column. The density and electrical charge of [^{3}H]IDU-Ol_2-loaded ^{125}I-NeoHDL were determined by density gradient centrifugation

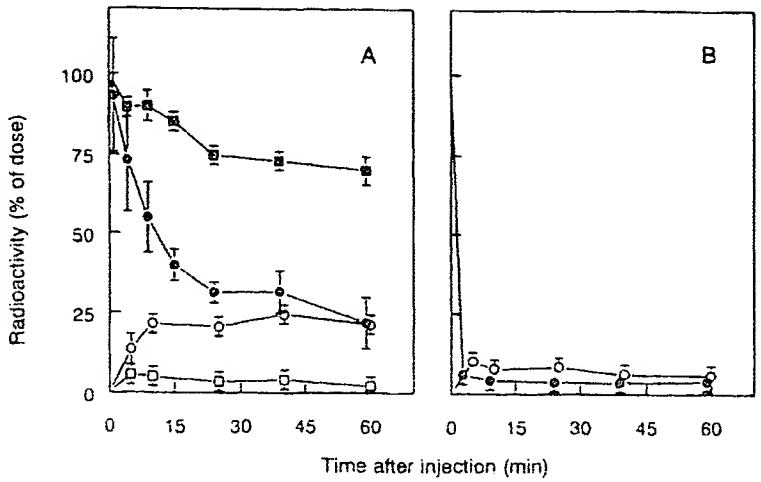

FIGURE 5: Plasma clearance and liver association of [^{3}H]IDU-Ol$_2$-loaded ^{125}I-NeoHDL (A) and [^{3}H]IDU (B). Rats were intravenously injected with [^{3}H]IDU-Ol$_2$-loaded ^{125}I-NeoHDL (A) or [^{3}H]IDU (B). The animals received 5 μg of IDU or an equivalent amount of IDU-Ol$_2$ per kg body weight. At the indicated times, the amounts of radioactivity in plasma and liver were determined. Values are means ± SEM of 3 rats. ●, ^{3}H in plasma; ○, ^{3}H in liver; ■, ^{125}I in plasma; □, ^{125}I in liver.

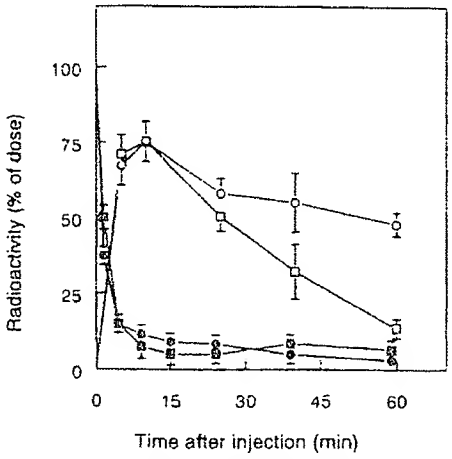

FIGURE 6: Plasma clearance and liver association of lactosylated [^{3}H]IDU-Ol$_2$-loaded ^{125}I-NeoHDL. Rats were intravenously injected with lactosylated [^{3}H]IDU-Ol$_2$-loaded ^{125}I-NeoHDL at a dose equivalent to 5 μg of IDU per kg body weight. At the indicated times, the amounts of radioactivity in plasma and liver were determined. Values are means ± SEM of 3 rats. ●, ^{3}H in plasma; ○, ^{3}H in liver; ■, ^{125}I in plasma; □, ^{125}I in liver.

and agarose gel electrophoresis, respectively. It was found that the prodrug-loaded particles had the same characteristics as native HDL. As in all assays the prodrug and apoproteins of the particle behaved similarly, it can be concluded that under the conditions employed the particles are stable.

The stability of the the prodrug-loaded particle in serum was investigated by *in vitro* incubation studies. Upon incubation with rat serum, NeoHDL-associated IDU-Ol$_2$ was not rapidly metabolized. Furthermore, it was found that the prodrug does not rapidly exchange with other lipoproteins, such as LDL, during *in vitro* incubation with human serum.

Derivatization of IDU and the subsequent incorporation of the prodrug into neoHDL drastically altered the biological fate of the drug. Underivatized IDU is rapidly cleared from the circulation after injection, and 10−15% of the injected amount was found in the liver. We showed earlier that the remainder is distributed nonspecifically over the total body. Major recovery sites were bulky tissues like muscles and skin (Biessen et al., 1994). As judged by the behavior of the apoproteins, IDU-Ol$_2$-loaded NeoHDL particles are only slowly cleared from the circulation, just like native HDL. Only a very small proportion became associated with the liver. As even a limited oxidative modification of lipoproteins results in a substantial hepatic uptake of lipoprotein particles (Van Berkel et al., 1991), this result indicates that no significant oxidative damage was provoked to the particles during preparation. The labeled prodrug, however, disappeared more rapidly from the circulation, and it associated to a higher extent with the liver. As mentioned above, NeoHDL-associated IDU-Ol$_2$, during *in vitro* incubations in serum, is not rapidly hydrolyzed nor does it readily exchange with LDL. Apparently, NeoHDL-associated IDU-Ol$_2$ *in vivo* is subject to selective release from HDL. It has been reported for a number of tissues, including liver, that cholesterol esters from native HDL are selectively taken up without a parallel uptake of the apoproteins (Glass et al., 1985). The rate of selective cellular uptake of various cholesterol esters can be up to 40-fold higher than the uptake of apoproteins (Sattler & Stocker, 1993). The observed higher rate of plasma clearance and liver uptake of IDU-Ol$_2$ from the circulation may thus, at least in part, be explained by HDL-specific natural processing of the prodrug-loaded particles.

We showed, earlier, that if (neo)HDL is provided with terminal galactose residues by reductive lactosamination, the resulting lactosylated (Neo)HDL is recognized by galactose receptors on parenchymal liver cells (Bijsterbosch & van Berkel, 1992; Schouten et al., 1994). In the present study, we show that lactosylated IDU-Ol$_2$-loaded NeoHDL is very rapidly cleared from the circulation. Within 10 min after injection, approximately 90% of the apoproteins as well as the prodrug is cleared from the circulation. The cleared radioactivity is largely (>80%) recovered in the liver. The hepatic association of prodrug and apoproteins was very similar. This finding indicates that, in the case of lactosylated IDU-Ol$_2$-loaded NeoHDL, the particles are taken up as an entity. In preliminary experiments it was found that preinjection of asialofetuin substantially reduced the rate of plasma clearance and liver uptake of both the prodrug and the apoproteins of lactosylated IDU-Ol$_2$-loaded NeoHDL (data

not shown). As asialofetuin specifically inhibits uptake by the asialoglycoprotein receptor on parenchymal liver cells (Van Berkel et al., 1987), this finding indicates that this receptor is mainly responsible for the hepatic uptake of lactosylated IDU-Ol_2-loaded NeoHDL. The approach to use lactosylated NeoHDL as a carrier to target lipophilic prodrugs to the galactose receptor on parenchymal liver cells affords a number of advantages over previously published carrier systems like (neo)glycoproteins and lactosylated poly-L-lysine (Jansen et al., 1993; Biessen et al., 1994). During transport in the circulation, the lipophilic prodrug is hidden in the lipid moiety (probably the apolar core), protected from the biological environment. Furthermore, as the lipophilic prodrugs are incorporated in the lipid moiety, high drug loads are possible without interfering with the receptor-mediated recognition of the lactose residues that are present on the surface of the apoproteins.

In conclusion, our findings indicate that it is possible to convert a hydrophilic drug like IDU into a lipophilic prodrug that can be efficiently incorporated into a reconstituted HDL particle with similar physicochemical properties as native HDL. The prodrug-loaded particles are *in vitro* stable in serum, their *in vivo* behavior resembles that of native HDL, and lactosylation induces selective uptake by parenchymal liver cells. The latter result is particularly interesting, as this approach may also be used to target other lipophilic derivatives of water-soluble drugs highly specifically to liver parenchymal cells. This may lead to a more effective therapy of infectious diseases like hepatitis B.

ACKNOWLEDGMENT

The authors wish to thank Dr. E. A. L. Biessen and Dr. H. C. P. F. Roelen for their help with recording and interpreting NMR spectra and Ms. R. B. Tijdens for the HPLC analysis of [^{3}H]IDU.

REFERENCES

Atkinson, D., & Small, D. M. (1986) *Annu. Rev. Biophys. Biophys. Chem. 15*, 403−456.
Biessen, E. A. L., Beuting, D. M., Vietsch, H., Bijsterbosch, M. K., & van Berkel, Th. J. C. (1994) *J. Hepatol.* (in press).
Bijsterbosch, M. K., & van Berkel, Th. J. C. (1990) *Adv. Drug Delivery Rev. 5*, 231−251.
Bijsterbosch, M. K., & van Berkel, Th. J. C. (1992) *Mol. Pharmacol. 41*, 404−411.
Bijsterbosch, M. K., Ziere, G. J., & van Berkel, Th. J. C. (1989) *Mol. Pharmacol. 36*, 484−489.
Caster, W. O., Simon, A. B., & Armstrong, W. D. (1955) *Am. J. Physiol. 183*, 317−321.
Counsell, R. E., & Pohland, R. C. (1982) *J. Med. Chem. 25*, 1115−1120.
De Smidt, P. C., & van Berkel, Th. J. C. (1990) *Cancer Res. 50*, 7476−7482.
De Smidt, P. C., Versluis, A. J., & van Berkel, Th. J. C. (1993) *Biochemistry 32*, 2916−2922.
Firestone, R. A. (1994) *Bioconjugate Chem. 5*, 105−113.
Firestone, R. A., Pisano, J. M., Falck, J. R., McPhaul, M. M., & Krieger, M. (1984) *J. Med. Chem. 27*, 1037−1043.
Folch, J., Lees, M., & Stanley, G. H. S. (1957) *J. Biol. Chem. 226*, 497−509.
Ghosh, M. K., & Mitra, A. K. (1991) *Pharm. Res. 8*, 771−775.
Glass, C., Pittman, R. C., Civen, M., & Steinberg, D. (1985) *J. Biol. Chem. 260*, 744−750.
Jansen, R. W., Kruijt, J. K., van Berkel, Th. J. C., & Meijer, D. K. F. (1993) *Hepatology 18*, 146−152.
Jonas, A., Kezdy, K. E., & Wald, J. H. (1989) *J. Biol. Chem. 264*, 4818−4824.
Lowry, O. H., Rosebrough, N. J., Farr, A. L., & Randall, R. J. (1951) *J. Biol. Chem. 193*, 265−275.
Mraz, W., Reble, B., Kemkes, B. M., & Knedel, M. (1986) *Transplant. Proc. 18*, 1281−1284.
Nagelkerke, J. F., Bakkeren, H. F., Kuipers, F., Vonk, R. J., & van Berkel, Th. J. C. (1986) *J. Biol. Chem. 261*, 8908−8913.
Narurkar, M. M., & Mitra, A. K. (1988) *Pharm. Res. 5*, 734−737.
Nishizawa, Y., Casida, J. E., Anderson, S. W., & Heidelberger, C. (1965) *Biochem. Pharmacol. 14*, 1605−1619.
Pittman, R. C., Glass, D. K., Atkinson, D., & Small, D. M. (1987) *J. Biol. Chem. 262*, 2435−2442.
Poznanski, M. J., & Juliano, R. L. (1984) *Pharmacol. Rev. 36*, 277−336.
Prusoff, W. H. (1959) *Biochim. Biophys. Acta 32*, 295−296.
Prusoff, W. H., & Goz, B. (1974) *Fed. Proc. 32*, 1679−1687.
Redgrave, T. G., Roberts, D. C. K., & West, C. E. (1975) *Anal. Biochem. 65*, 42−49.
Santos, O., Pant, K. D., Blank, E. W., & Ceriani, R. L. (1992) *J. Nucl. Med. 33*, 1530−1534.
Sattler, W., & Stocker, R. (1993) *Biochem. J. 294*, 771−778.
Schouten, D., Kleinherenbrink-Stins, M. F., Brouwer, A., Knook, D. L., & van Berkel, Th. J. C. (1988) *Biochem. J. 256*, 615−621.
Schouten, D., van der Kooij, M., Muller, J., Pieters, M. N., Bijsterbosch, M. K., & van Berkel, Th. J. C. (1993) *Mol. Pharmacol. 44*, 486−492.
Shaw, J. M., Shaw, K. V., Yanovich, S., Iwanik, M., Futch, W. S., Rosowsky, A., & Schook, L. B. (1987) *Ann. N.Y. Acad. Sci. 507*, 252−271.
Sinkula, A. A., & Yalowski, S. H. (1975) *J. Pharm. Sci. 64*, 181−210.
Tomlinson, E. (1987) *Adv. Drug Delivery Rev. 1*, 87−198.
Van Berkel, Th. J. C., Dekker, C. J., Kruijt, J. K., & Van Eijk, H. G. (1987) *Biochem. J. 243*, 715−722.
Van Berkel, Th. J. C., de Rijke, Y. B., & Kruijt, J. K. (1991) *J. Biol. Chem. 266*, 2282−2289.
Vitols, S. G., Masquelier, M., & Peterson, C. O. (1985) *J. Med. Chem. 28*, 451−454.
Weisgraber, K. H., & Mahley R. W. (1980) *J. Lipid Res. 21*, 316−325.